Weyl and Transport

© Nature

Claudia Felser

Graphene

- Graphene’s conductivity exhibits values close to the conductivity quantum e2/h per carrier type
- Graphene’s charge carriers can be tuned continuously between electrons and holes in concentrations $n = 10^{13}\ cm^{-2}$
- Mobilities μ can exceed 15,000 $cm^2\ V^{-1}\ s^{-1}$ under ambient conditions
- InSb has μ ≈77,000 $cm^2\ V^{-1}\ s^{-1}$

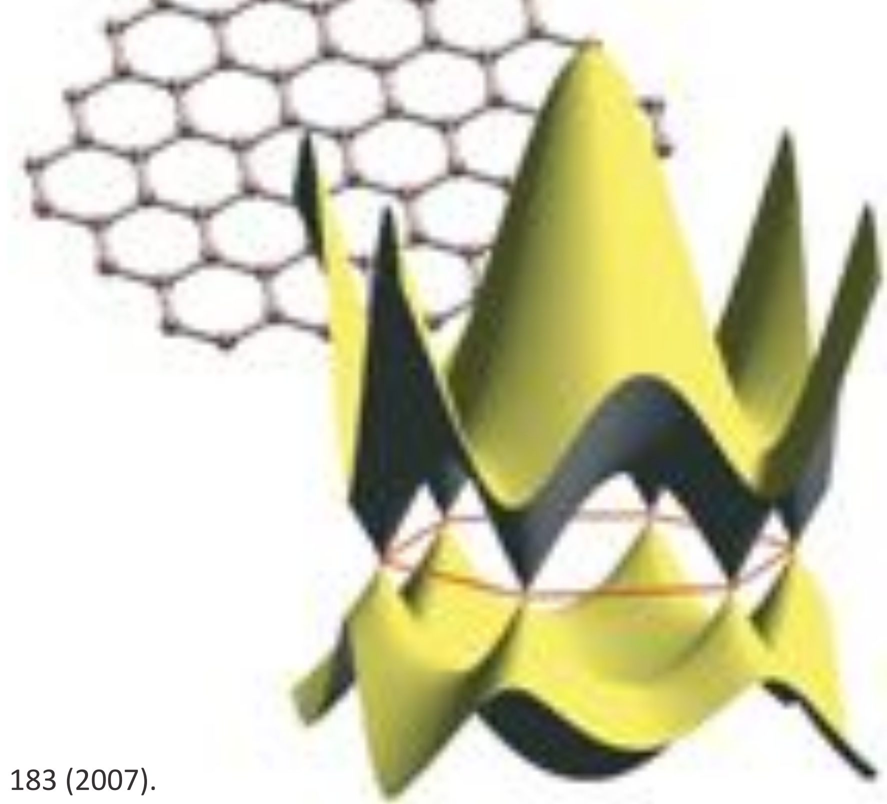

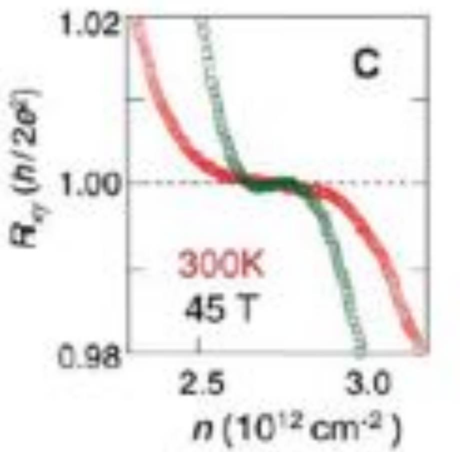

Geim, A. K. & Novoselov, K. S. The rise of graphene. Nature Mater. 6, 183 (2007).

Graphene

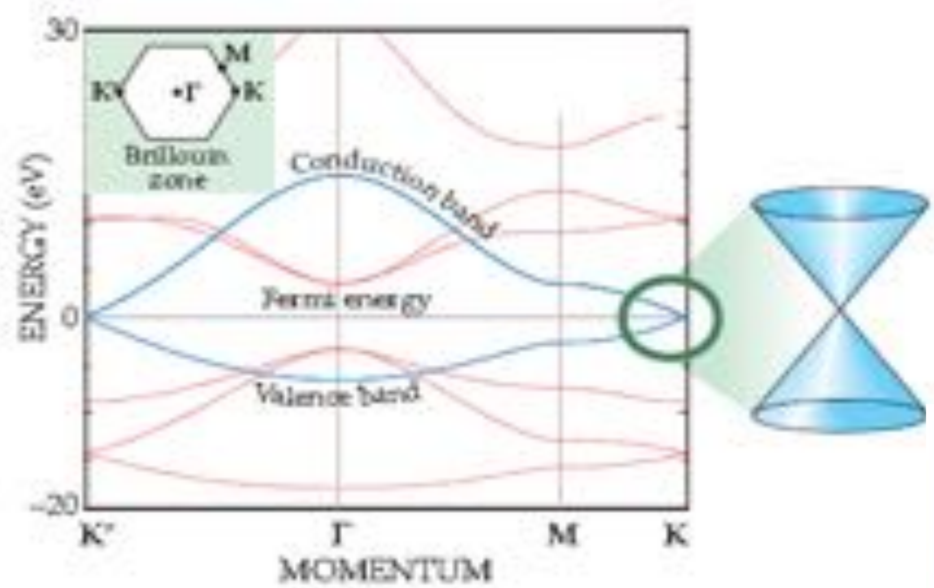

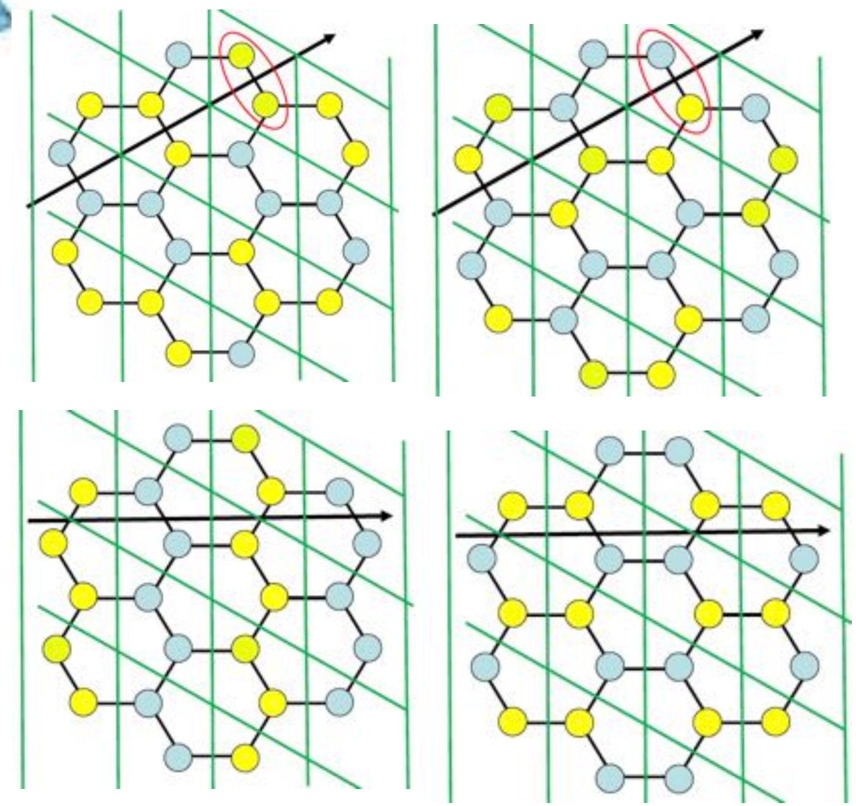

Geim, A. K. & Novoselov, K. S. The rise of graphene. Nature Mater. 6, 183 (2007).

Particles – Universe –Condensed matter

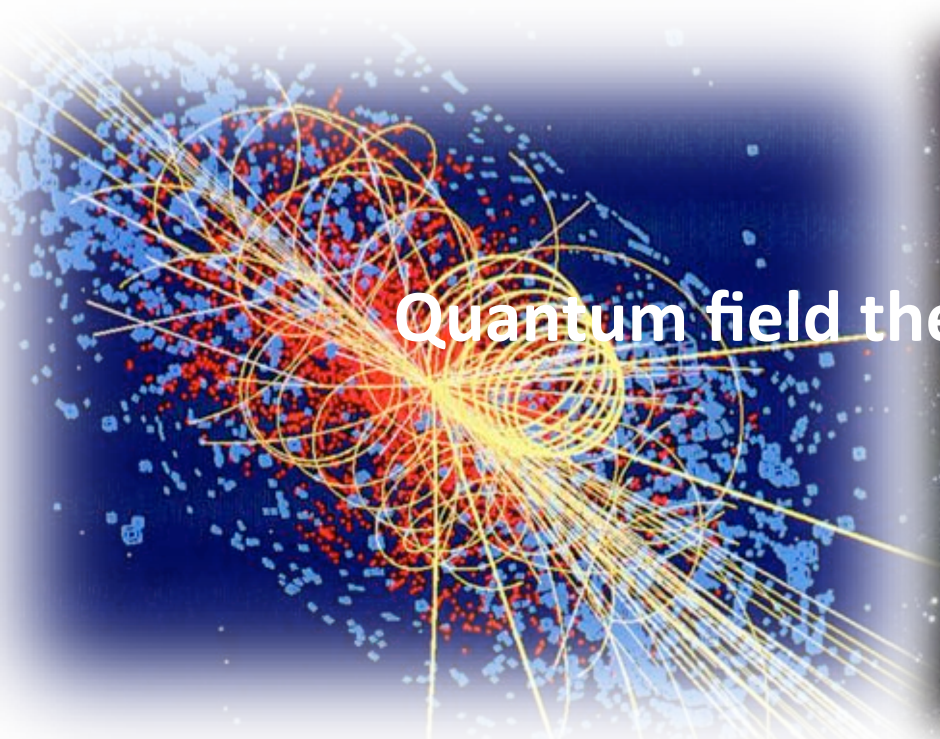

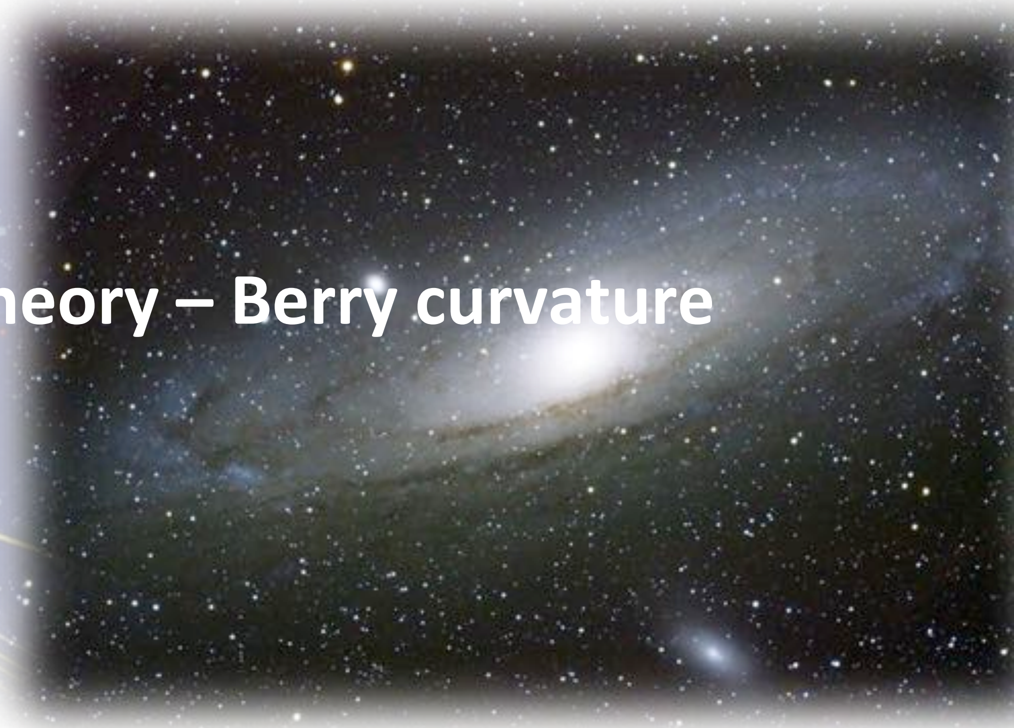

Quantum field theory – Berry curvature

Dirac
Cd_3As_2
Guido Kreiner

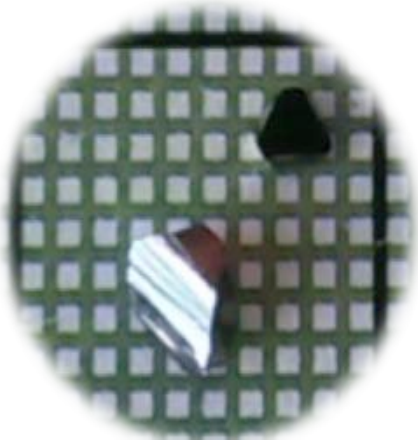

Higgs
$YMnO_3$
Lichtenberg Spaldin

Weyl
TaAs
Vicky Süss, Marcus Schmidt

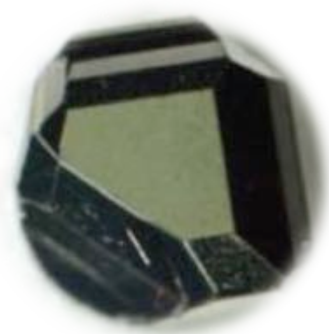

Majorana
YPtBi
Chandra Shekhar

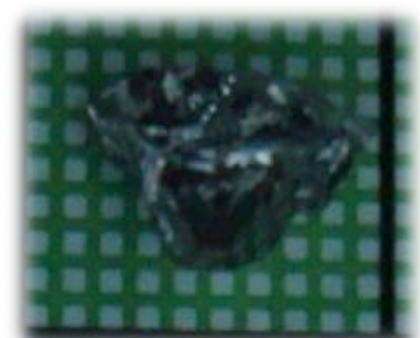

Family of Quantum Hall Effects

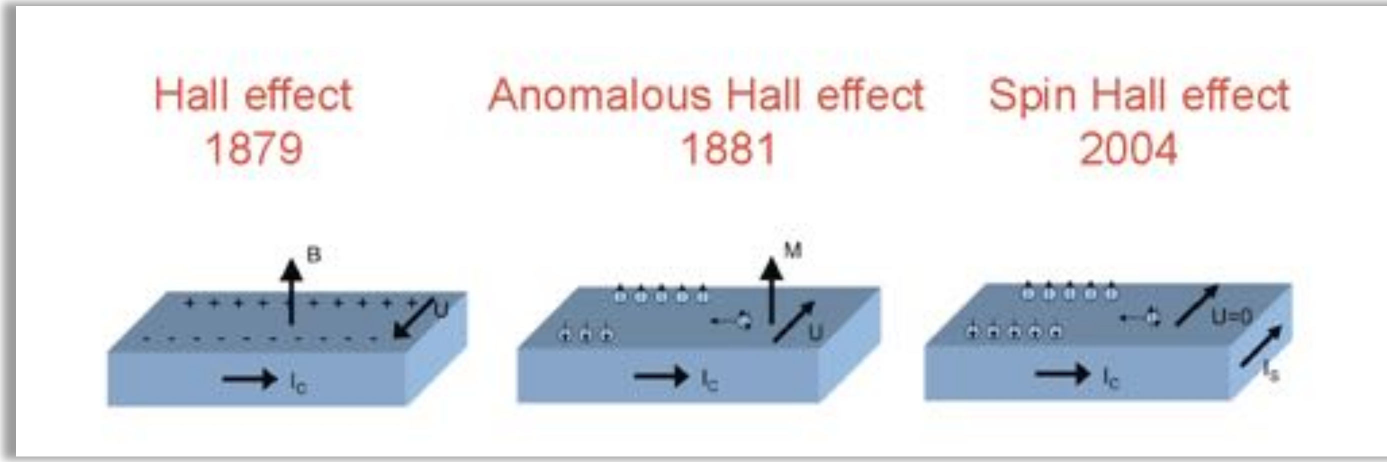

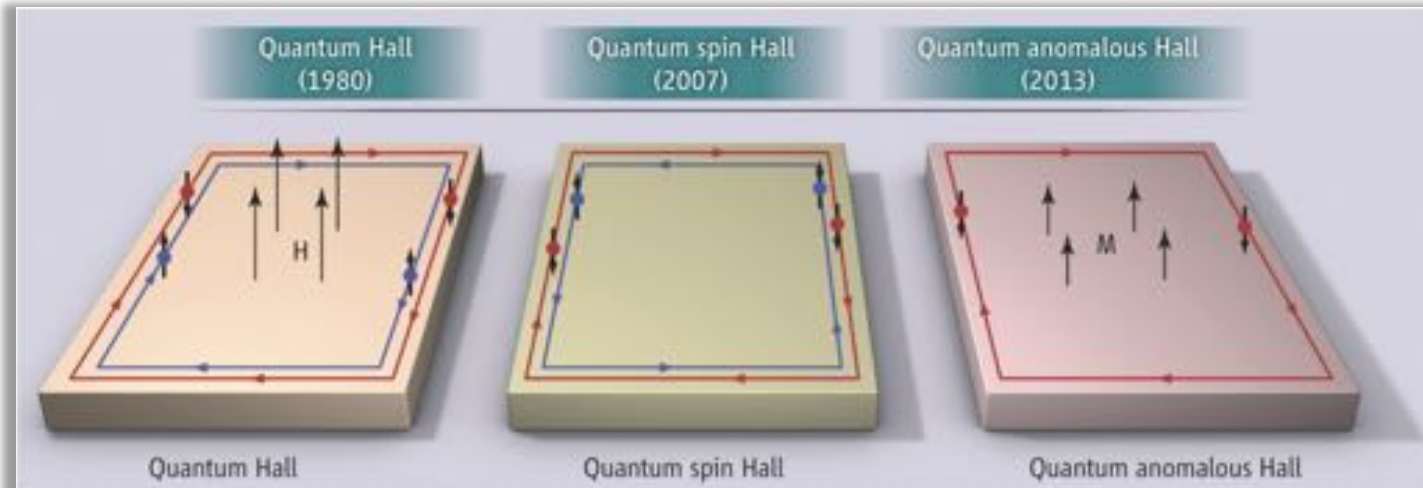

S Oh Science 340 (2013) 153

1985
Klaus von Klitzing
1998
Horst Ludwig Störmer and Daniel Tsui
2010
Andre Geim and Konstantin Novoselov

2016
David Thouless, Duncan Haldane und Michael Kosterlitz

Hall effect

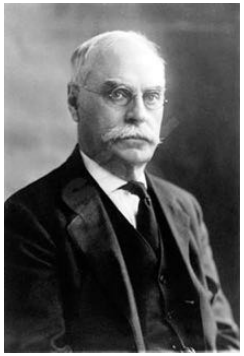

Edwin Herbert Hall

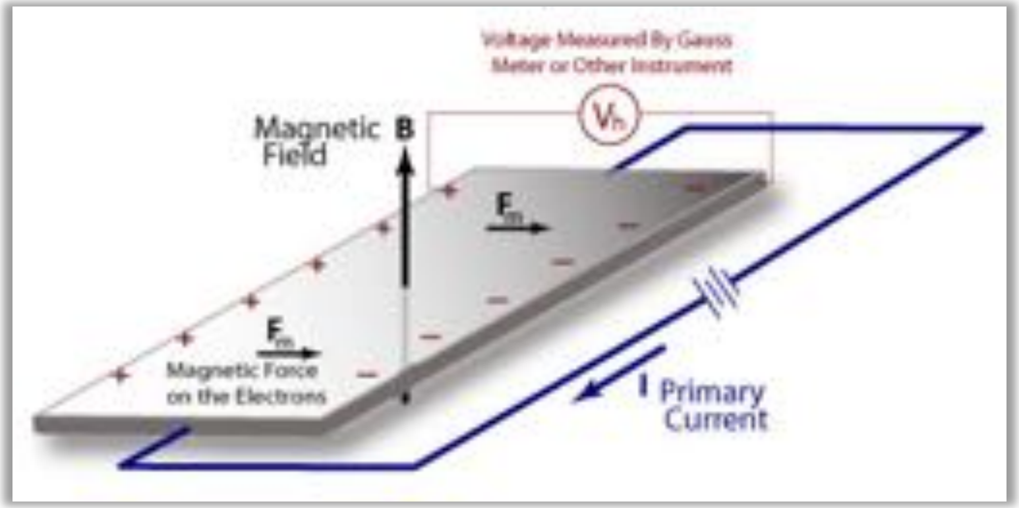

Lorentz force deflect charge particles

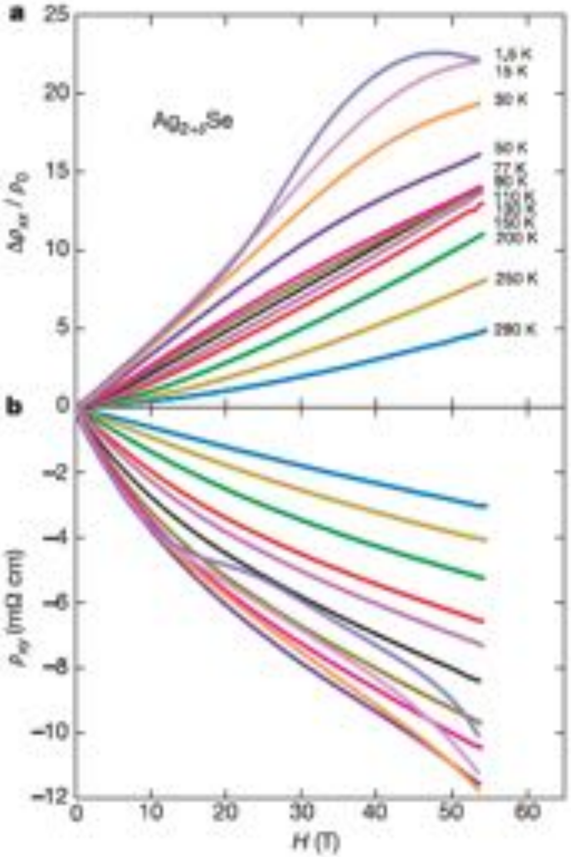

We measure the resistance without and with a magnetic field

- Metal, semiconductor, or insulator
- Electron or hole conductivity
- Resistance in a magnetic field: Magnetoresistance

A. Husmann et al., Nature 417 (2002) 421

Hall effect

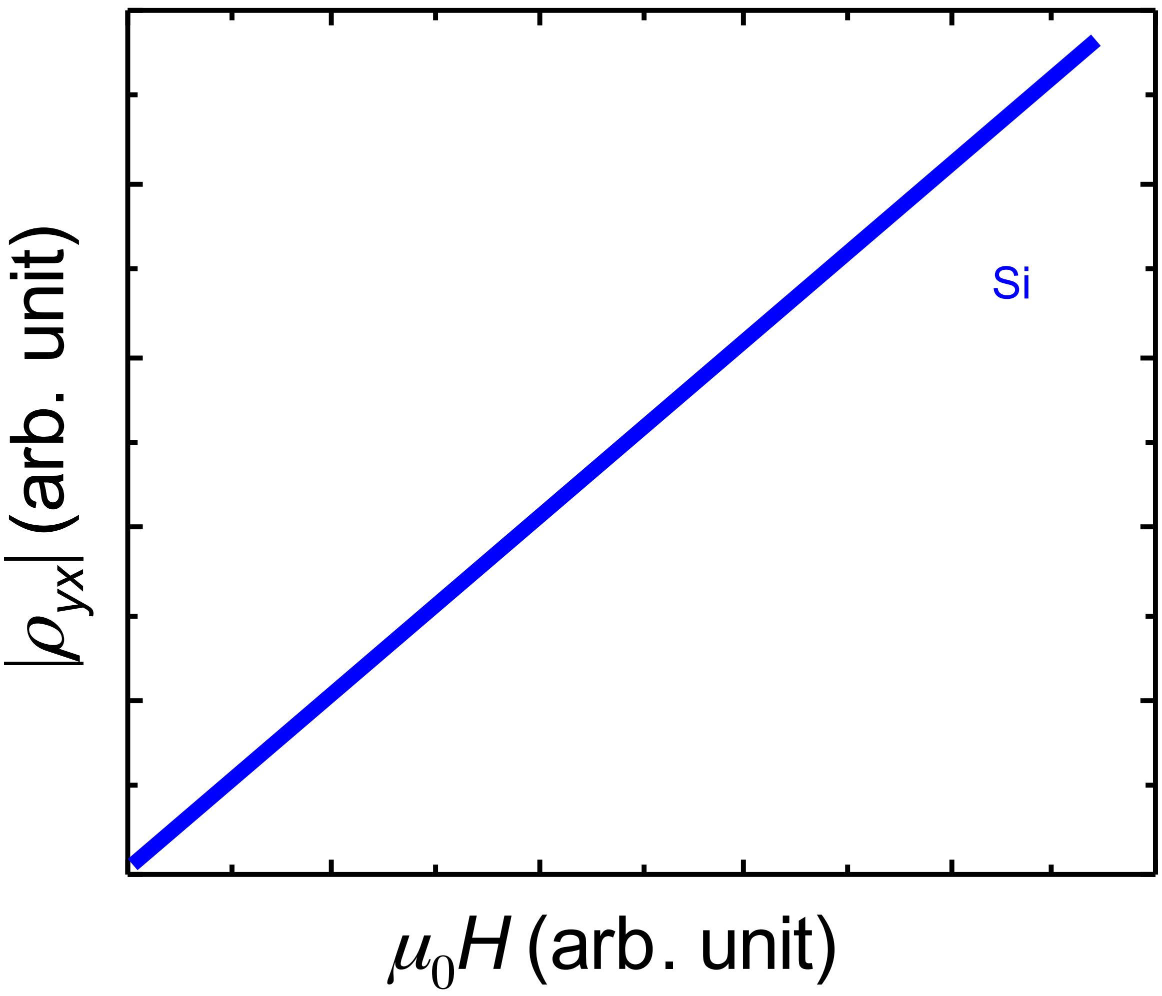

Anomalous-Hall effect

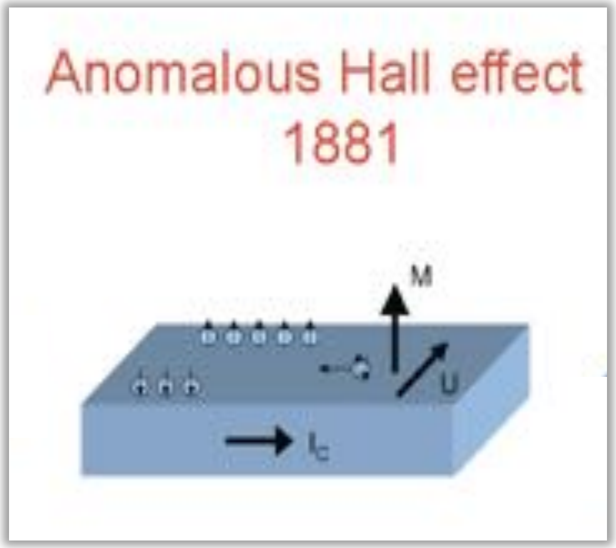

- Ferromagnetic materials have internal magnetic field
- No effect so far in antiferromagnets
- AHE scales with the Magnetization
- External effects
- Much larger than normal Hall Effect, but not well understood ; Possible Berry-phase effect

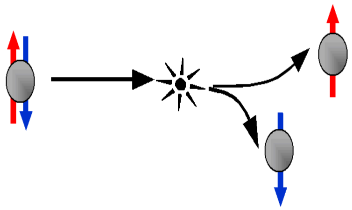

$$\rho_H = R_0 B + \boxed{4\pi R_s M}$$

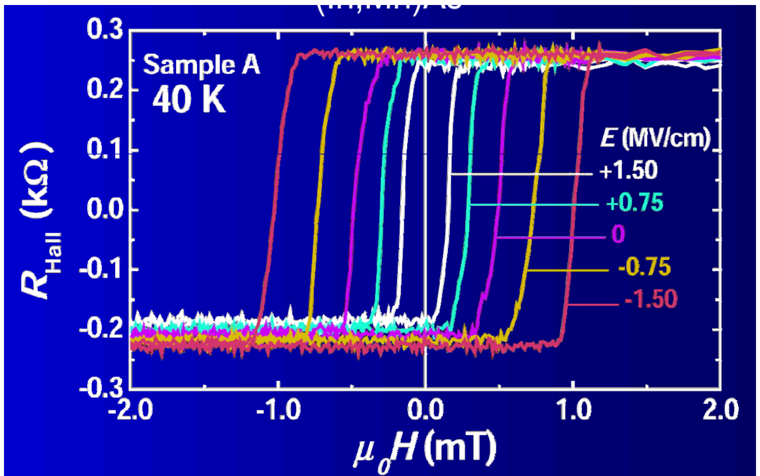

D. Chiba *et al.*, Science **301**, 943 (2003)

$$\boxed{-\frac{e^2}{\hbar}\mathbf{E}\times\int d^3k\sum_n f_n\mathbf{\Omega}_n(\mathbf{k}) - \frac{e}{\hbar}\int d^3k\sum_n \delta f_n(\mathbf{k})\frac{\partial\varepsilon_n}{\partial\mathbf{k}}}$$

$$\boxed{\mathbf{\Omega}_n(\mathbf{k}) = -\,\mathrm{Im}\,\langle\nabla_{\mathbf{k}}u_{n\mathbf{k}}|\times|\nabla_{\mathbf{k}}u_{n\mathbf{k}}\rangle}$$

Berry curvature:

M.V. Berry, Proc. Royal Soc. London (1984)

Spin-Hall effect

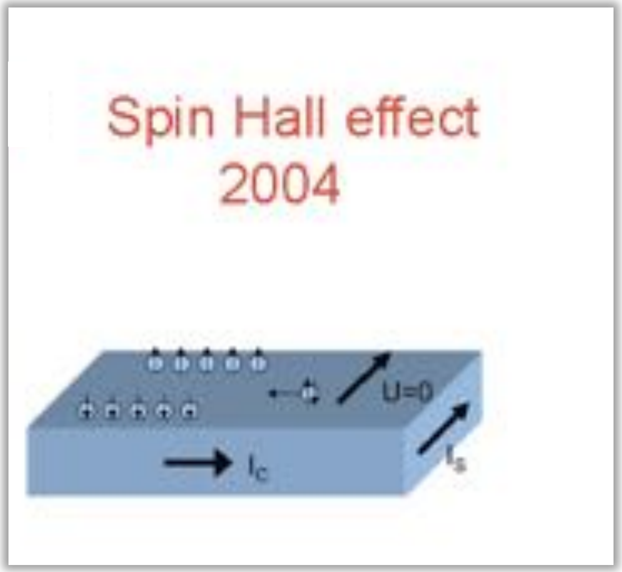

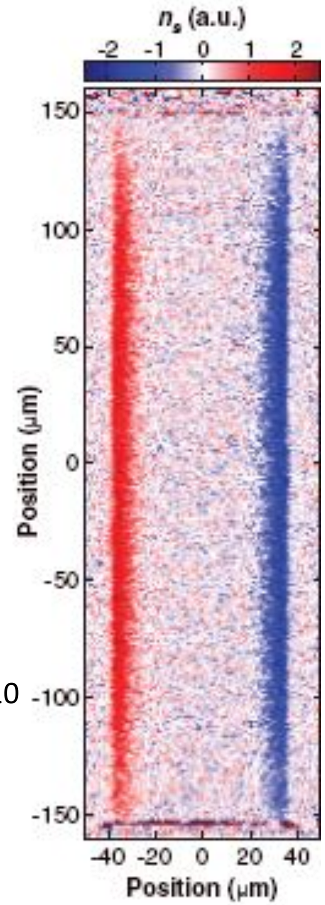

- Separation of electron spins without magnetic field
- Spin-current generation in non-magnetic systems
- Predicted in 1971 or 2004?
- Observed in semiconductors (2004) and metals
- Extrinsic or intrinsic?

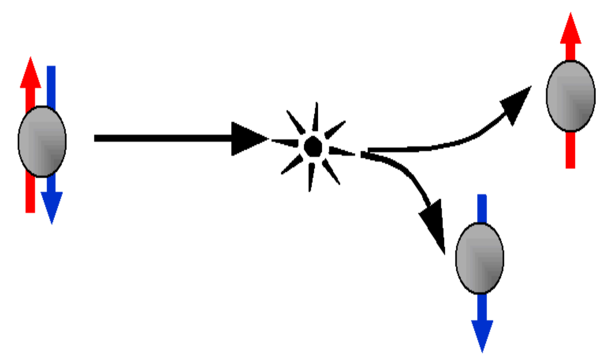

Experiment (2004):
Kato, Myars, Gossard, Awschalom, Science 306, 1910
Theory
D'yakonov & Perel', Exp. Theor. Phys. Lett. (1971)
INTRINSIC SPIN-HALL EFFECT:
Murakami et al Science 2003 (cond-mat/0308167)
Sinova et al PRL 2004 (cont-mat/0307663)

$$\boxed{-\frac{e^2}{\hbar}\mathbf{E}\times\int d^3k\sum_n f_n\mathbf{\Omega}_n(\mathbf{k}) - \frac{e}{\hbar}\int d^3k\sum_n \delta f_n(\mathbf{k})\frac{\partial\varepsilon_n}{\partial\mathbf{k}}}$$

$$\boxed{\mathbf{\Omega}_n(\mathbf{k}) = -\,\mathrm{Im}\,\langle\nabla_{\mathbf{k}}u_{n\mathbf{k}}|\times|\nabla_{\mathbf{k}}u_{n\mathbf{k}}\rangle}$$

Berry curvature:
M.V. Berry, Proc. Royal Soc. London (1984)

Anomalous Hall effect

REVIEWS OF MODERN PHYSICS, VOLUME 82, APRIL–JUNE 2010

Anomalous Hall effect

Naoto Nagaosa

Department of Applied Physics, University of Tokyo, Tokyo 113-8656, Japan and Cross-Correlated Materials Research Group (CMRG), and Correlated Electron Research Group (CERG), ASI, RIKEN, Wako, 351-0198 Saitama, Japan

Jairo Sinova

Department of Physics, Texas A&M University, College Station, Texas 77843-4242, USA and Institute of Physics ASCR, Cukrovarnická 10, 162 53 Praha 6, Czech Republic

Shigeki Onoda

Condensed Matter Theory Laboratory, ASI, RIKEN, Wako, 351-0198 Saitama, Japan

A. H. MacDonald

Department of Physics, University of Texas at Austin, Austin, Texas 78712-1081, USA

N. P. Ong

Department of Physics, Princeton University, Princeton, New Jersey 08544, USA

(Published 13 May 2010)

The anomalous Hall effect (AHE) occurs in solids with broken time-reversal symmetry, typically in a ferromagnetic phase, as a consequence of spin-orbit coupling. Experimental and theoretical studies of the AHE are reviewed, focusing on recent developments that have provided a more complete framework for understanding this subtle phenomenon and have, in many instances, replaced controversy by clarity. Synergy between experimental and theoretical works, both playing a crucial role, has been at the heart of these advances. On the theoretical front, the adoption of the Berry-phase concepts has established a link between the AHE and the topological nature of the Hall currents. On the experimental front, new experimental studies of the AHE in transition metals, transition-metal oxides, spinels, pyrochlores, and metallic dilute magnetic semiconductors have established systematic trends. These two developments, in concert with first-principles electronic structure calculations, strongly favor the dominance of an intrinsic Berry-phase-related AHE mechanism in metallic ferromagnets with moderate conductivity. The intrinsic AHE can be expressed in terms of the Berry-phase curvatures and it is therefore an intrinsic quantum-mechanical property of a perfect crystal. An extrinsic mechanism, skew scattering from disorder, tends to dominate the AHE in highly conductive ferromagnets. The full modern semiclassical treatment of the AHE is reviewed which incorporates an anomalous contribution to wave-packet group velocity due to momentum-space Berry curvatures and correctly combines the roles of intrinsic and extrinsic (skew-scattering and side-jump) scattering-related mechanisms. In addition, more rigorous quantum-mechanical treatments based on the Kubo and Keldysh formalisms are reviewed, taking into account multiband effects, and demonstrate the equivalence of all three linear response theories in the metallic regime. Building on results from recent experiment and theory, a tentative global view of the AHE is proposed which summarizes the roles played by intrinsic and extrinsic contributions in the disorder strength versus temperature plane. Finally outstanding issues and avenues for future investigation are discussed.

Intrinisic Hall

- Berry curvature
- Magnetisation?

Extrinsic Hall

- Skew scattering
- Side jumps

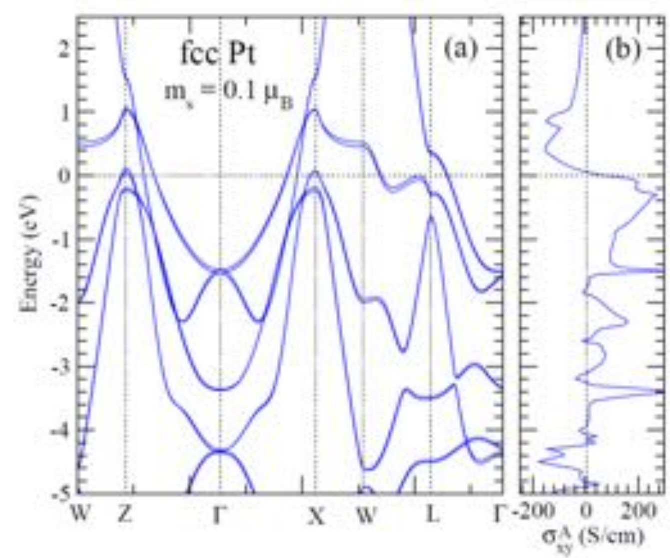

Anomalous Nernst and Hall effects in magnetized platinum and palladium

G. Y. Guo,[1,2,*] Q. Niu,[3,4] and N. Nagaosa[5,6]

The Spin Hall effect (SHE) → Spin Orbit Torque

Positive Spin Hall Angle (SHA)

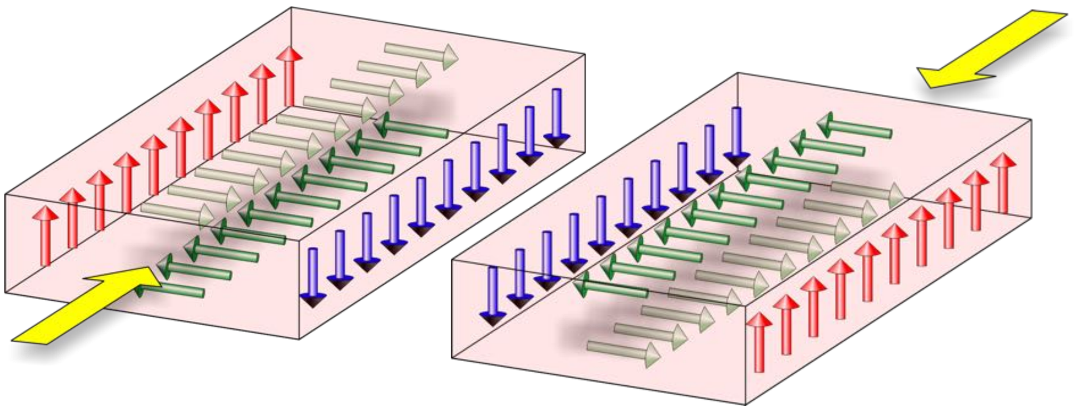

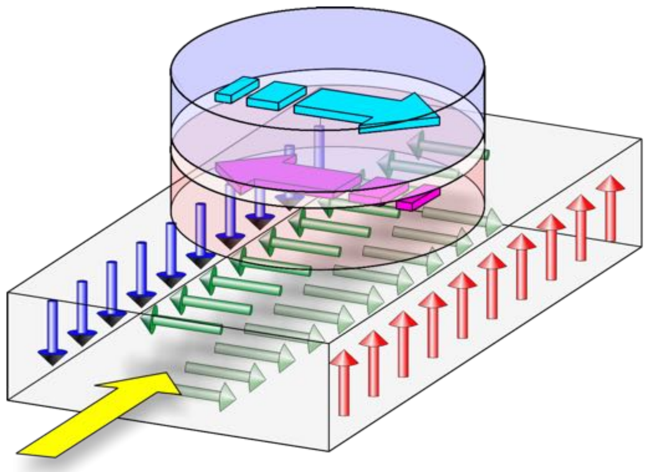

Miron *et* al., Nature (2011)
Liu *et al.*, Science (2012)

Spin Hall effect → Spin orbit torque

- Spin current flows across the interface and applies a torque on the FM layer
- Charge to spin conversion efficiency

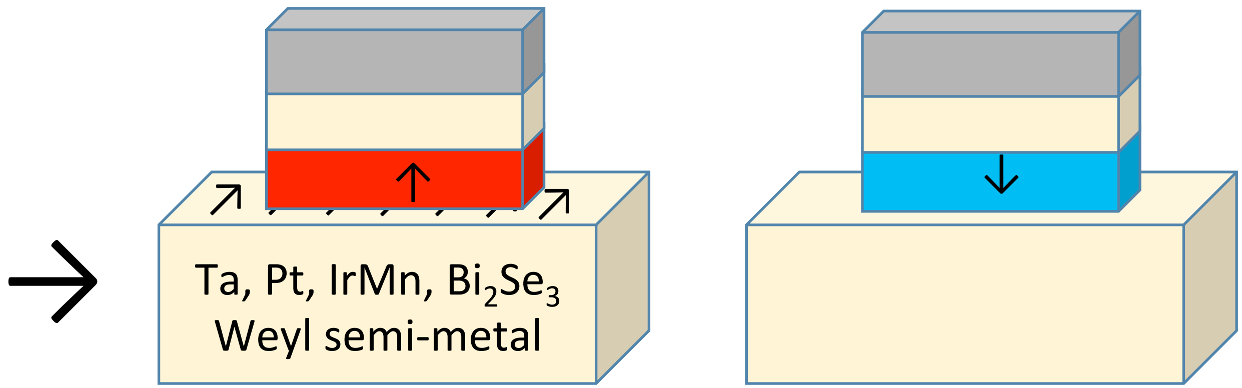

Fundamental limits: switching current

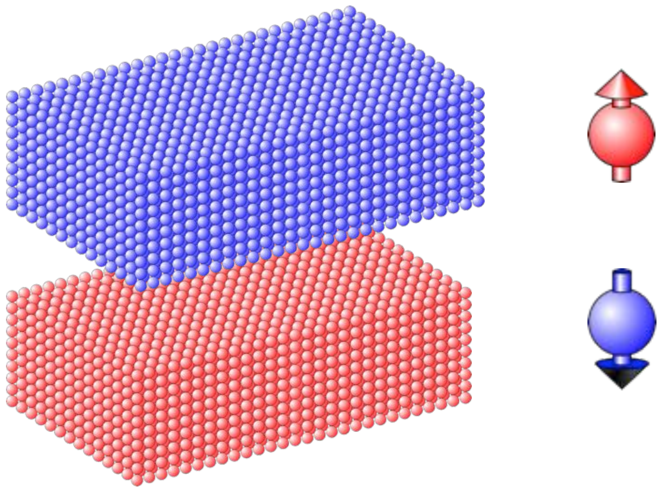

→ How many spin polarized electrons needs to switch nano-element?

→ Nano-element: 10 x 10 x 1 nm^3
- need ~100,000 electrons to switch magnetization
- requires that current (μA) x time interval (nsec) ~ 30 μA.nsec

→ 10 μA for 3 nsec

→ To reduce current could use orbital moments e.g. using spin-orbit coupling

→ Lower limit:

- need to overcome energy barrier that stabilizes MTJ against thermal fluctuations
- some angular momentum lost to lattice (damping)

Dirac and Weyl semimetals

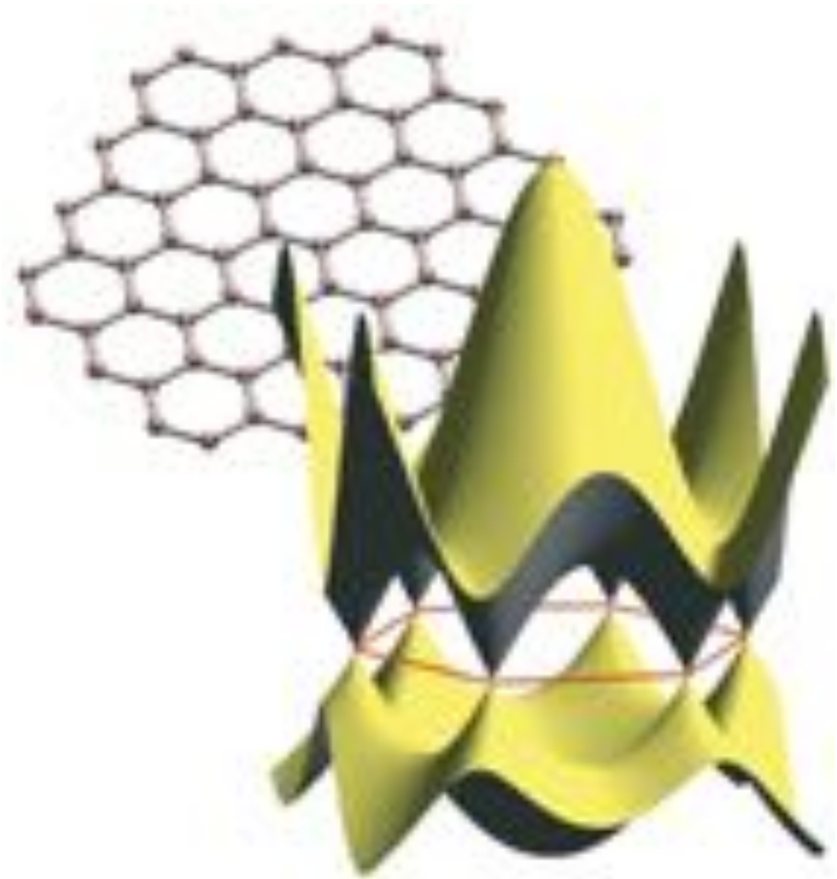

Paul Klee

Dirac semimetals

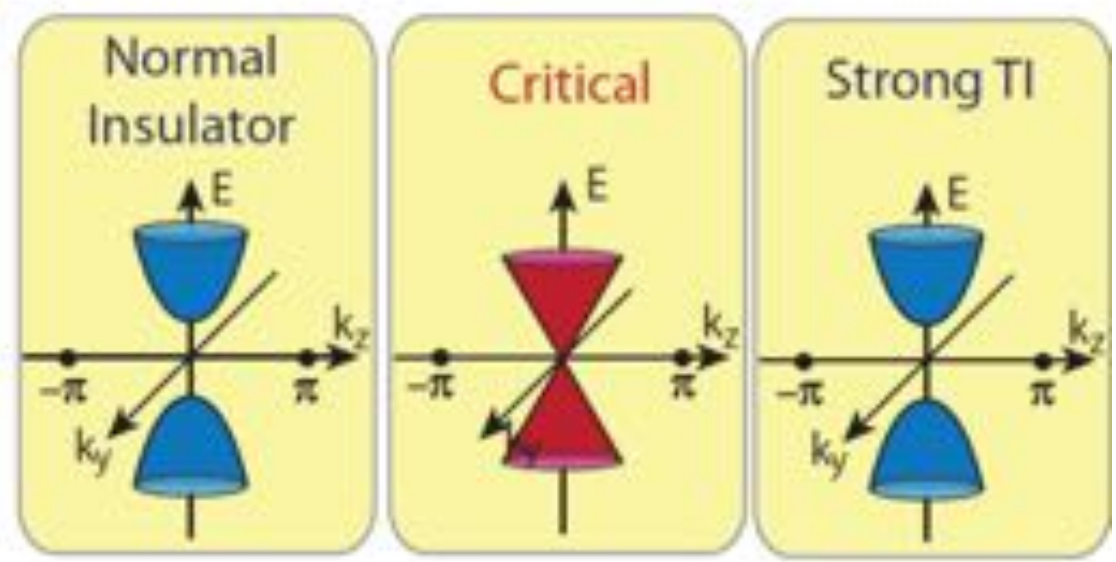

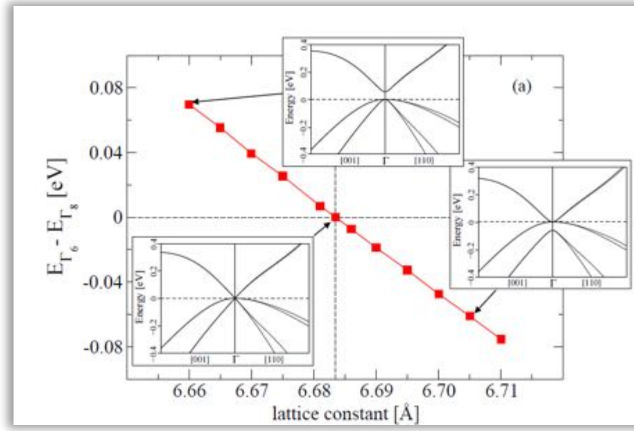

Bohm-Jung Yang and Naoto Nagaosa, arXiv:1404.0754

nature COMMUNICATIONS

ARTICLE

Received 2 Dec 2013 | Accepted 2 Apr 2014 | Published 7 May 2014 DOI: 10.1038/ncomms4786

Observation of a three-dimensional topological Dirac semimetal phase in high-mobility Cd_3As_2

Madhab Neupane[1,*], Su-Yang Xu[1,*], Raman Sankar[2,*], Nasser Alidoust[1], Guang Bian[1], Chang Liu[1], Ilya Belopolski[1], Tay-Rong Chang[3], Horng-Tay Jeng[3,4], Hsin Lin[5], Arun Bansil[6], Fangcheng Chou[2] & M. Zahid Hasan[1,7]

Science AAAS

Observation of Fermi arc surface states in a topological metal
Su-Yang Xu *et al.*
Science **347**, 294 (2015);
DOI: 10.1126/science.1256742

3D Dirac Cd_3As_2

Cd_3As_2—A Noncubic Semiconductor with Unusually High Electron Mobility*

ARTHUR J. ROSENBERG AND THEODORE C. HARMAN
Lincoln Laboratory, Massachusetts Institute of Technology, Lexington, Massachusetts
(Received June 17, 1959)

IN all reported studies of electron transport in solids, the electron mobility at room temperature determined by galvanomagnetic or drift experiments has been found to exceed 10 000 cm²/volt-sec in but four materials, namely, the compounds InSb, InAs, HgSe, and HgTe at accessible purities [Table I(A)]. Each

TABLE I. Electron Hall mobility at 300°K.[a]

Material	Carrier concentration, cm⁻³	Hall mobility, cm²/volt-sec
A. Highest measured values		
InSb	2×10^{16}	63 000[b]
InAs	1.7×10^{16}	30 000[c]
HgSe	4×10^{17}	18 000[d]
HgTe	2.6×10^{17}	19 000[e]
B. Measured values at 4×10^{18} carriers/cm³		
InSb		8000[f]
InAs		7000[c]
HgSe		6000[d]
Cd_3As_2		10 000

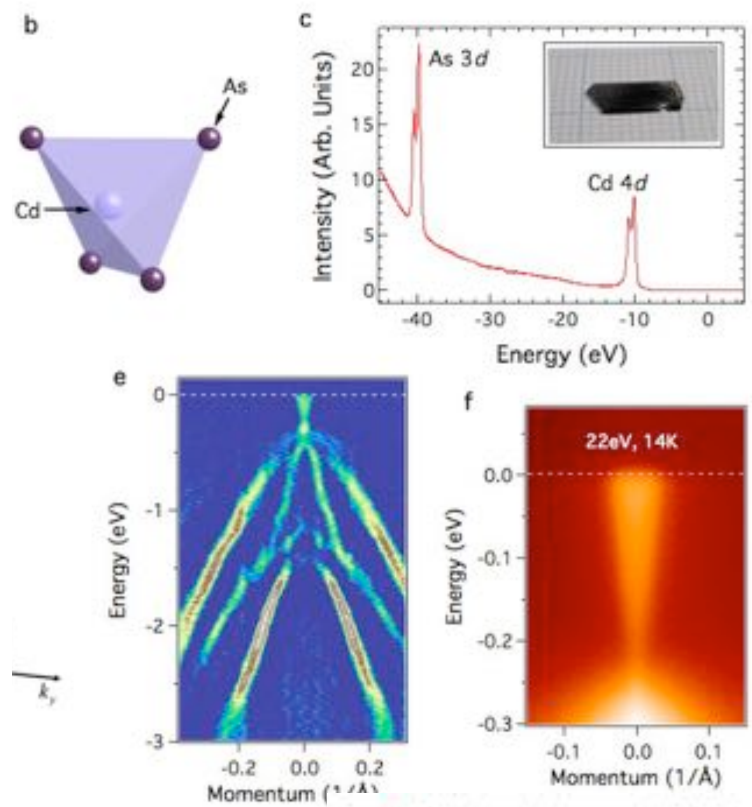

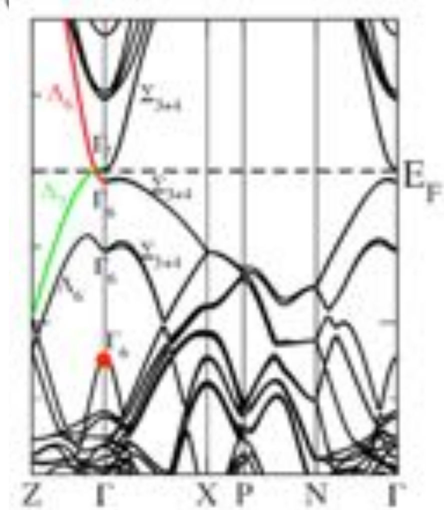

Arthur J. Rosenberg and Theodore C. Harman Journal of Applied Physics 30, 1621 (1959)
Wang, Z. J., Weng, H. M., Wu, Q. S., Dai, X. & Fang, Z., *Phys. Rev. B* 88, 125427 (2013).
Liu, Z. K. *et al*. *Nature Mater.* 13, 677-681 (2014).

Electronic structure

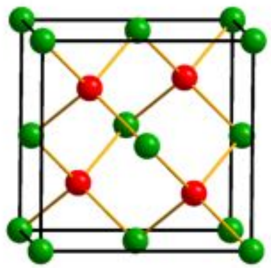

CdTe

HgTe

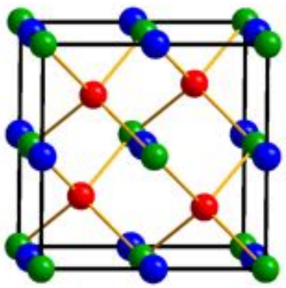

ScPtSb

ScPtBi

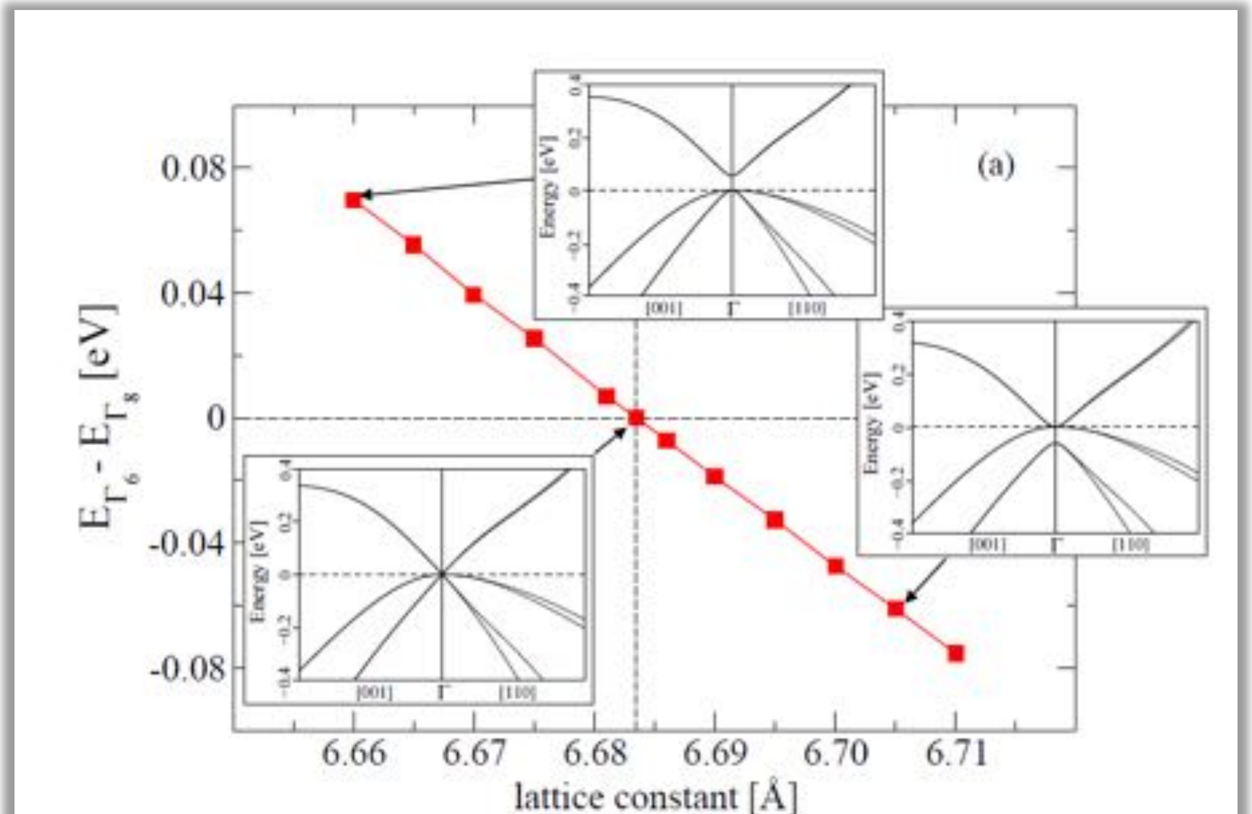

Chadov, Qi, Kübler, Zhang, Felser Nature Mat. 9 (2010) 541, arXiv:1003.0193

Application Spin Hall Effect

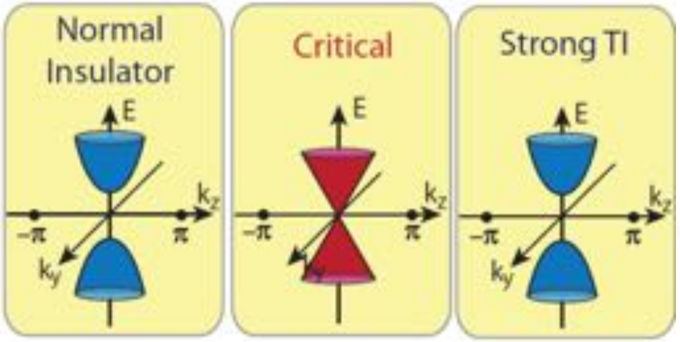

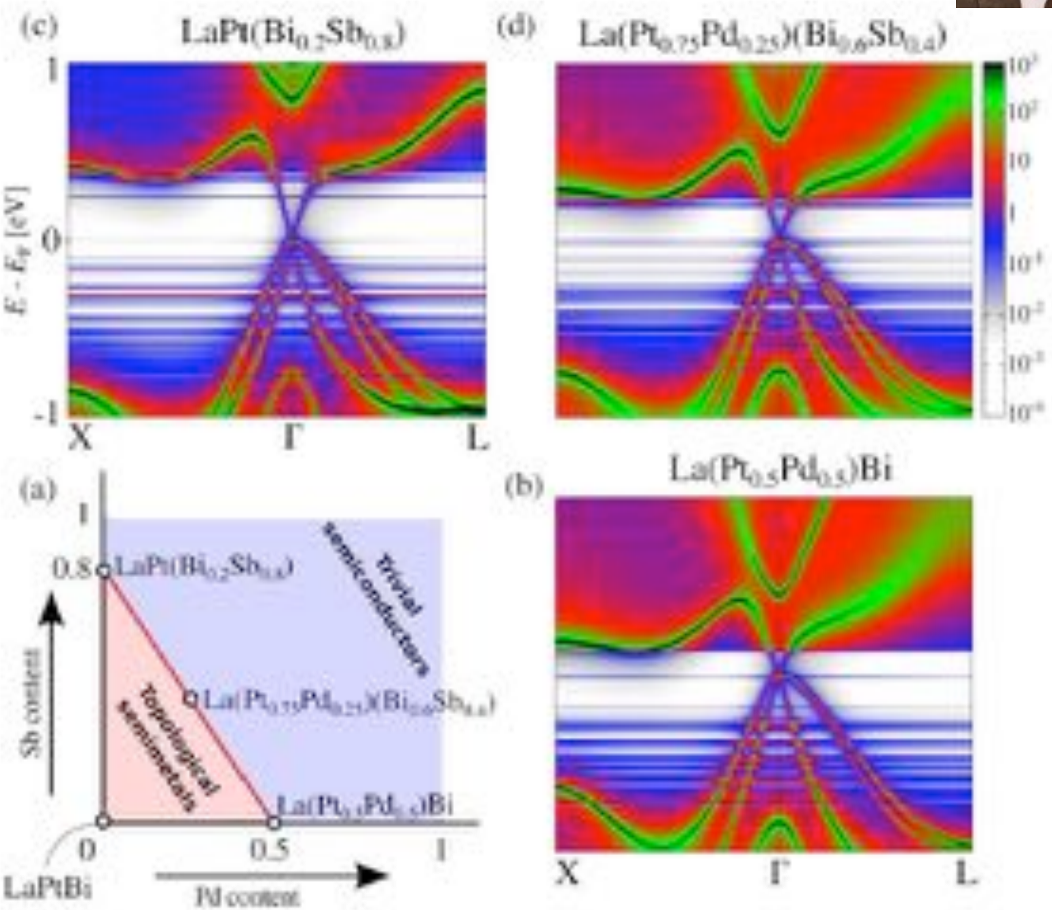

K. Chadova, et al., Phys. Rev. B 93 (2016) 195102 preprint: arXiv:1510.06935

Application Spin Hall Effect

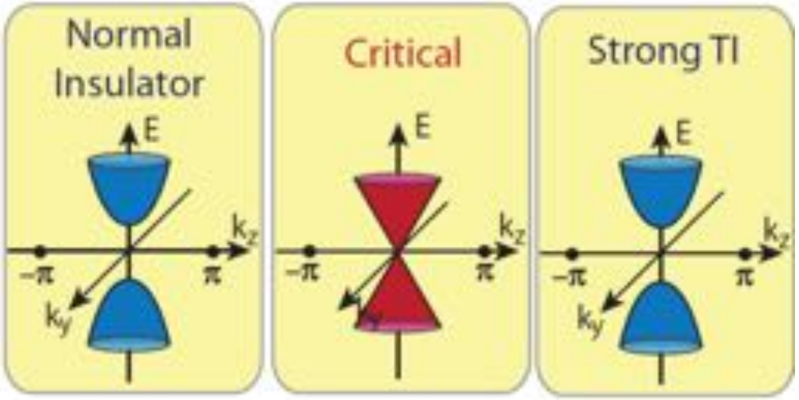

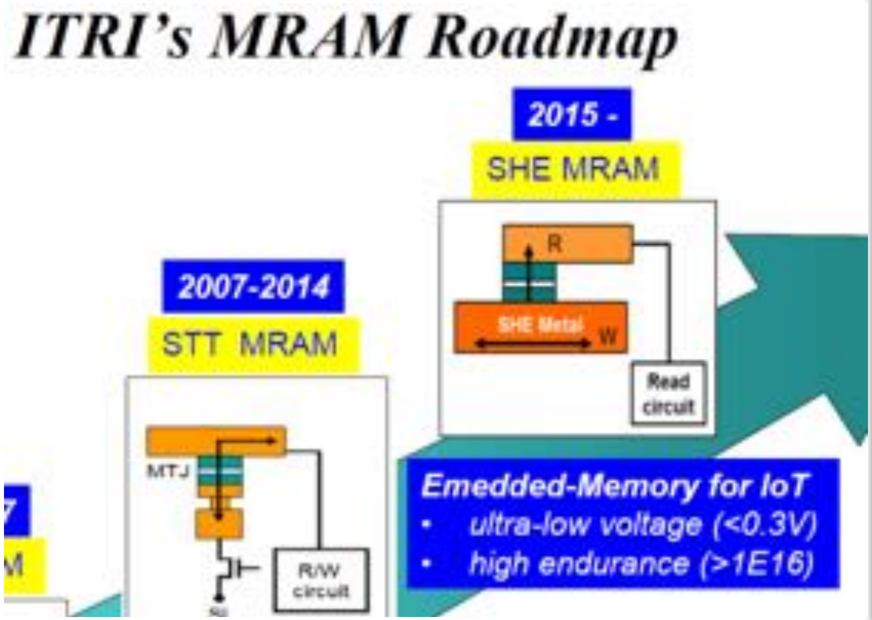

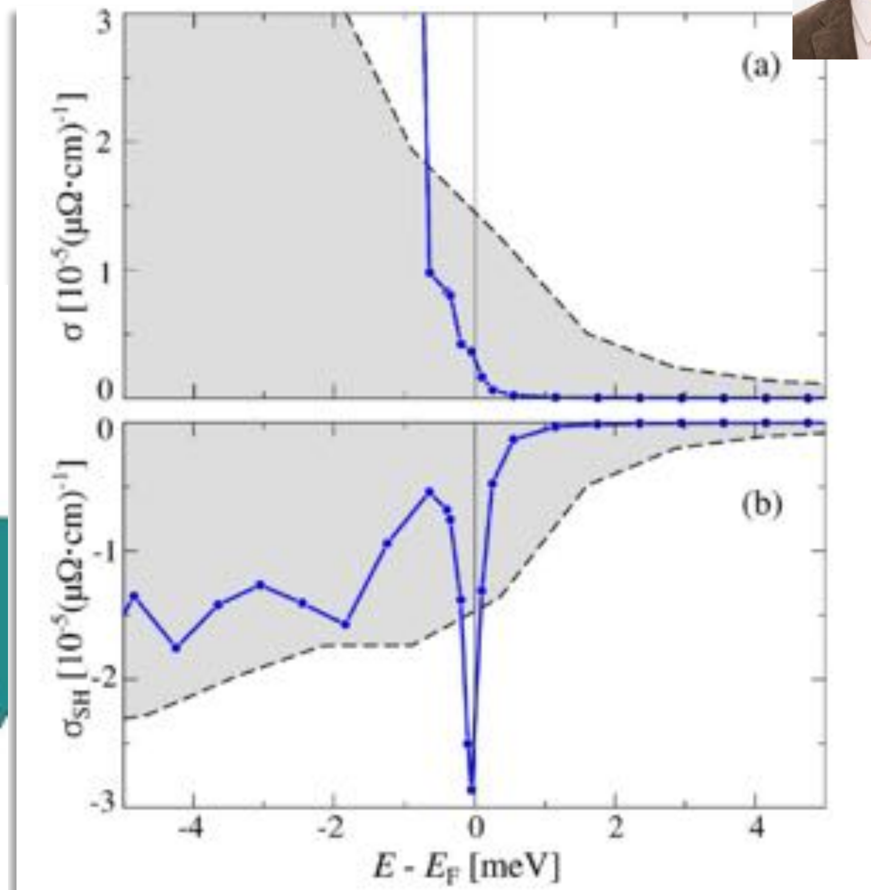

K. Chadova, et al., Phys. Rev. B 93 (2016) 195102 preprint: arXiv:1510.06935

The layered “Heusler”

Three-dimensional Critical Dirac semimetal in KMgBi

Congcong Le,[1,*] Shengshan Qin,[1,*] Xianxin Wu,[1] Xia Dai,[1] Peiyuan Fu,[1] and Jiangping Hu[1,2,†]

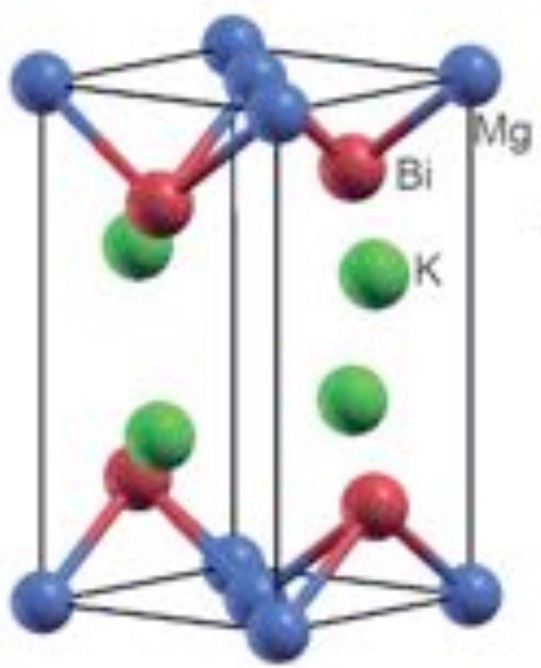

(a)

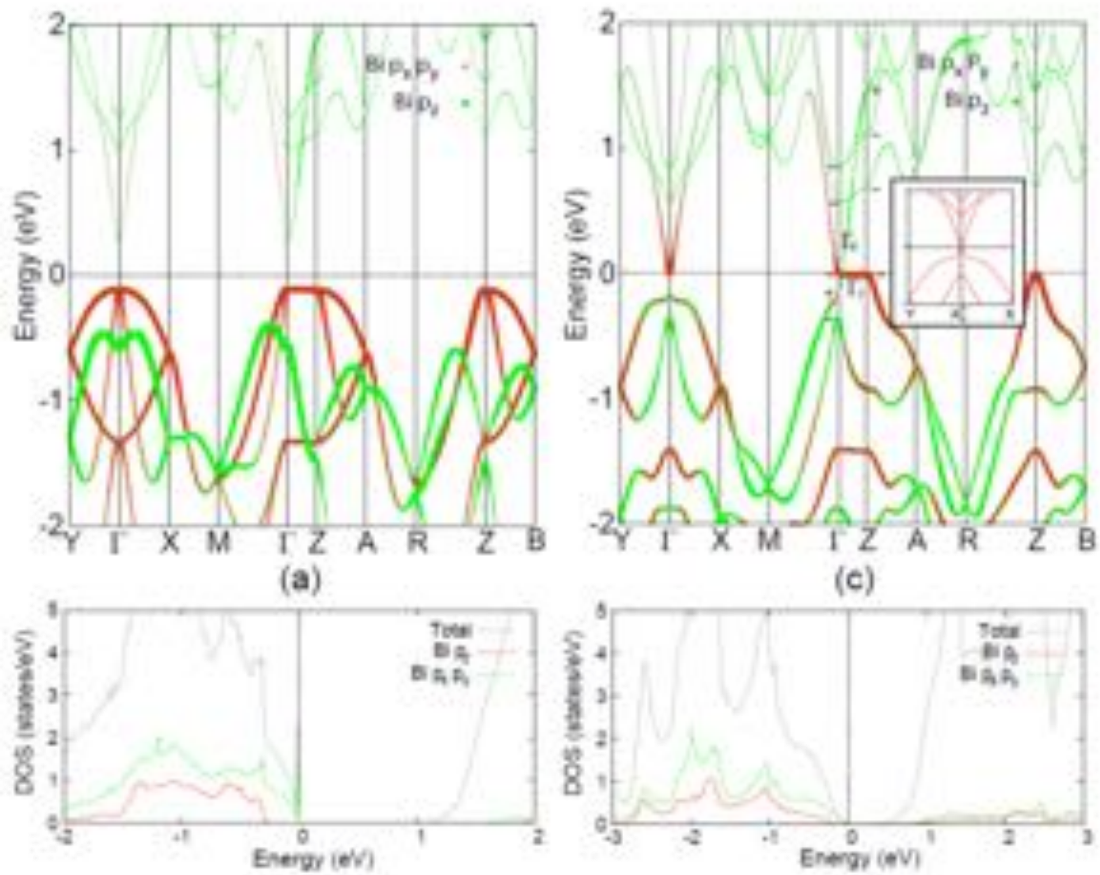

(a) (c)

(b) (d)

Weyl Semimetals

Breaking symmtery – NbP

Weyl Semimetal

- Breaking symmetry
  - Inversion symmetry (Structural distortion)
- Breaking time reversal symmetry
  - Magnetic field

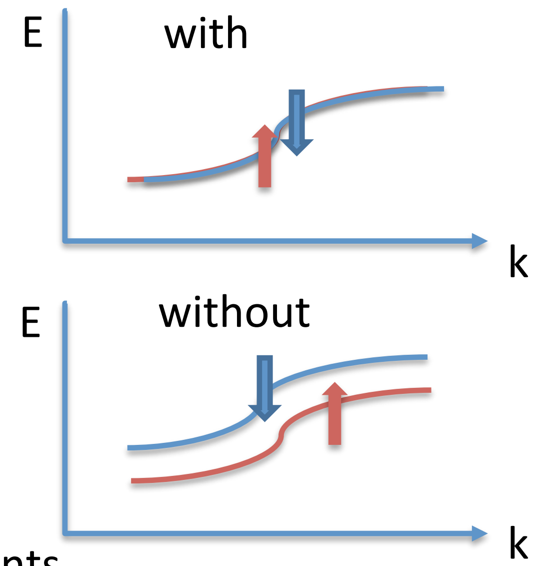

Dirac points are at high symmetry points

Weyl points are not at high symmetry points

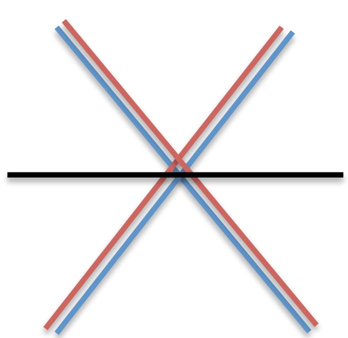

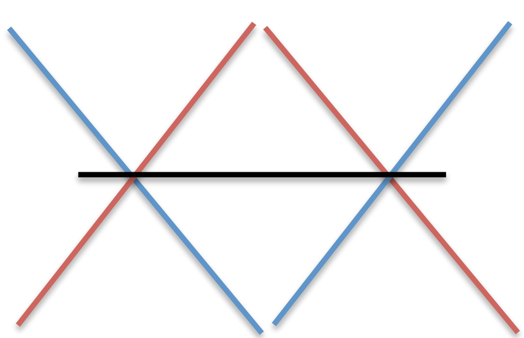

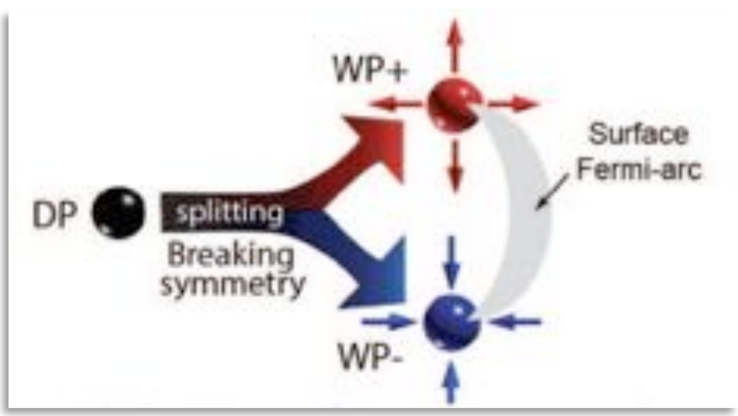

Weyl semimetals

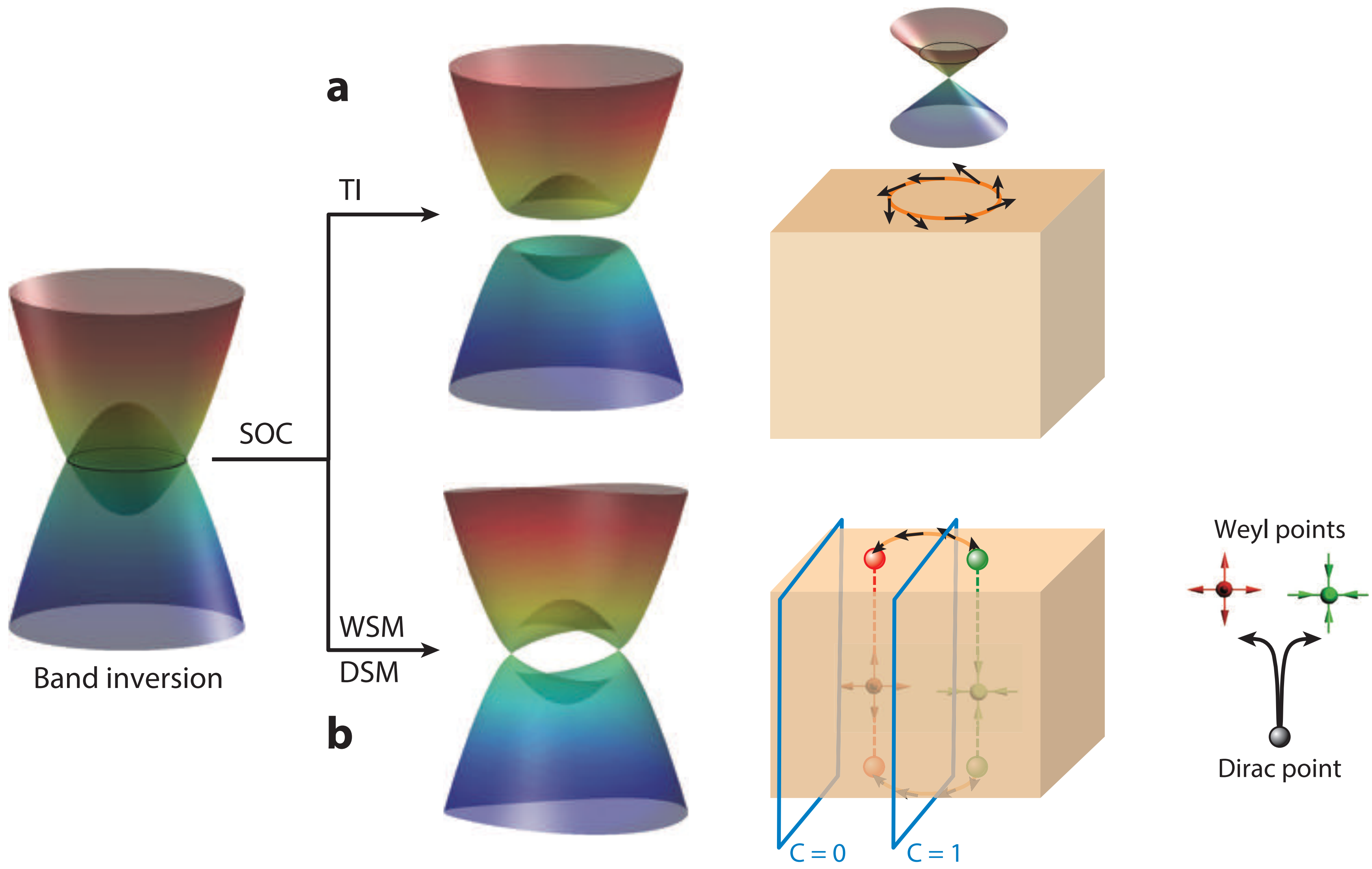

c

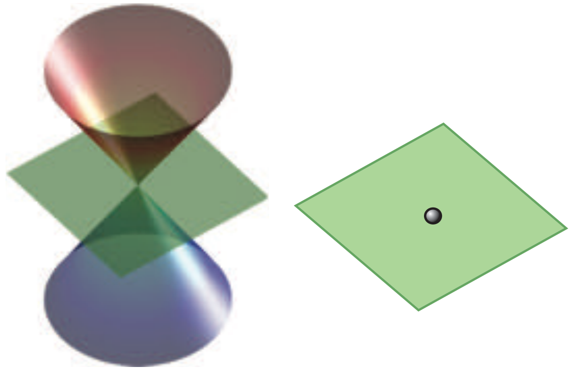

Type-I WSM

d

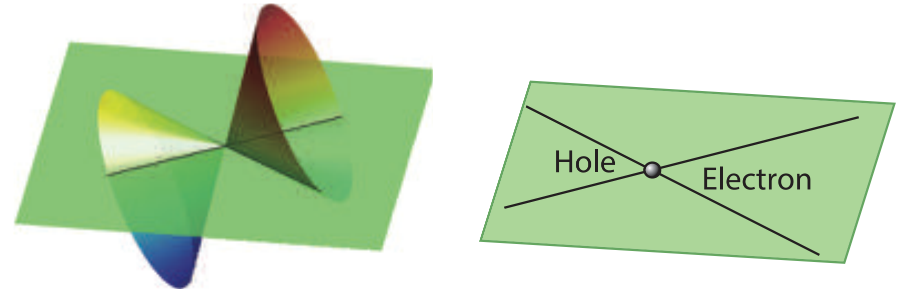

Type-II WSM

Alexey A. Soluyanov, et al., Nature 527, 495 (2005)

Graphene

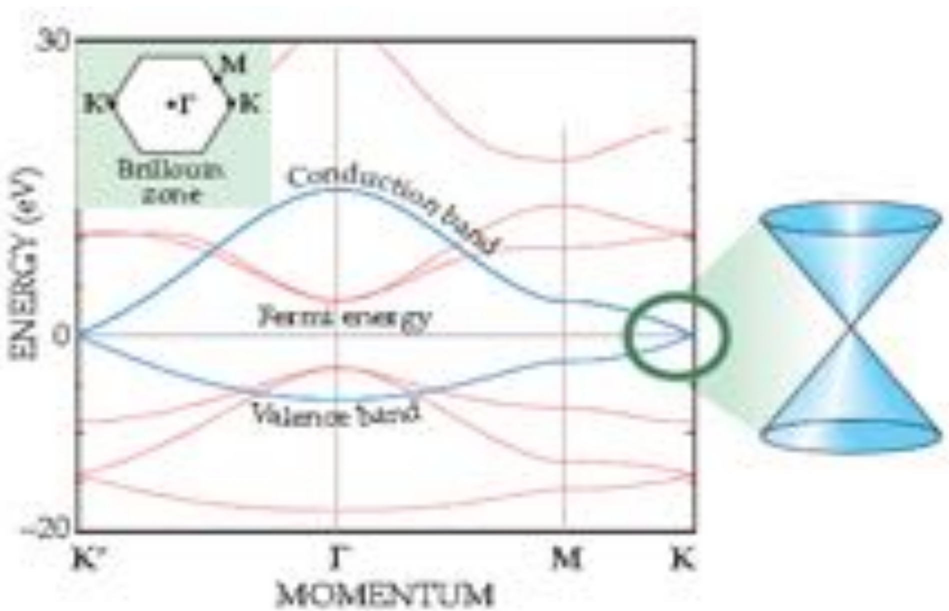

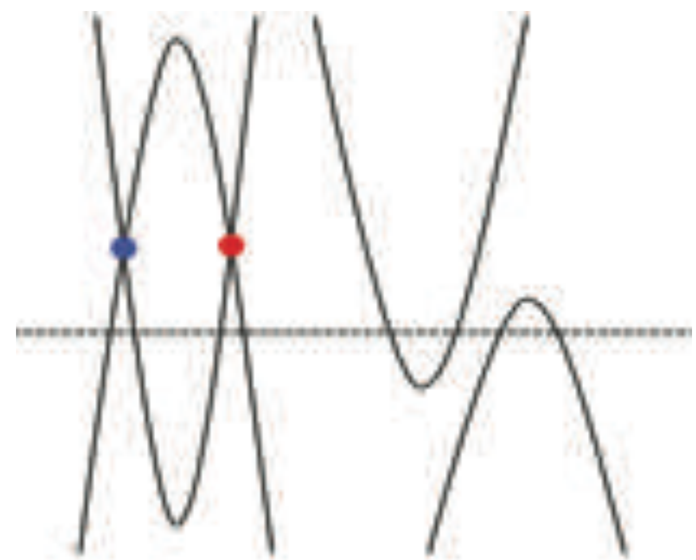

A. K. Geim, A. H. MacDonald Physics Today, 08.(2007), 35-41

Shekhar, et al. , Nature Physics 11 (2015) 645

Weyl semimetals

3D topological Weyl semimetals - breaking time reversal symmetry – in transport measurement
we should see:

1. Fermi arc

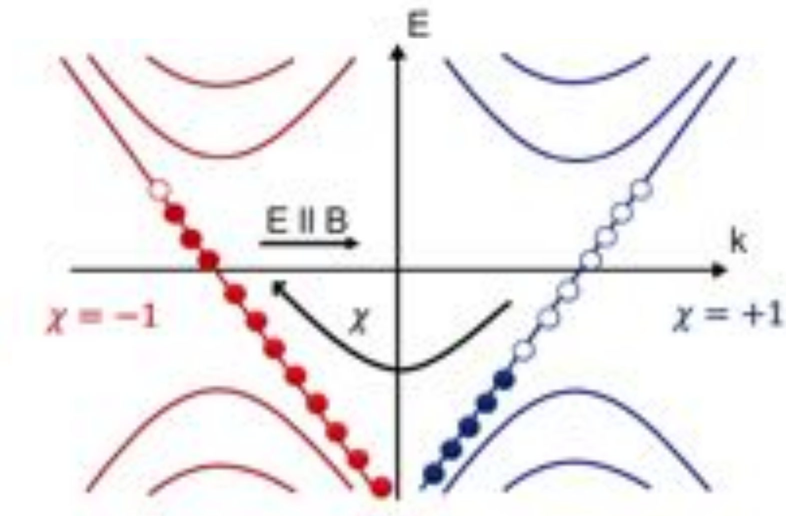

2. Chiral anomaly

$$\partial_\mu j^\mu_\chi = \boxed{-}\chi \frac{e^3}{4\pi^2\hbar^2} \boldsymbol{E}\cdot\boldsymbol{B}$$

$$\sigma_a = \frac{e^3 v_f^3}{4\pi^2\hbar\mu^2 c}\boxed{B^2},$$

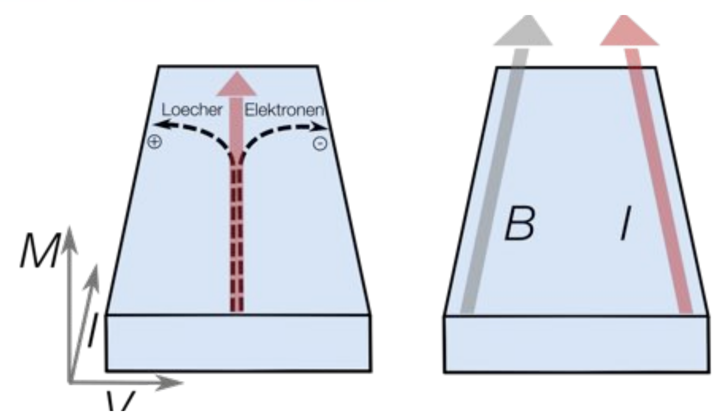

S. L. Adler, Phys. Rev. 177, 2426 (1969)
J. S. Bell and R. Jackiw, Nuovo Cim. A60, 47 (1969)
AA Zyuzin, AA Burkov - Physical Review B (2012)
AA Burkov, L Balents, PRL 107 12720 (2012)

Violation of chiral symmetry.

In Quantum Electro Dynamics (relativistic quantum field theory) chiral charge conservation can be violated for massless fermions!

Pion decay:

Neutral Pion

Photon

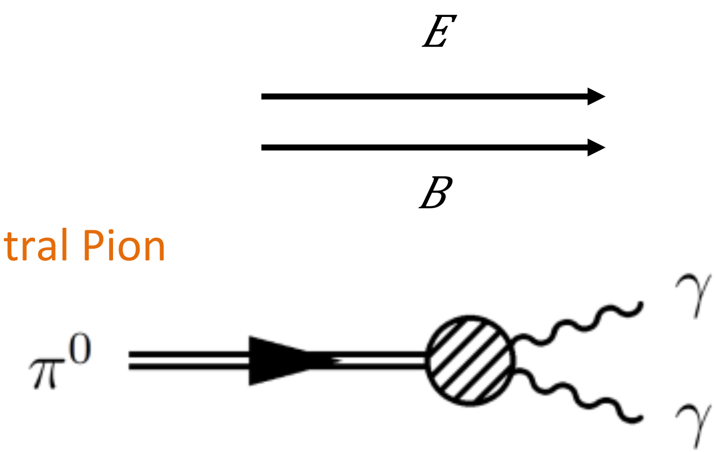

Photon

Electric charge: 0	0		
Spin: half-integer	integer	⇒	Chiral anomaly

Adler, S. L. *Phys. Rev.* **177,** 5 (1969).
Bell, J. S. & Jackiw, R. *Nuovo Cim.* **A60,** 4 (1969)

Weyl semimetals in non-centro NbP

NbP, NbAs,
TaP, TaAs

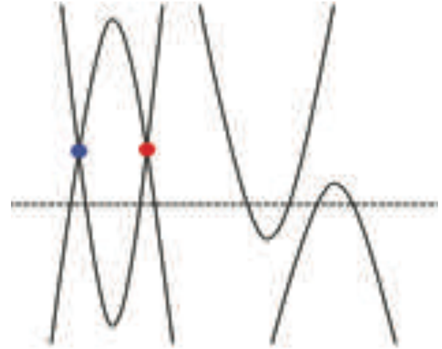

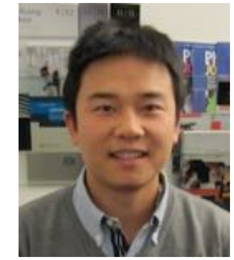

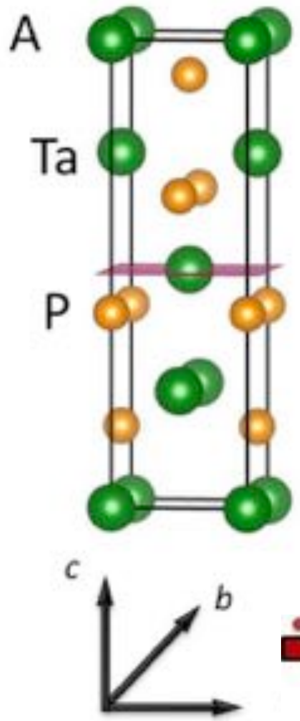

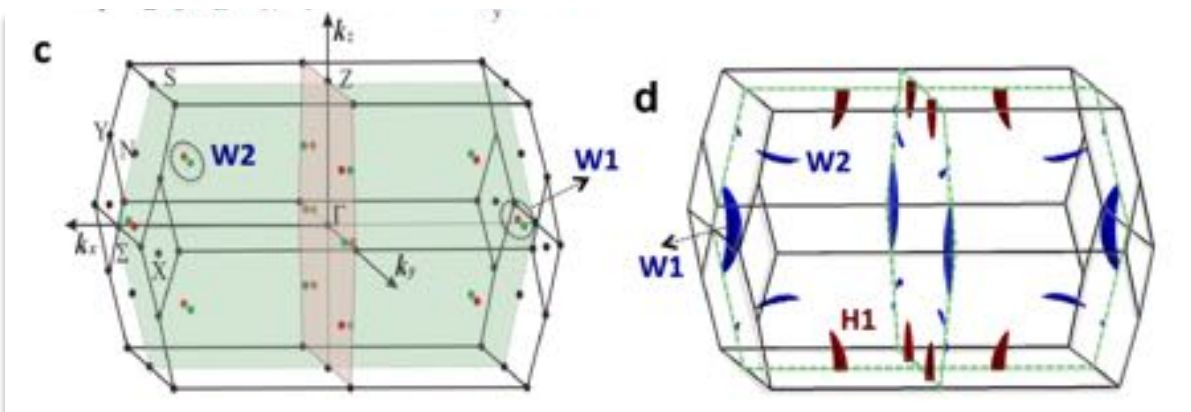

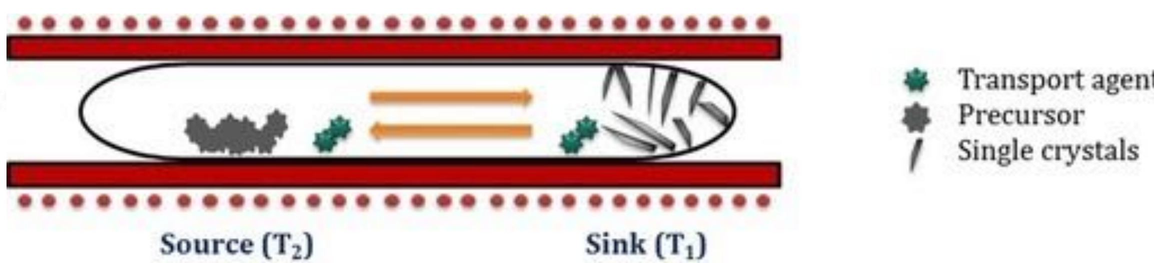

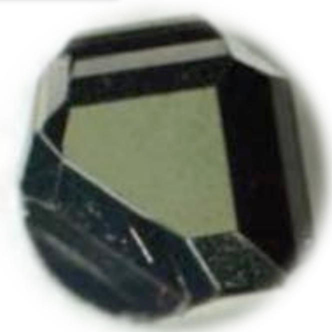

Shekhar, et al. , Nature Physics 11 (2015) 645,
Frank Arnold, et al. Nature Communication 7 (2016) 11615

Weng, et al. Phys. Rev. X 5, 11029 (2015)
Huang et al. preprint arXiv:1501.00755

NbP, TaP, TaAs

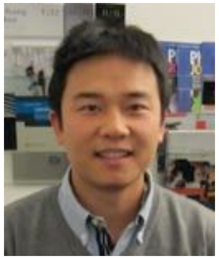

Increasing spin orbit coupling increases – heavier elements
Distance between the Weyl points increases

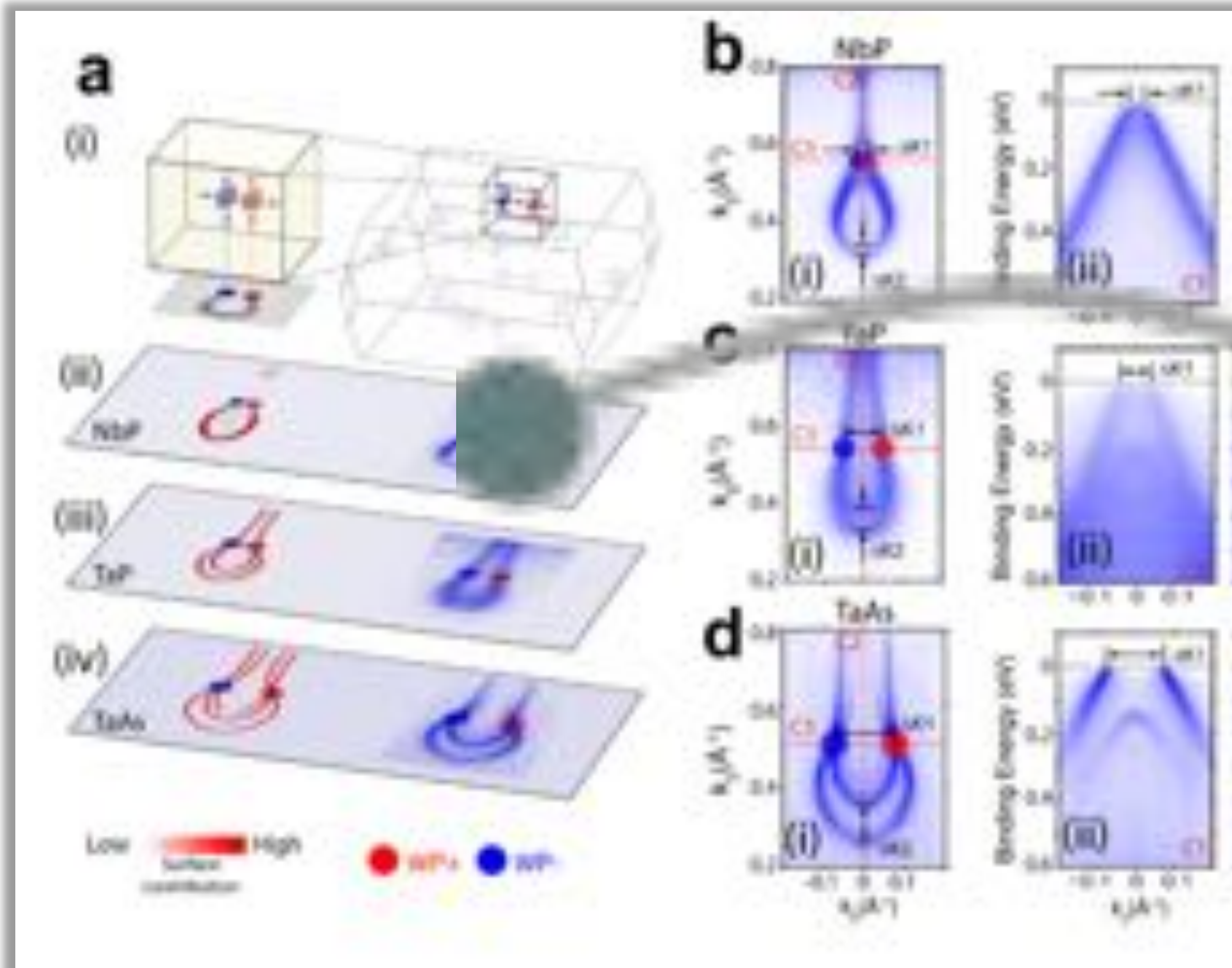

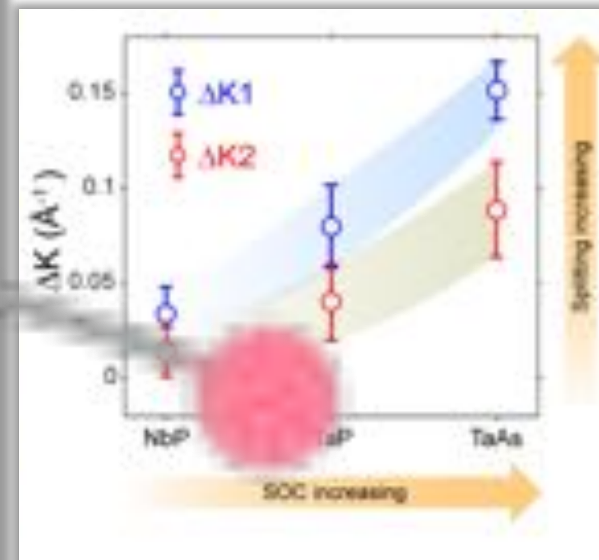

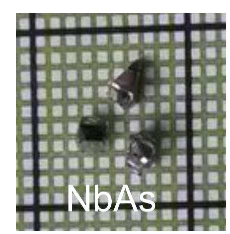

Z. K. Liu et al., Nature Mat. 15 (2016) 27
Yang, et al. Nature Phys. 11 (2015) 728

Resistance Measurement

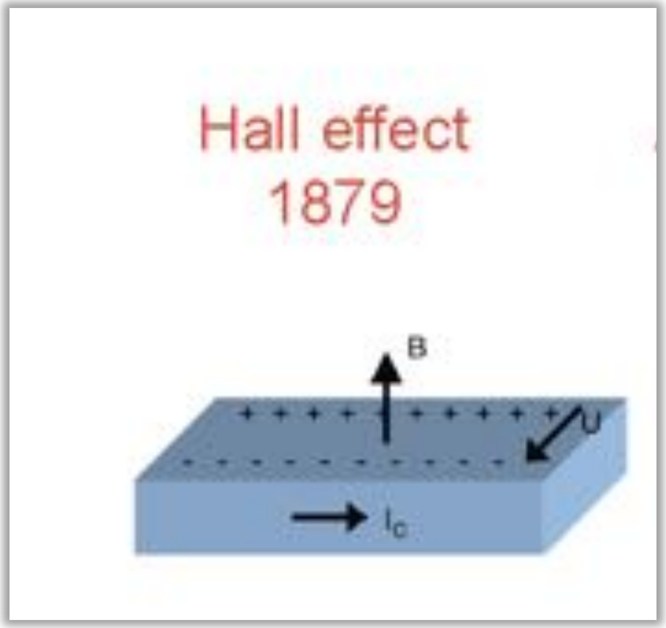

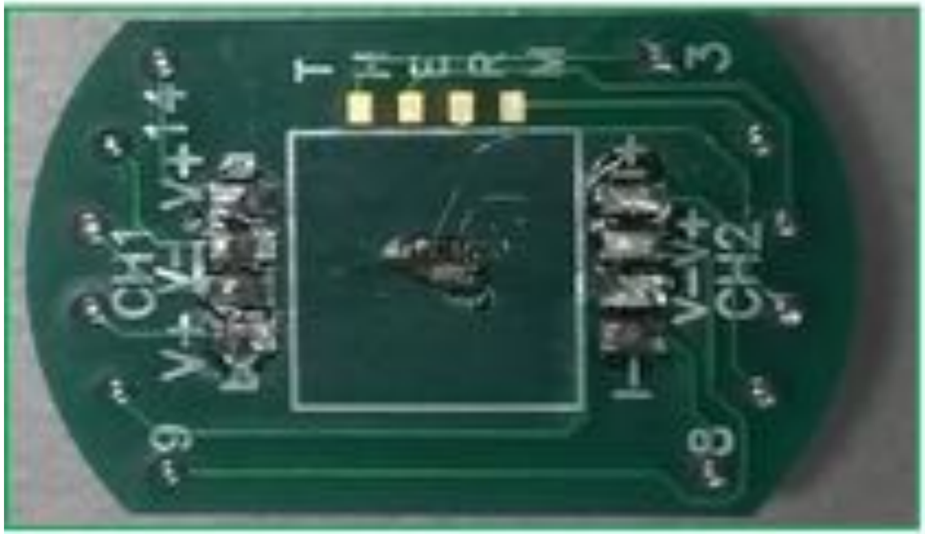

We measure the resistance without and with a magnetic field

- Metal, semiconductor, or insulator
- Electron or hole conductivity
- Resistance in a magnetic field: Magnetoresistance

Weyl Points in non-centro NbP

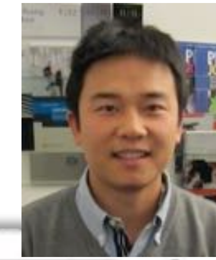

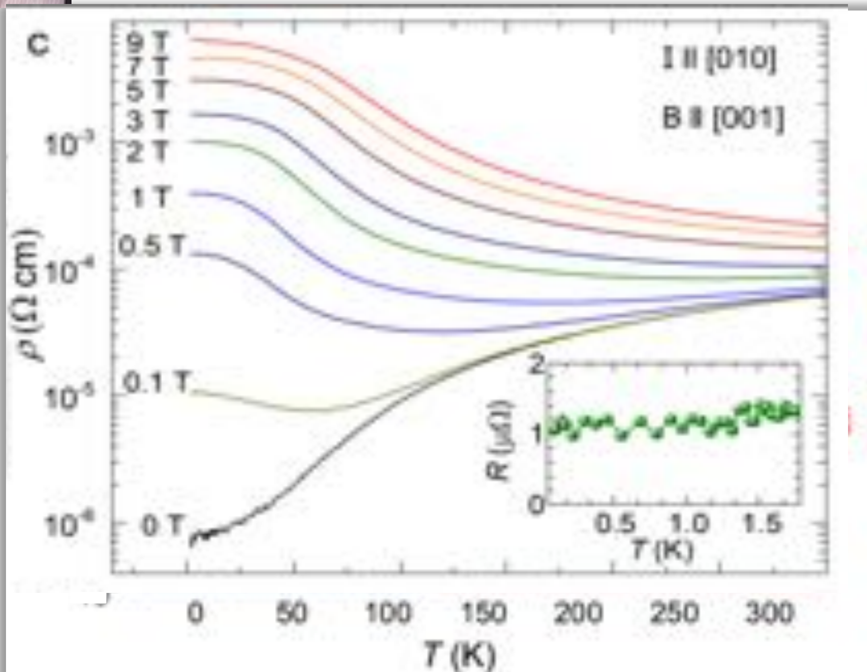

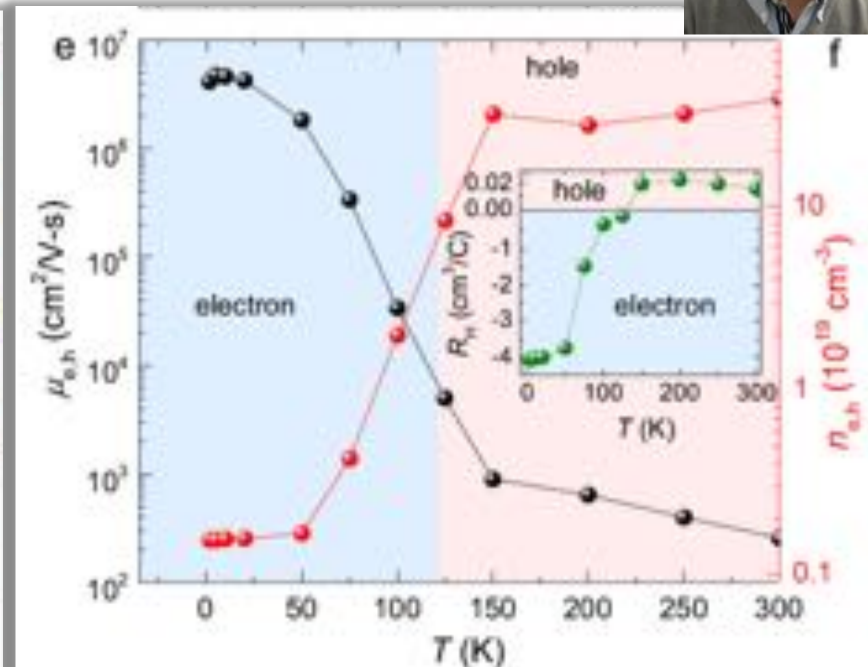

NbP is a topological Weyl semimetal

- with massless relativistic electrons
- extremely large magnetoresistance of **850,000%** at 1.85 K, 9T (250% at room temperature)
- an ultrahigh carrier mobility of **$5*10^6$ cm^2 / V s**

Shekhar, et al. , Nature Physics 11 (2015) 645,
Frank Arnold, et al. Nature Communication 7 (2016) 11615

Weng, et al. Phys. Rev. X 5, 11029 (2015)
Huang . et al. preprint arXiv:1501.00755

TaP Quantum Oscillations

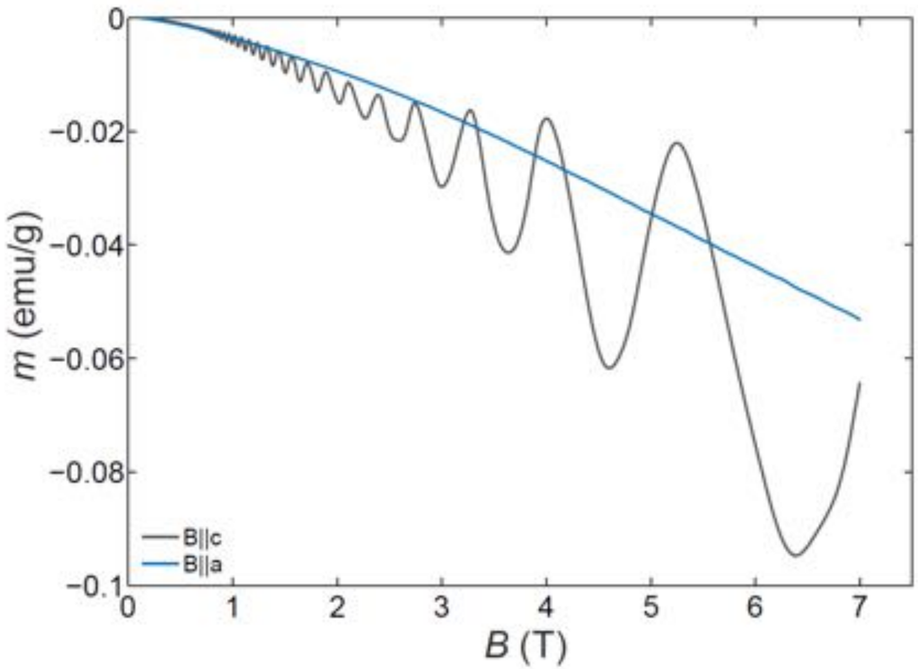

SQUID-VSM magnetization

- In c-direction the diamagnetic magnetization is superimposed by quantum oscillations starting at 0.6 T
- In a-direction only weak quantum oscillations are visible
- The frequency proportional to the extremal Fermi surface perpendicular to ***B***

NbP and the Fermi surface

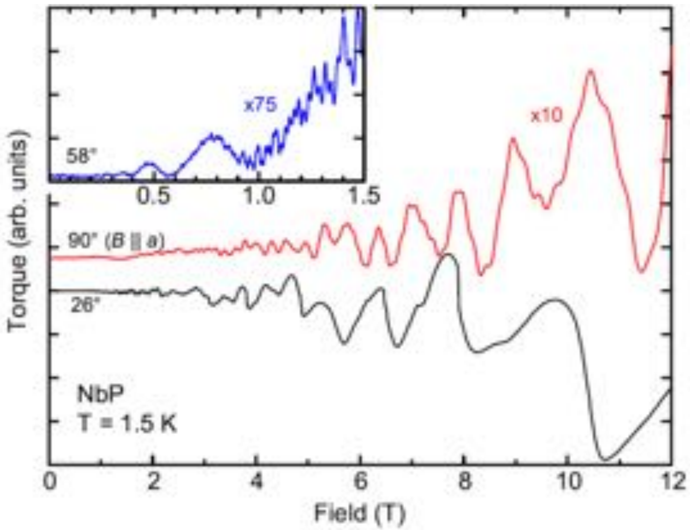

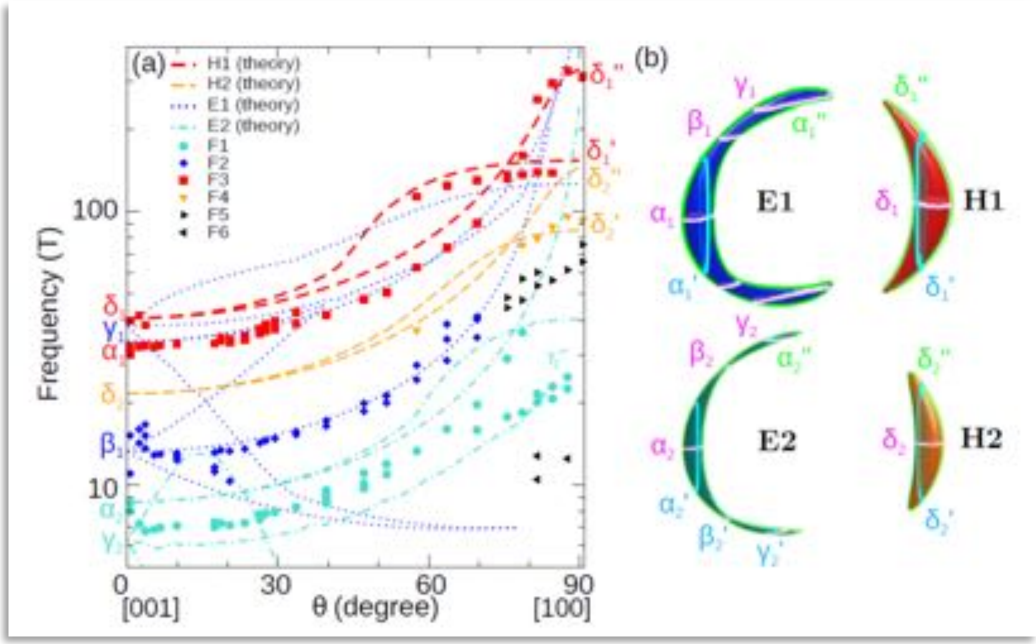

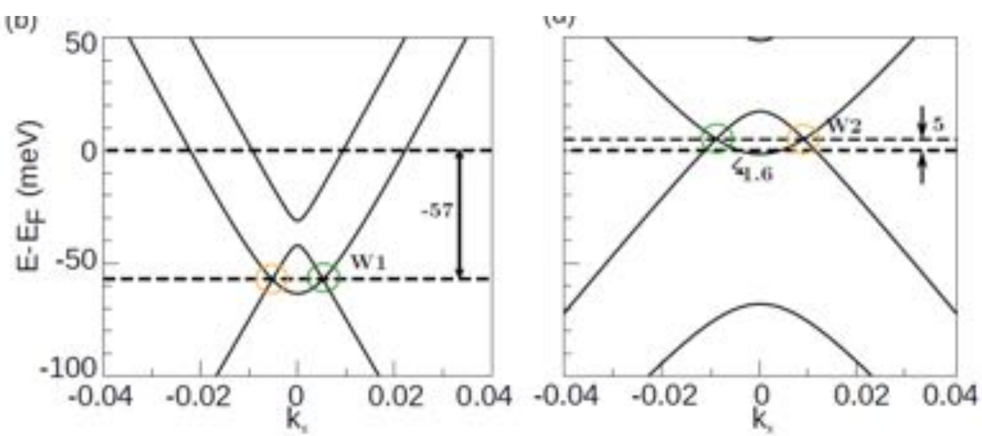

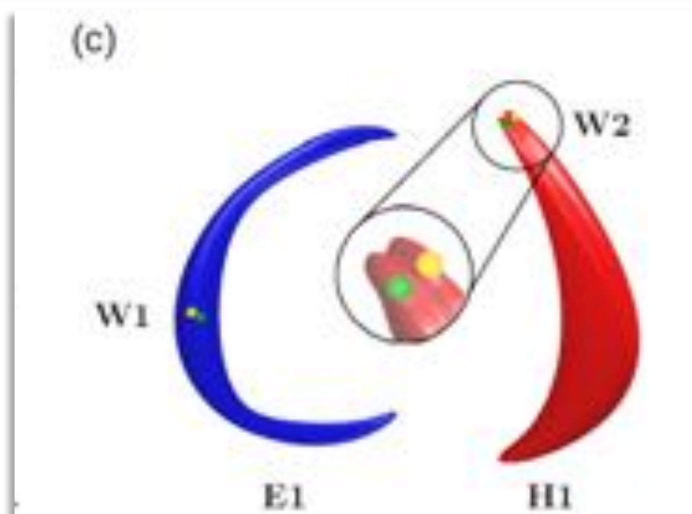

Klotz et al. Phys. Rev. Lett. 2016

Chiral Anomaly

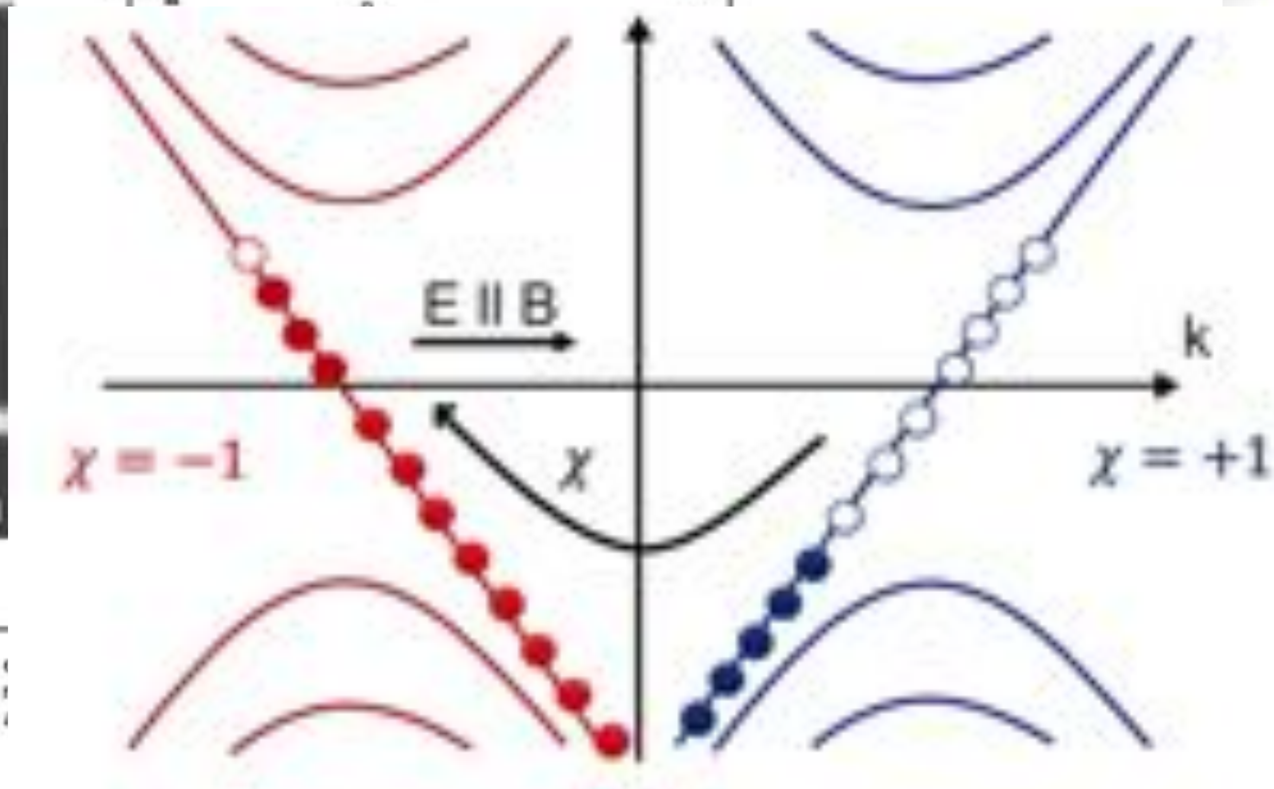

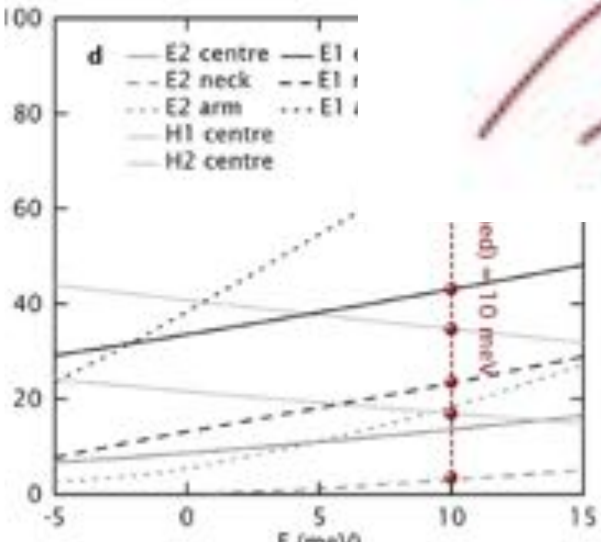

Ga-doping relocate the Fermi energy in NbP close to the W2 Weyl points
Therefore we observe a negative MR as a signature of the chiral anomaly the, NMR survives up to room temperature

Anna Corinna Niemann, Johannes Gooth et al. Scientific Reports 7 (2017) 43394 doi:10.1038/srep4339 preprint arXiv:1610.01413

Chiral Anomaly

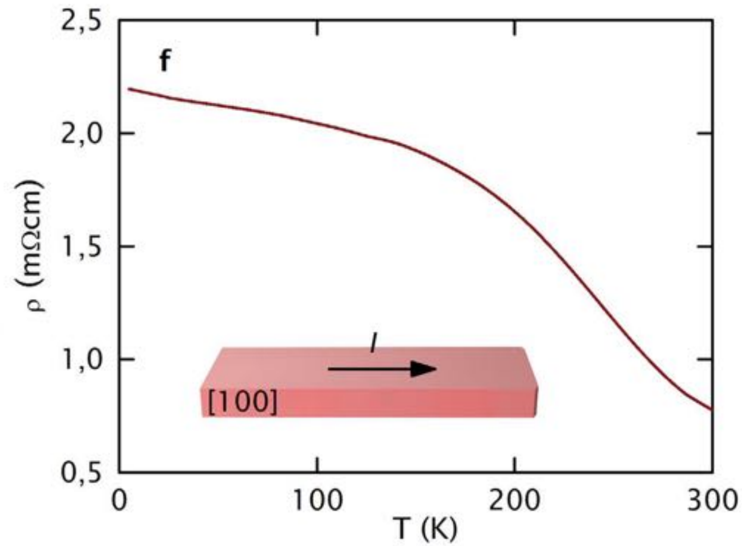

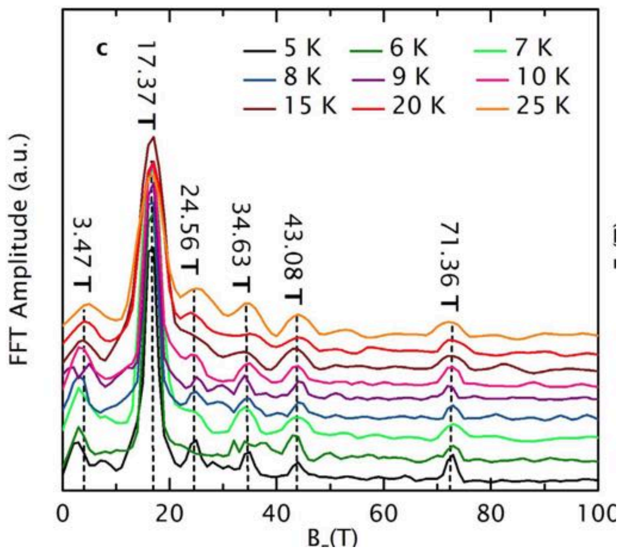

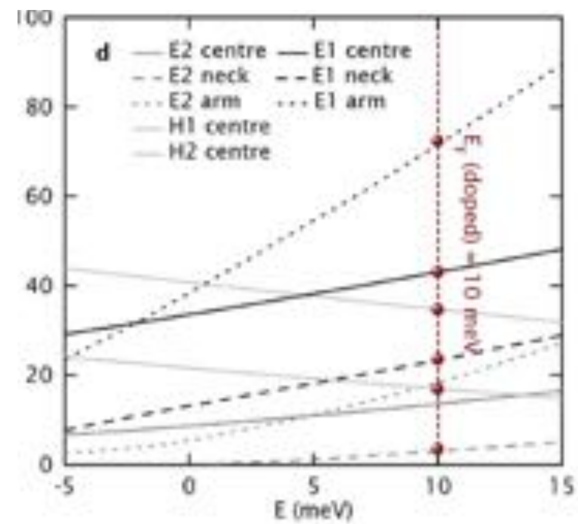

Ga-doping relocate the Fermi energy in NbP close to the W2 Weyl points

Anna Corinna Niemann, Johannes Gooth et al. Scientific Reports 7 (2017) 43394 doi:10.1038/srep4339 preprint arXiv:1610.01413

Longitudinal magneto-transport – E||B

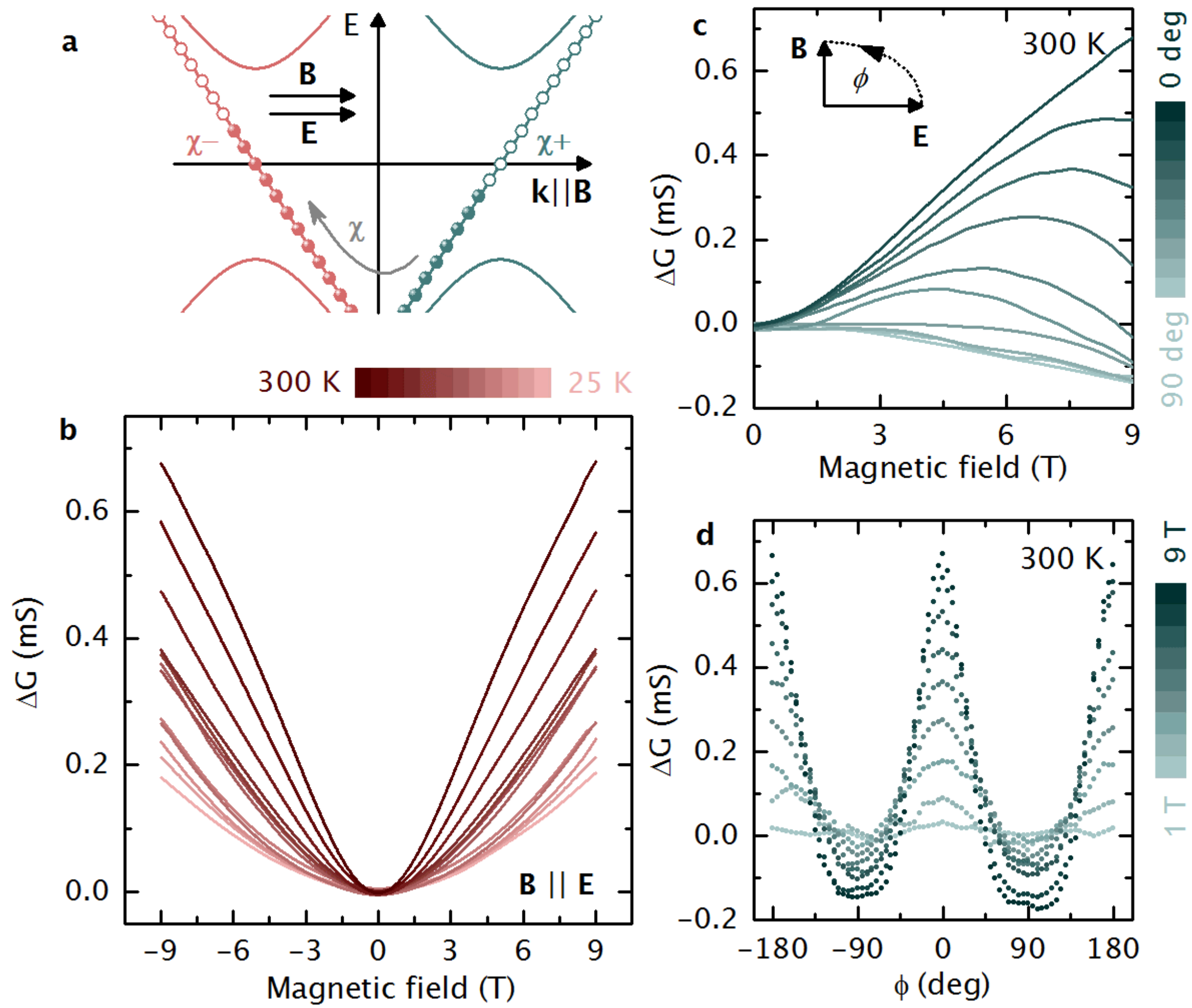

The PMC is locked to E||B, as expected for Chiral anomaly.

[Shekhar, C. et al. Nat. Phys. 11, 3372 (2015)]

Experimental signatures for the mixed axial-gravitational anomaly in Weyl semimetals

- In solid state physics, mixed axial-gravitational anomaly can be identified by a positive magneto-thermoelectric conductance (PMTG) for $\Delta T \parallel B$.

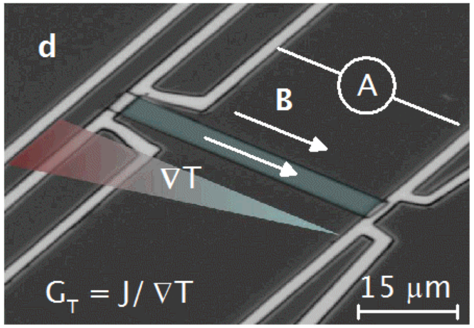

- Low fields: quadratic

$$G_T = d_{\mathrm{th}} + c_2 a_\chi a_g B_{\|}^2$$

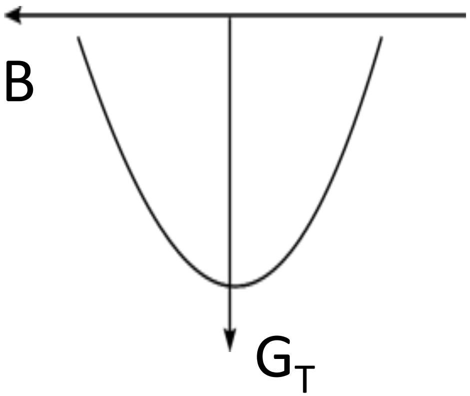

- High fields: deminishes

- $\Delta T \parallel B$ dictates sensitivity on alignement of B and ΔT.

[Lucas, *et al. Proceedings of the National Academy of Sciences* **113,** 9463 (2016)]

Gravitational Anomaly

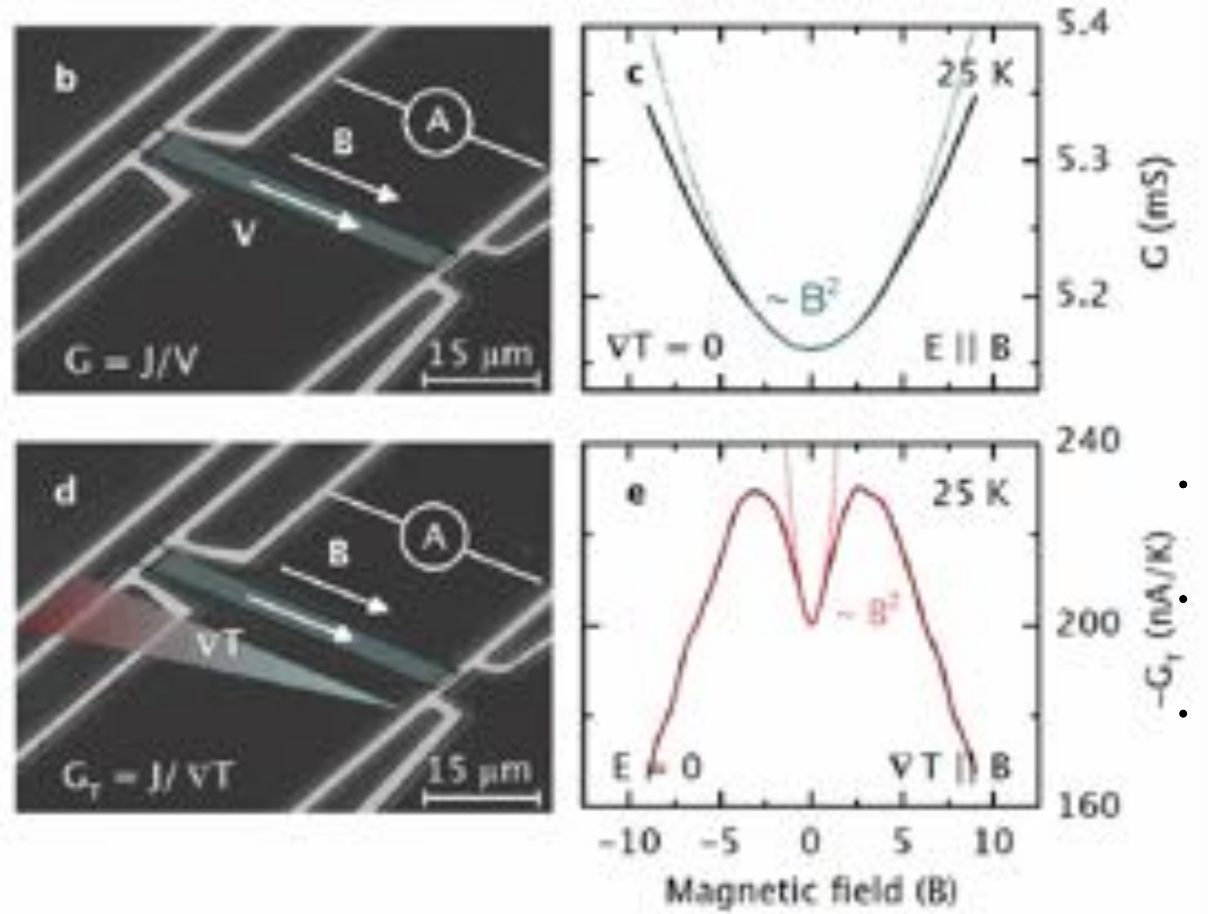

- Landsteiner, et al. Gravitational anomaly and transport phenomena. Phys. Rev. Lett. 107, 021601 (2011). URL
- Jensen, et al. Thermodynamics, gravitational anomalies and cones. Journal of High Energy Physics 2013, 88 (2013).
- Lucas, A., Davison, R. A. & Sachdev, S. Hydrodynamic theory of thermoelectric transport and negative magnetoresistance in weyl semimetals. PNAS 113, 9463–9468 (2016).

A positive longitudinal magneto-thermoelectric conductance (PMTC) in the Weyl semimetal NbP for collinear temperature gradients and magnetic fields that vanishes in the ultra quantum limit.

Johannes Gooth et al. Experimental signatures of the gravitational anomaly in the Weyl semimetal NbP, Nature accepted arXiv:1703.10682

Gravitational Anomaly

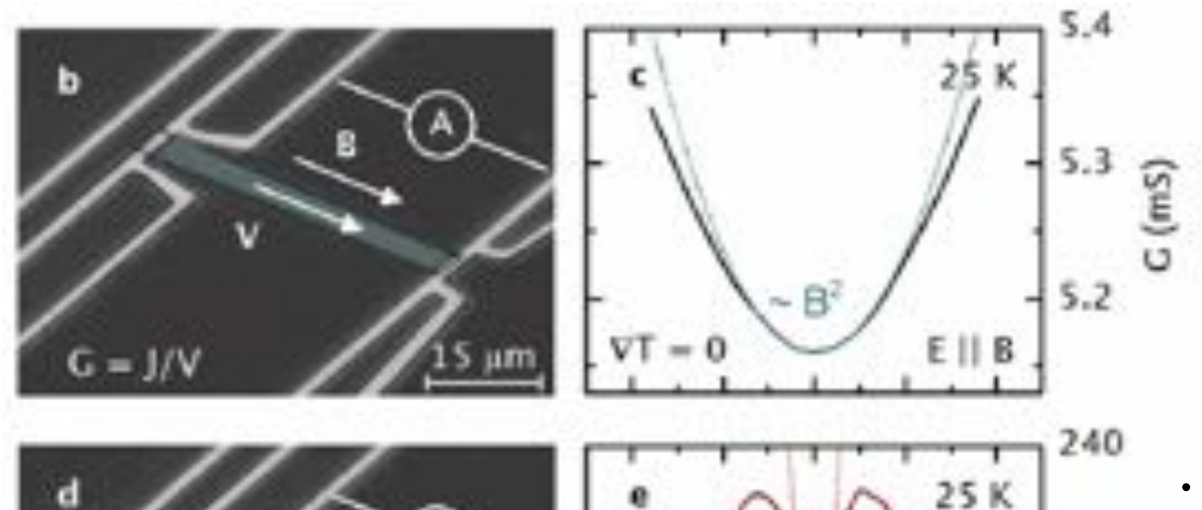

- Landsteiner, et al. Gravitational anomaly and

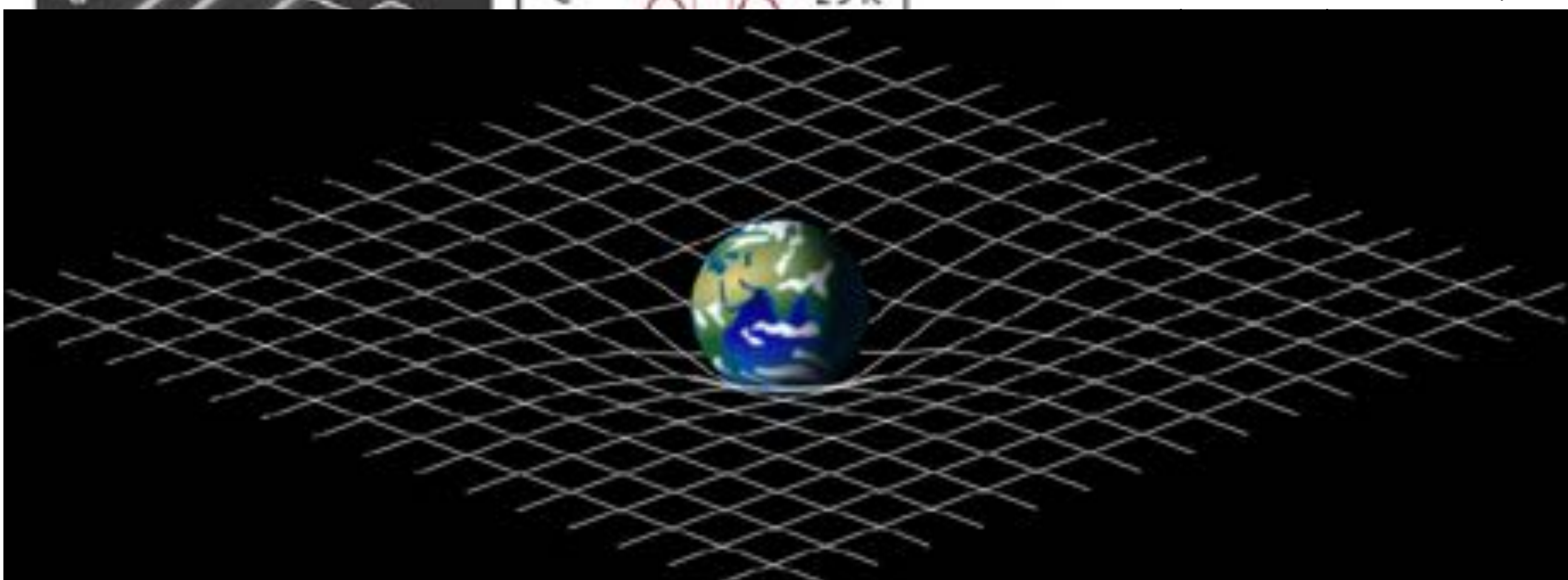

rt

Hydrodynamics

PHYSICS

Electrons go with the flow in exotic material systems

Electronic hydrodynamic flow—making electrons flow like a fluid—has been observed

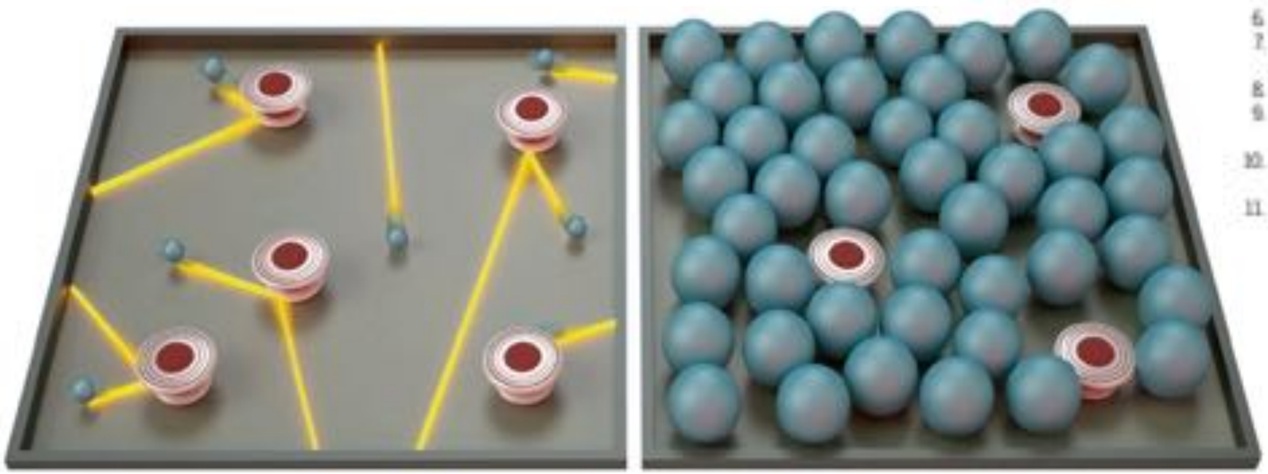

REFERENCES

1. J. Crossno, J. K. Shi, K. Wang, X. Liu, A. Harzheim, A. Lucas, S. Sachdev, P. Kim, T. Taniguchi, K. Watanabe, T. A. Ohki, K. C. Fong, Science **351**, 1058 (2016).
2. D. A. Bandurin, I. Torre, R. Krishna Kumar, M. Ben Shalom, A. Tomadin, A. Principi, G. H. Auton, E. Khestanova, K. S. Novoselov, I. V. Grigorieva, L. A. Ponomarenko, A. K. Geim, M. Polini, Science **351**, 1055 (2016).
3. P. J. W. Moll et al., Science **351**, 1061 (2016).
4. J. Zaanen, Y.-W. Sun, Y. Liu, K. Schalm, *Holographic Duality in Condensed Matter Physics* (Cambridge Univ. Press, 2015).
5. S. A. Hartnoll, P. K. Kovtun, M. Mueller, S. Sachdev, *Phys. Rev. B* **76**, 144502 (2007).
6. A. H. Castro Neto et al., *Rev. Mod. Phys.* **81**, 109 (2009).
7. M. Mueller, J. Schmalian, L. Fritz, *Phys. Rev. Lett.* **103**, 025301 (2009).
8. M. S. Foster, I. L. Aleiner, *Phys. Rev. B* **79**, 085415 (2009).
9. A. Lucas, J. Crossno, K. C. Fong, P. Kim, S. Sachdev, http://arxiv.org/abs/1510.01738 (2015).
10. L. Levitov, G. Falkovich, http://arxiv.org/abs/1508.00836 (2015).
11. M. J. M. de Jong, L. W. Molenkamp, *Phys. Rev. B* **51**, 13389 (1995).

- Hydrodynamic electron fluid is defined by momentum-conserving electron-electron scattering
- Violation of Wiedeman-Franz law
- Viscosity-induced shear forces making the electrical resistivity a function of the channel width

Hydrodynamics

Evidence for hydrodynamic electron flow in $PdCoO_2$

Philip J. W. Moll,[1,2,3] Pallavi Kushwaha,[3] Nabhanila Nandi,[3] Burkhard Schmidt,[3] Andrew P. Mackenzie[3,4*]

Experimental evidence that the resistance of restricted channels of the ultra-pure two-dimensional metal PdCoO2 has a large viscous contribution

Negative local resistance caused by viscous electron backflow in graphene

D. A. Bandurin,[1] I. Torre,[2] R. Krishna Kumar,[1,3] M. Ben Shalom,[1,4] A. Tomadin,[5] A. Principi,[6] G. H. Auton,[4] E. Khestanova,[1,4] K. S. Novoselov,[4] I. V. Grigorieva,[1] L. A. Ponomarenko,[1,3] A. K. Geim,[1*] M. Polini[7*]

ELECTRON TRANSPORT

Observation of the Dirac fluid and the breakdown of the Wiedemann-Franz law in graphene

Jesse Crossno,[1,2] Jing K. Shi,[1] Ke Wang,[1] Xiaomeng Liu,[1] Achim Harzheim,[1] Andrew Lucas,[1] Subir Sachdev,[1,3] Philip Kim,[1,2*] Takashi Taniguchi,[4] Kenji Watanabe,[4] Thomas A. Ohki,[5] Kin Chung Fong[5*]

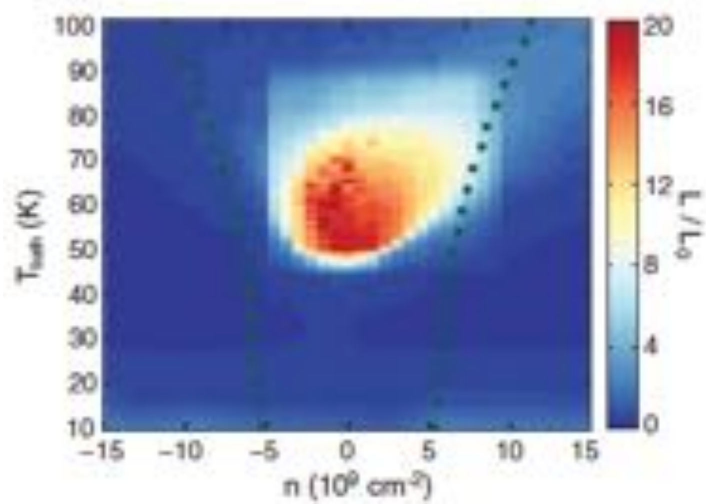

High mobility wires

PHYSICAL REVIEW B VOLUME 51, NUMBER 19 15 MAY 1995-I

Hydrodynamic electron flow in high-mobility wires

M. J. M. de Jong* and L. W. Molenkamp†
Philips Research Laboratories, 5656 AA Eindhoven, The Netherlands
(Received 24 October 1994)

Hydrodynamic electron flow is experimentally observed in the differential resistance of electrostatically defined wires in the two-dimensional electron gas in (Al,Ga)As heterostructures. In these experiments current heating is used to induce a controlled increase in the number of electron-electron collisions in the wire. The interplay between the partly diffusive wire-boundary scattering and the electron-electron scattering leads first to an increase and then to a decrease of the resistance of the wire with increasing current. These effects are the electronic analog of Knudsen and Poiseuille flow in gas transport, respectively. The electron flow is studied theoretically through a Boltzmann transport equation, which includes impurity, electron-electron, and boundary scattering. A solution is obtained for arbitrary scattering parameters. By calculation of flow profiles inside the wire it is demonstrated how normal flow evolves into Poiseuille flow. The boundary-scattering parameters for the gate-defined wires can be deduced from the magnitude of the Knudsen effect. Good agreement between experiment and theory is obtained.

A Better Weyl Semimetals

WP_2 protected Weyl

PRL 117, 066402 (2016) PHYSICAL REVIEW LETTERS week ending 5 AUGUST 2016

Robust Type-II Weyl Semimetal Phase in Transition Metal Diphosphides XP_2 ($X = $ Mo, W)

G. Autès,[1,2] D. Gresch,[3] M. Troyer,[3] A. A. Soluyanov,[3,4] and O. V. Yazyev[1,2]

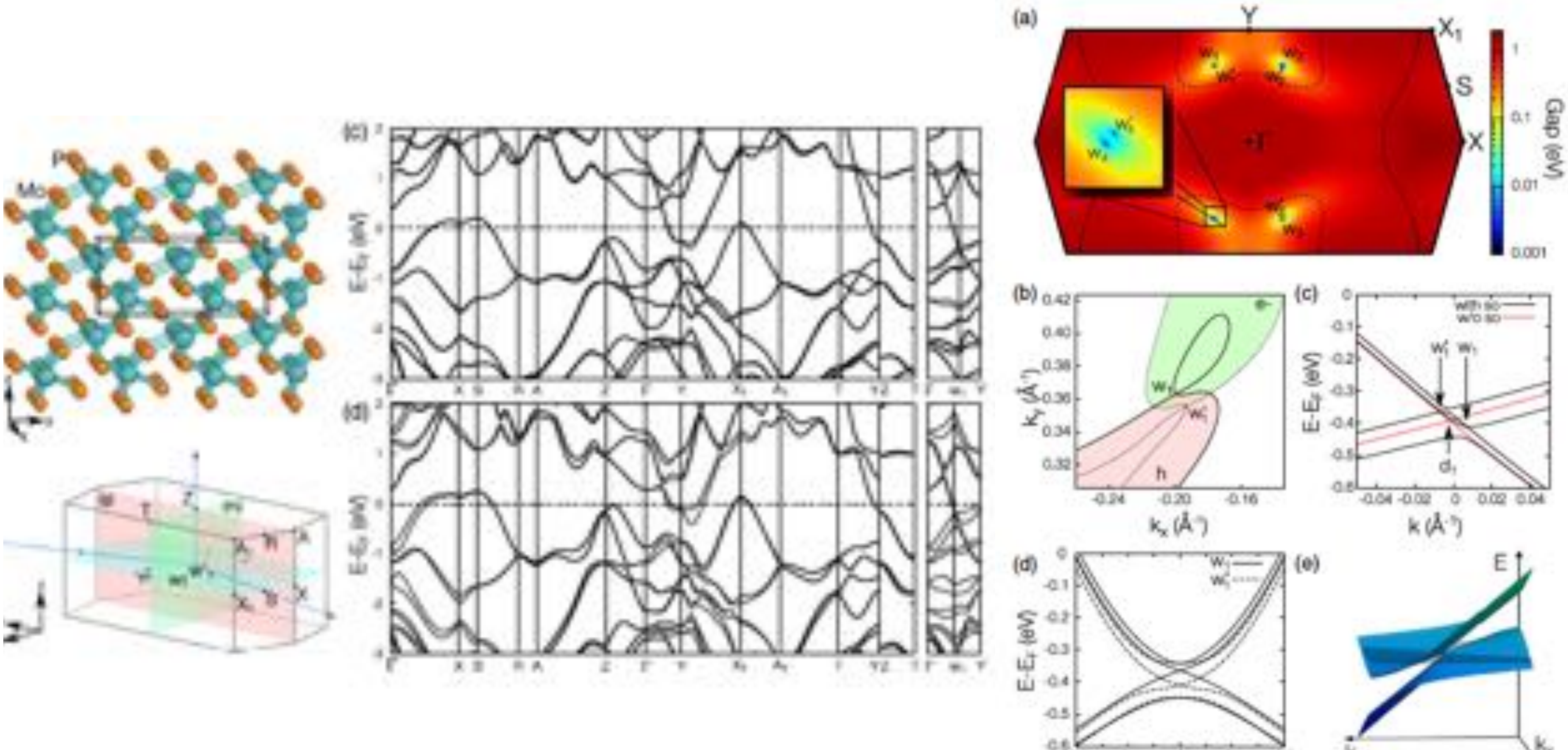

Prediction: G. Autès, et al.; Phys. Rev. Lett. 117 (2016) 066402

WP_2 protected Weyl

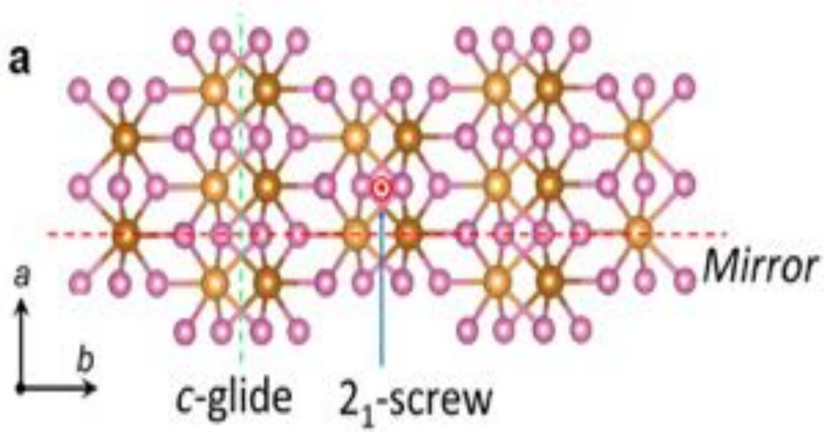

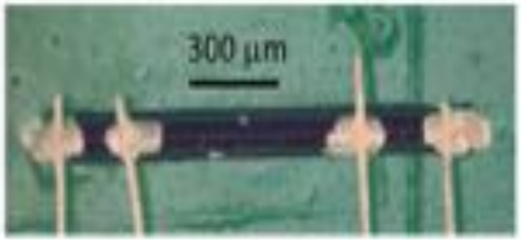

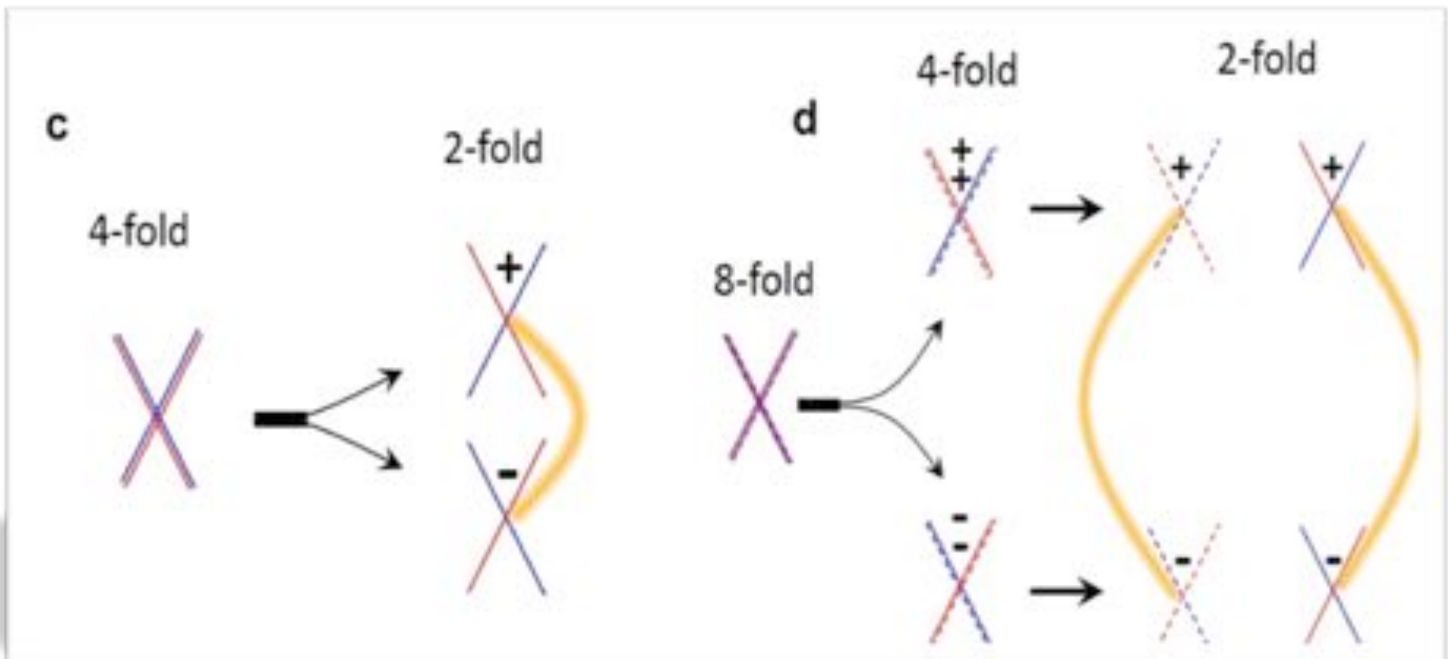

Prediction: G. Autès, et al.; Phys. Rev. Lett. 117 (2016) 066402 Extremely high magnetoresistance and conductivity in the type-II Weyl semimetal WP2, Nitesh, et al.; **arXiv:1703.04527**

WP_2 protected Weyl

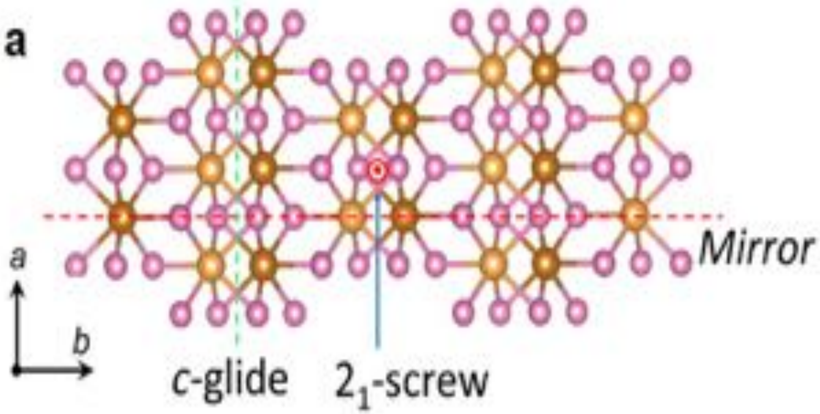

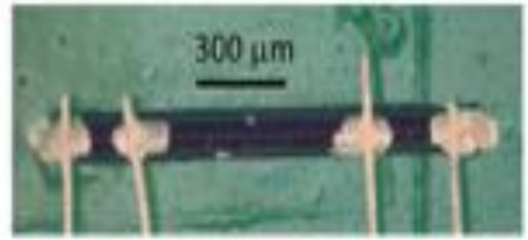

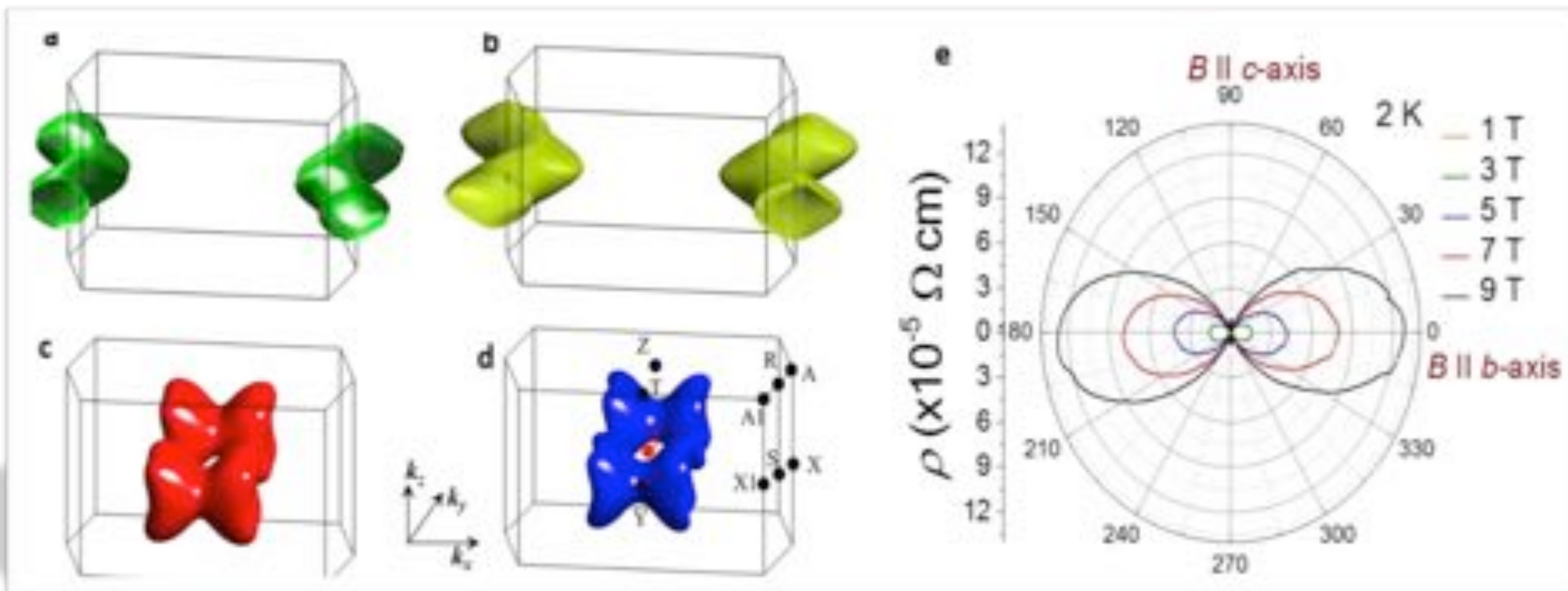

Prediction: G. Autès, et al.; Phys. Rev. Lett. 117 (2016) 066402 Extremely high magnetoresistance and conductivity in the type-II Weyl semimetal WP2, Nitesh, et al.; **arXiv:1703.04527**

ARPES and the Band Structure

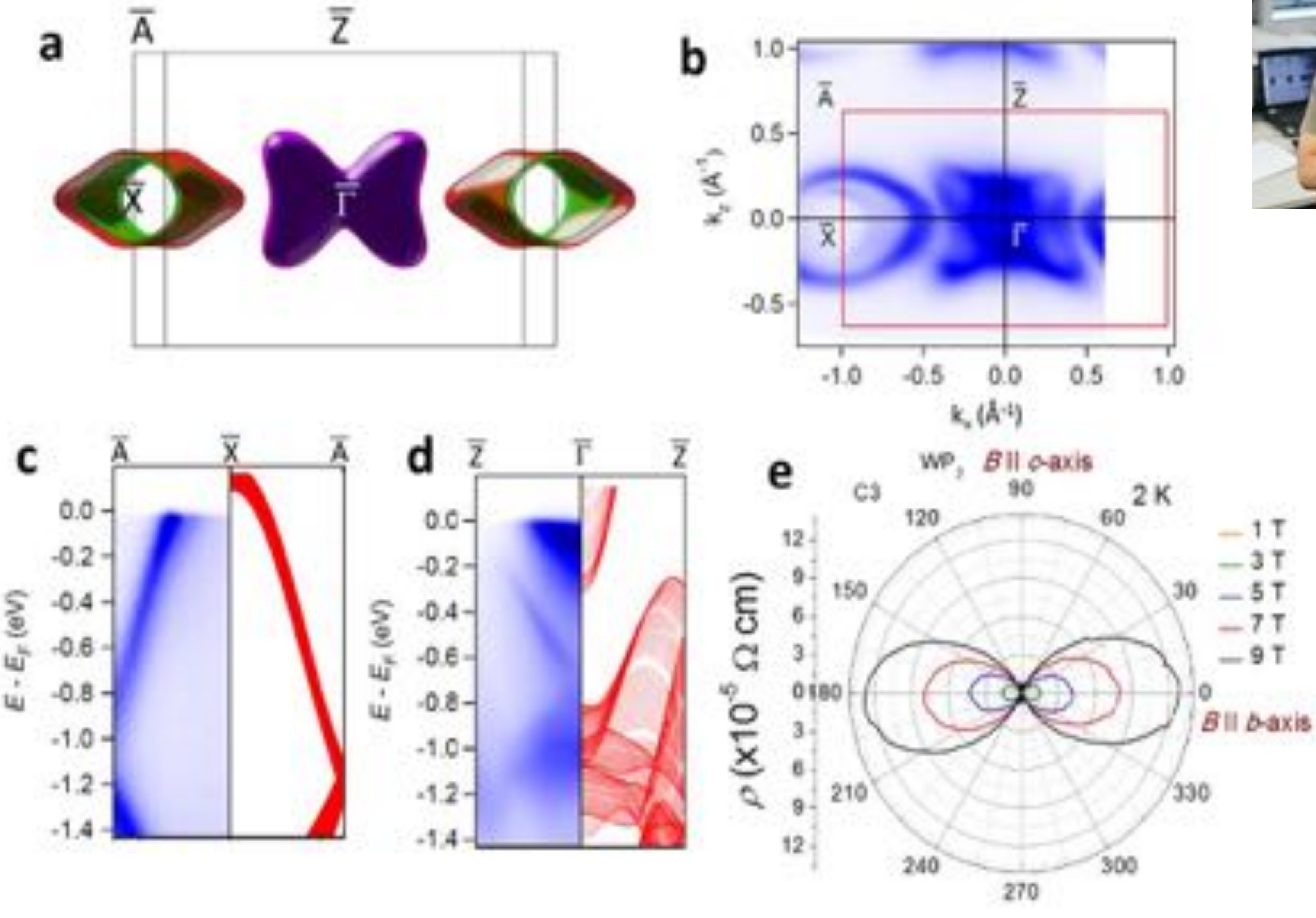

Photoemission, Nan Xu, Ming Shi, Paul Scherrer Institute, Swiss Light Source, CH-5232 Villigen PSI, Switzerland.
Extremely high magnetoresistance and conductivity in the type-II Weyl semimetal WP2, Nitesh, et al.; arXiv:1703.04527

WP_2 protected Weyl

Magnetotransport in a novel Weyl WP_2

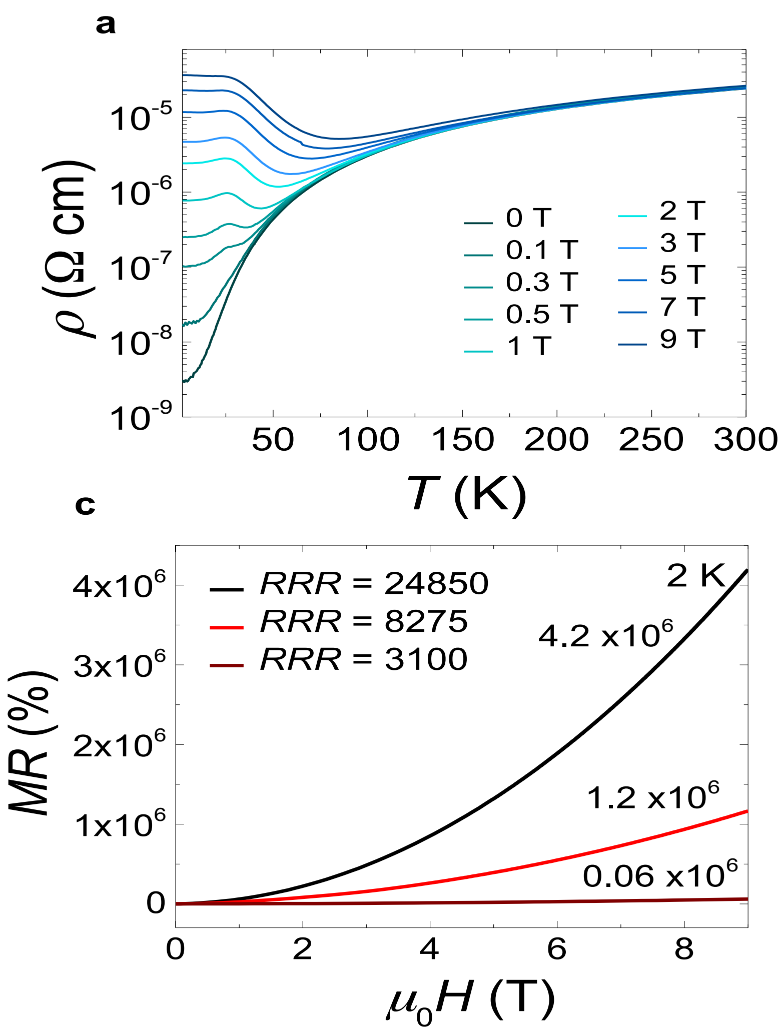

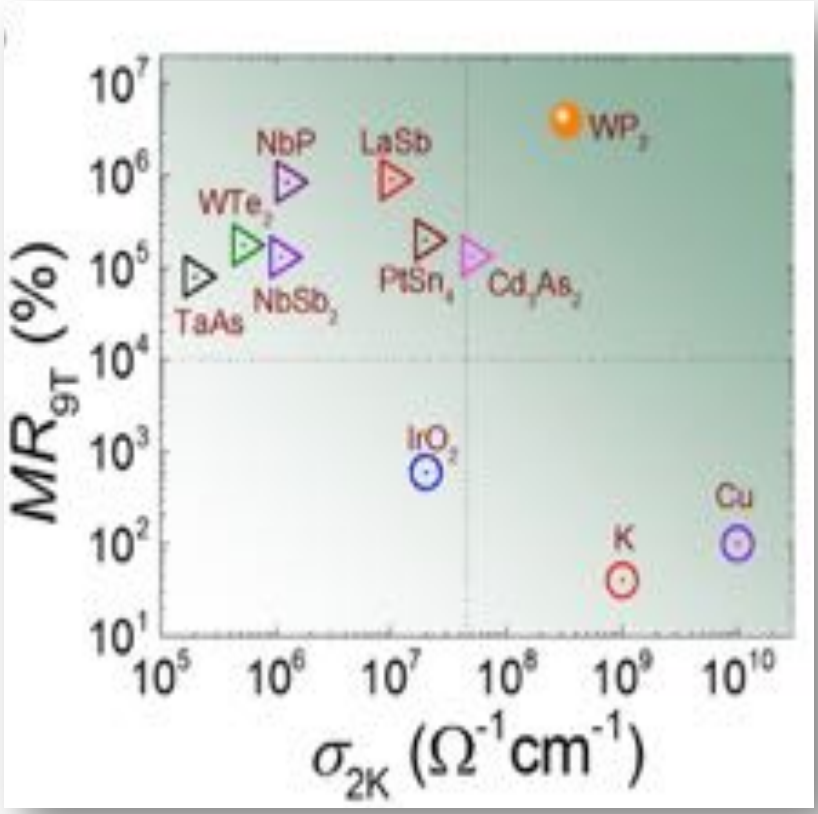

Prediction: G. Autès, et al.; Phys. Rev. Lett. 117 (2016) 066402 Extremely high magnetoresistance and conductivity in the type-II Weyl semimetal WP2, Nitesh, et al.; **arXiv:1703.04527**

Macroscopic Mean Free Path

Compound	ρ (Ωcm)	l (μm)	μ ($cm^2V^{-1}s^{-1}$)	n (cm^{-3})
MoP	6×10^{-9}	11	2.4×10^{4}	2.9×10^{22}
WP_2	3×10^{-9}	530	4×10^{6}	5×10^{20}
WC	0.35×10^{-6}		$\sim1\times10^{4}$	4×10^{20}
$PtCoO_2$	40×10^{-9}	5	0.7×10^{4}	2.2×10^{22}
$PdCoO_2$	9×10^{-9}	20	$2.8\text{x}10^{4}$	2.4×10^{22}

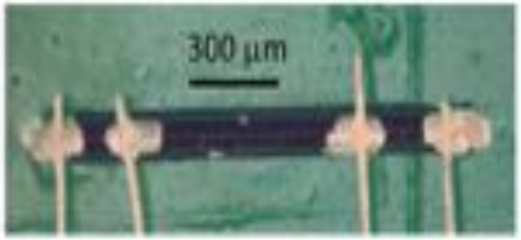

WC J. B. He et al. arXiv:1703.03211
Pallavi Kushwaha, et al. Sci. Adv.1 (2015) e150069
P. Moll Science 351, (2016) 1061

Chandra Shekhar et al. arXiv:1703.03736
Nitesh, et al.; arXiv:1703.04527

Hydrodynamics

PRL 118, 226601 (2017) PHYSICAL REVIEW LETTERS week ending 2 JUNE 2017

Hydrodynamic Electron Flow and Hall Viscosity

Thomas Scaffidi,[1] Nabhanila Nandi,[2] Burkhard Schmidt,[2] Andrew P. Mackenzie,[2,3] and Joel E. Moore[1,4]

In the ballistic regime ($w << l_{er}, l_{mr}$): $\rho \sim w^{-1}$

Hydrodynamic effects become dominant

- electron-electron scattering $l_{er} << w << l_{mr}$,
- with electron-electron scattering length $l_{er} = v_F \tau_{er}$
- w the sample width,
- $l_{mr} = v_F \tau_{mr}$ the mean free path and v_F the Fermi velocity

In the Navier-Stokes flow limit: $\rho = m^*/(e^2 n) \cdot 12 \eta w^{-2}$

R. N. Gurzhy, A. N. Kalinenko, A. I. Kopeliovich, Hydrodynamic effects in the electrical conductivity of impure metals. *Sov. Physics-JETP*. **69**, 863–870 (1989).

P. S. Alekseev, Negative magnetoresistance in viscous flow of two-dimensional electrons. *Phys. Rev. Lett.* **117** (2016).

T. Scaffidi, N. Nandi, B. Schmidt, A. P. Mackenzie, J. E. Moore, Hydrodynamic Electron Flow and Hall Viscosity. *Phys. Rev. Lett.* **118**, 226601 (2017).

Water, Gas or Electrons

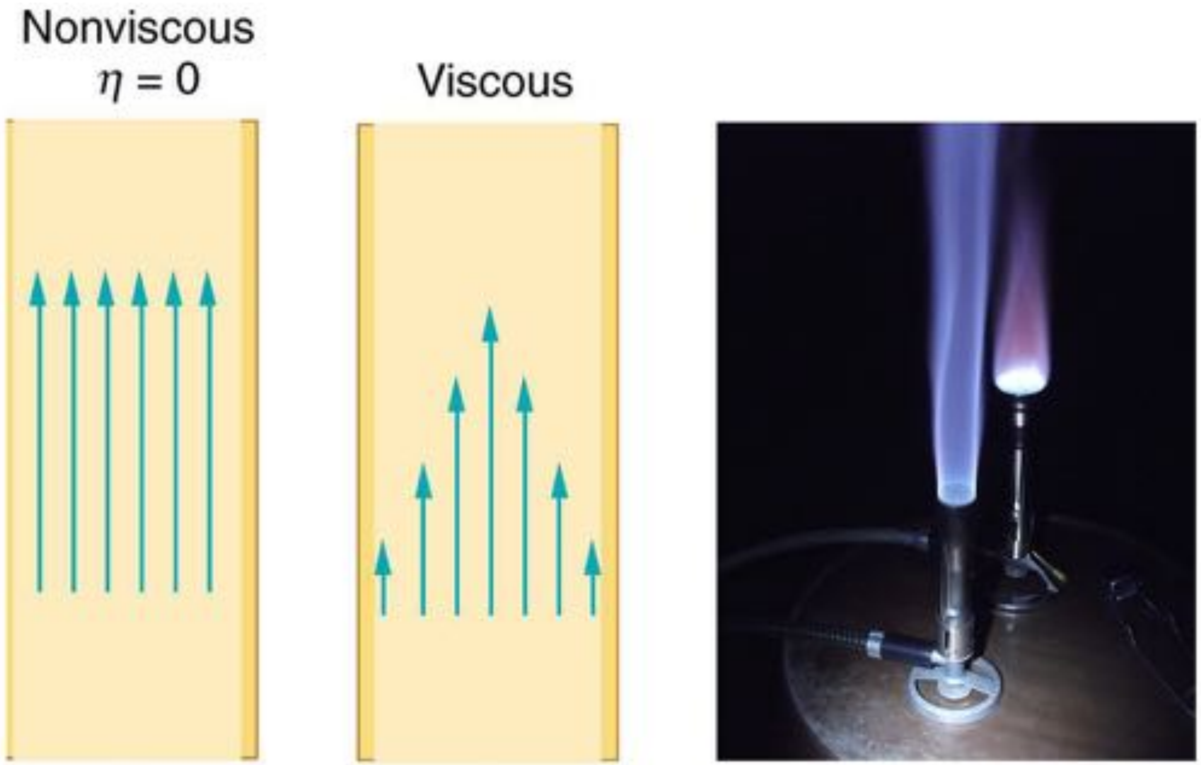

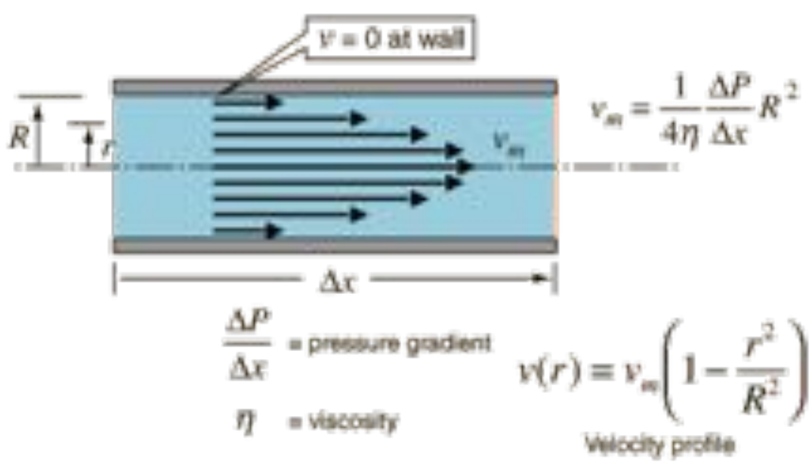

Hydrodynamic flow

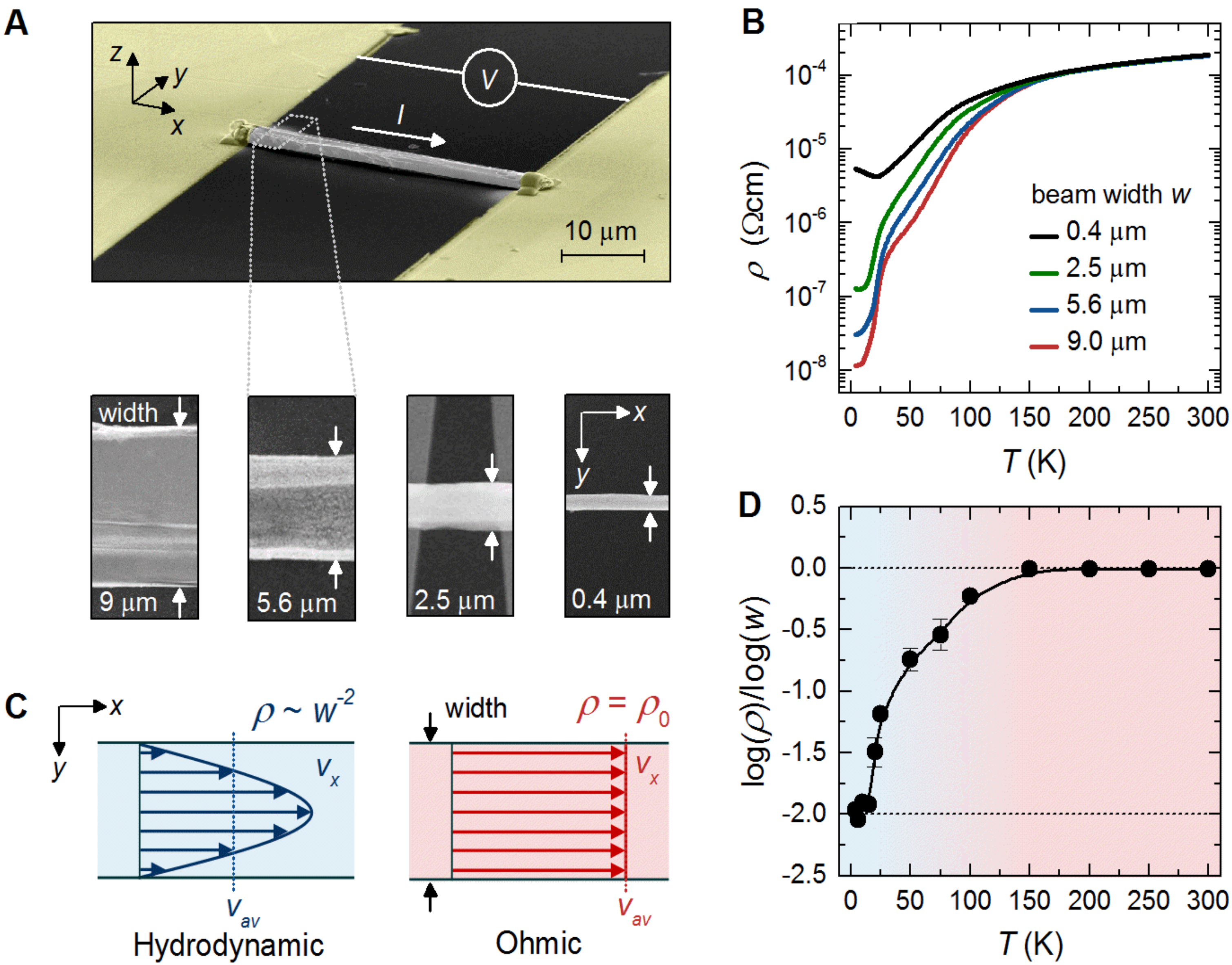

J. Gooth et al. submitted, arXiv:1706.05925

Hydrodynamic flow

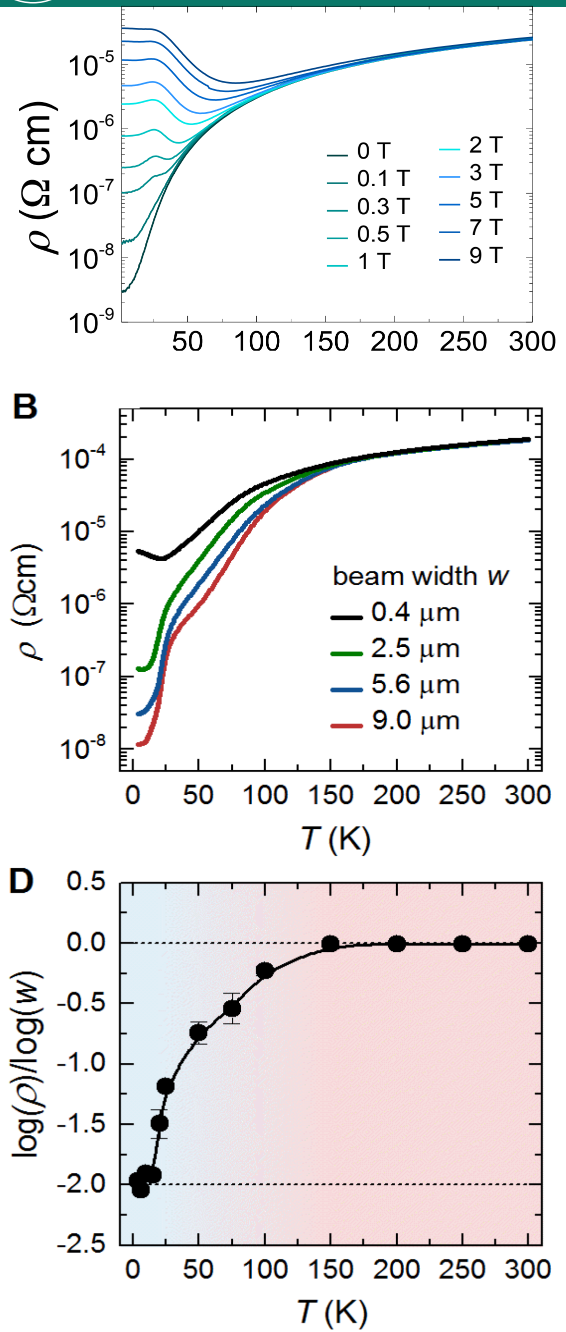

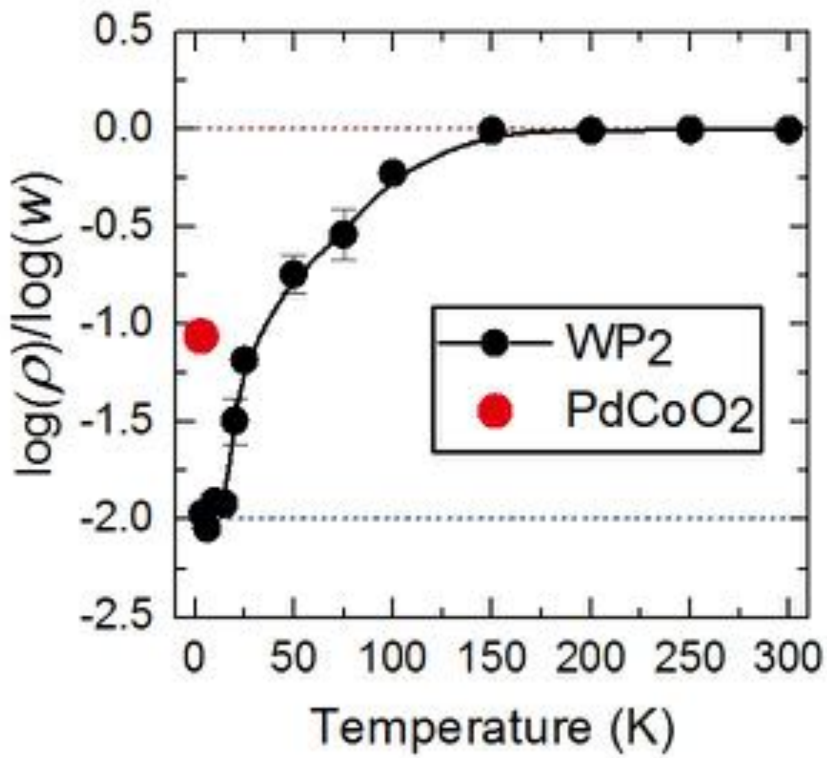

P. J. W. Moll *et al.*, *Science* 10.1126/science.aac8385 (2016).

J. Gooth et al. submitted, arXiv:1706.05925

Hydrodynamic flow

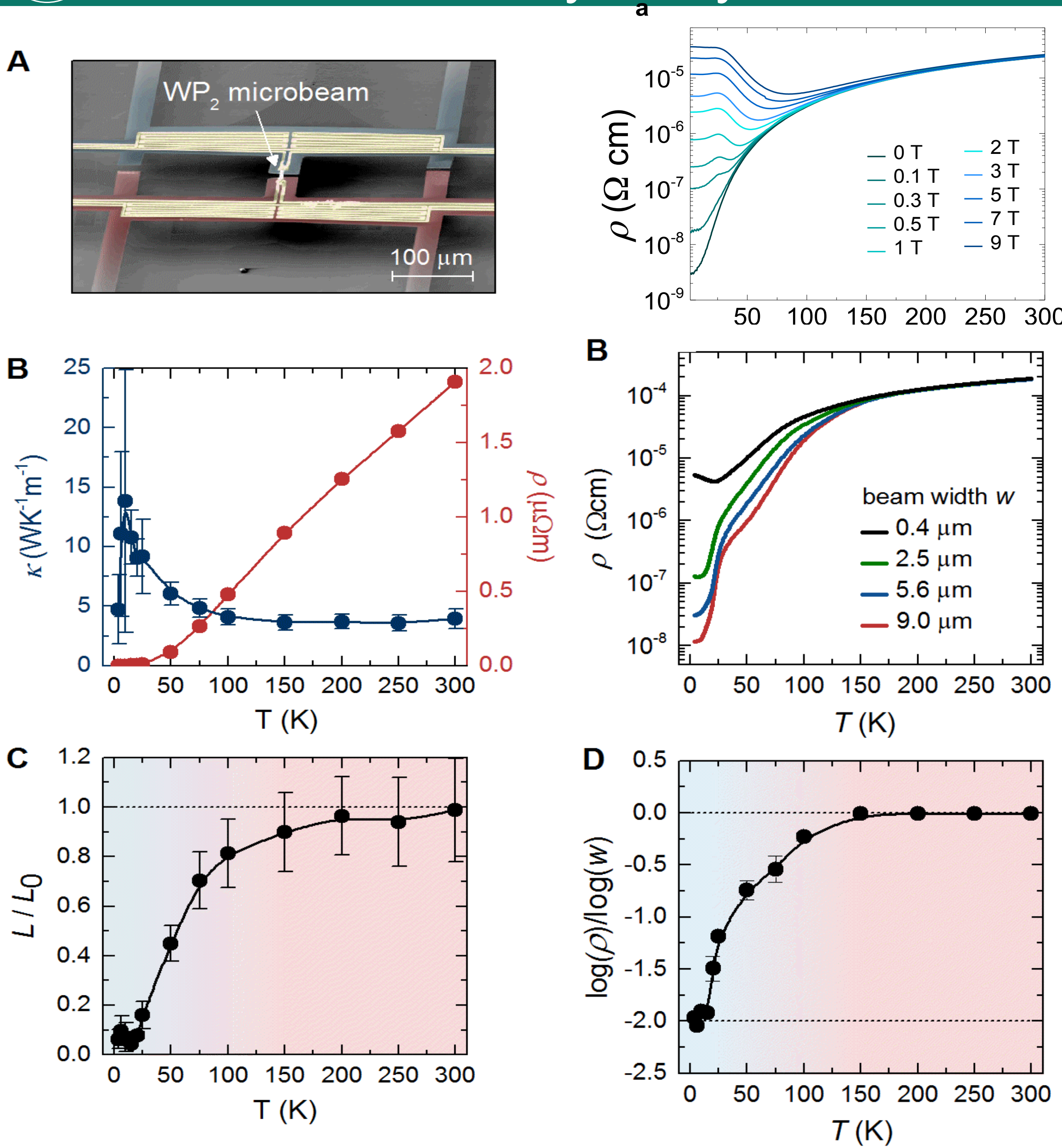

- Hydrodynamic electron fluid <15K
- conventional metallic state at T higher 150K

The hydrodynamic regime:

- a viscosity-induced dependence of the electrical resistivity on the square of the channel width

$$\rho = m^{*}/(e^{2}n)\cdot 12\eta w^{-2}$$

- a strong violation of the

$$L \equiv \frac{\kappa}{\sigma T} = \frac{\pi^2}{3} \equiv L_0$$

J. Gooth et al. submitted, arXiv:1706.05925

Hydrodynamic flow

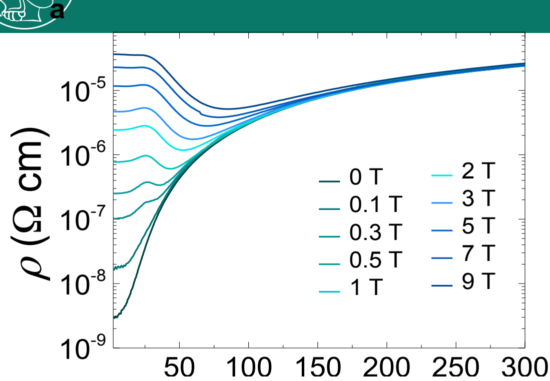

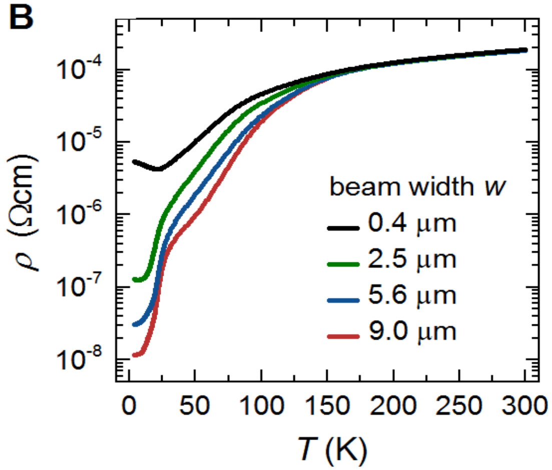

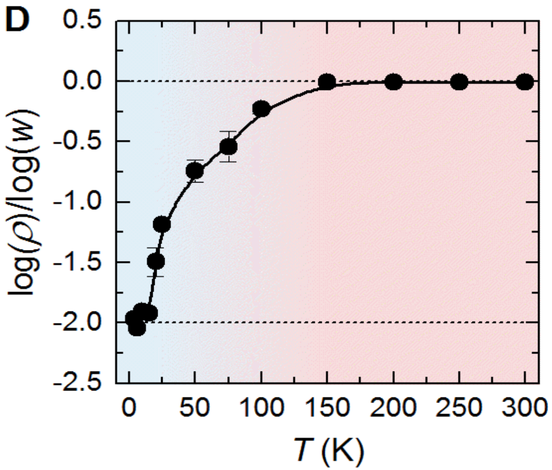

$PdCoO_2$

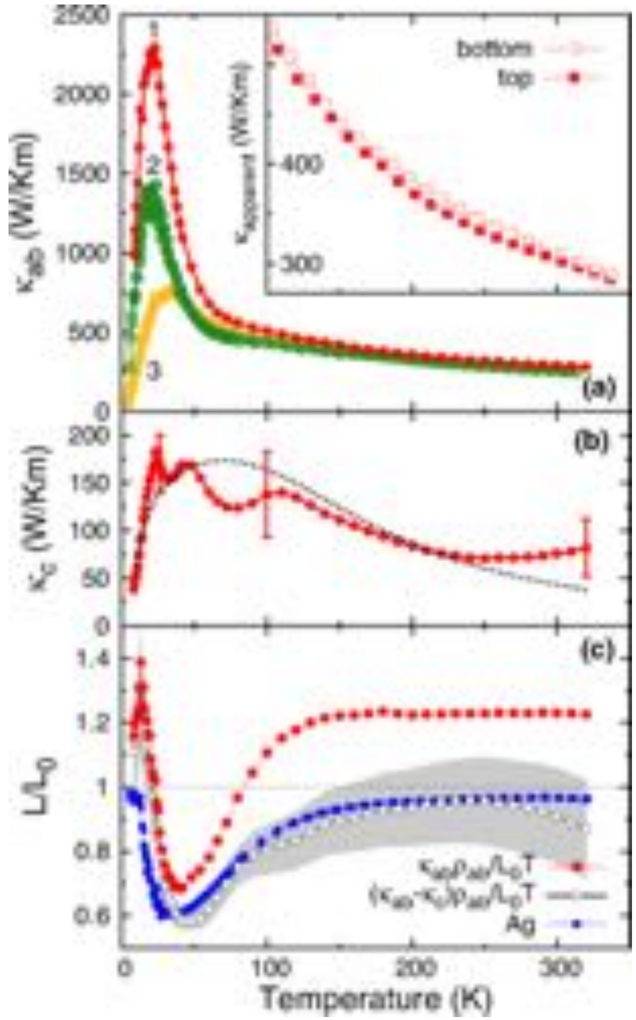

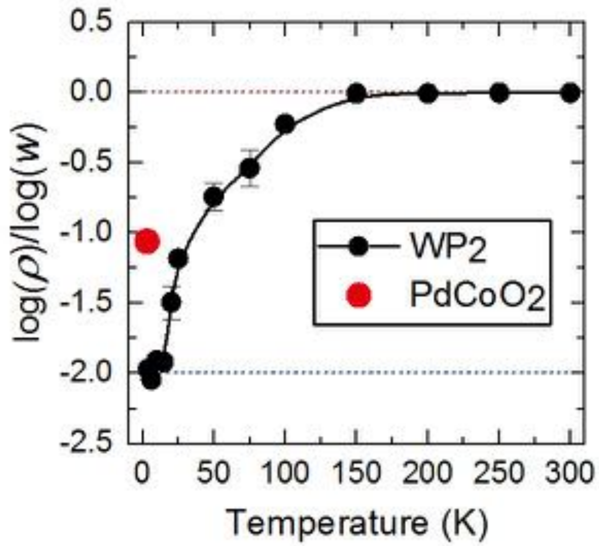

P. J. W. Moll *et al.*, *Science* 10.1126/science.aac8385 (2016)
R. Daou, et al. and Antoine Maignan, Phys. Rev. B 91, 041113(R) (2015)
J. Gooth et al. submitted, arXiv:1706.05925

Giant Nernst – Topology - Hydrodynamic

Rep. Prog. Phys. 79 (2016) 046502 (23pp)
doi:10.1088/0034-4885/79/4/046502

Review

Nernst effect in metals and superconductors: a review of concepts and experiments

Kamran Behnia and Hervé Aubin

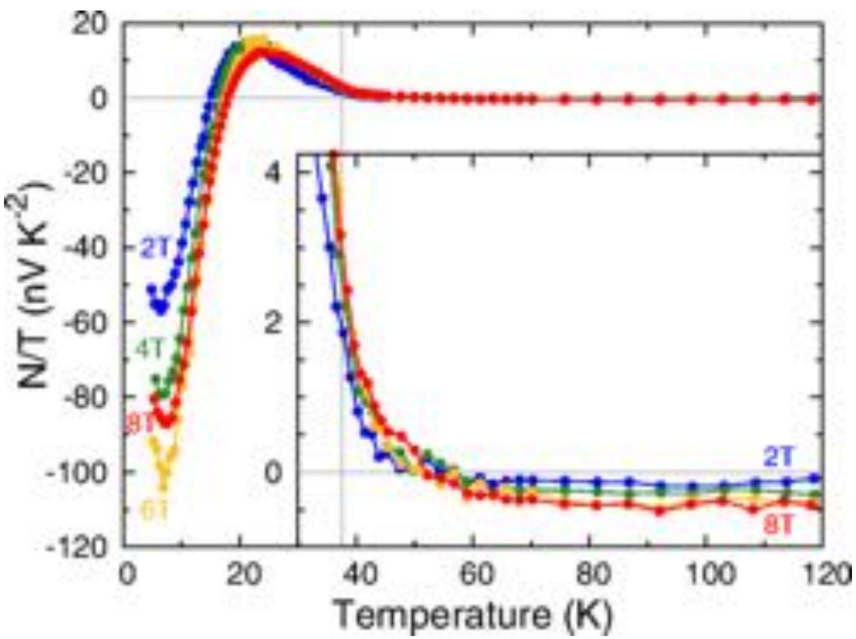

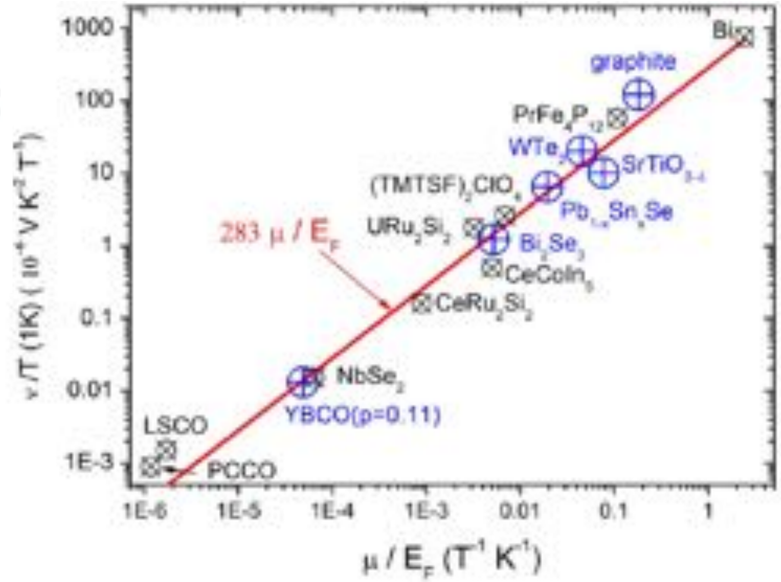

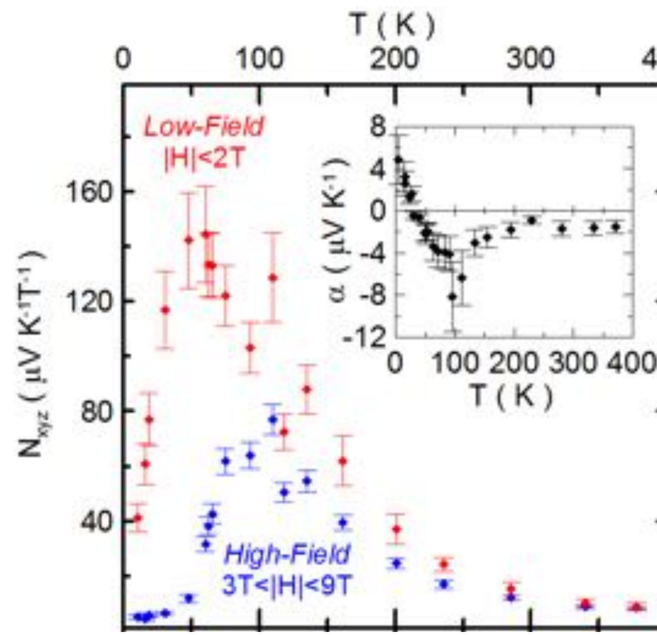

Ramzy Daou, Raymond Frésard, Sylvie Hébert, and Antoine Maignan, Phys. Rev. B 92, 245115 (2015)
Sarah J. Watzman, et al. preprint arXiv:1704.02241

Magnetohydrodynamics, Planckian bound of dissipation

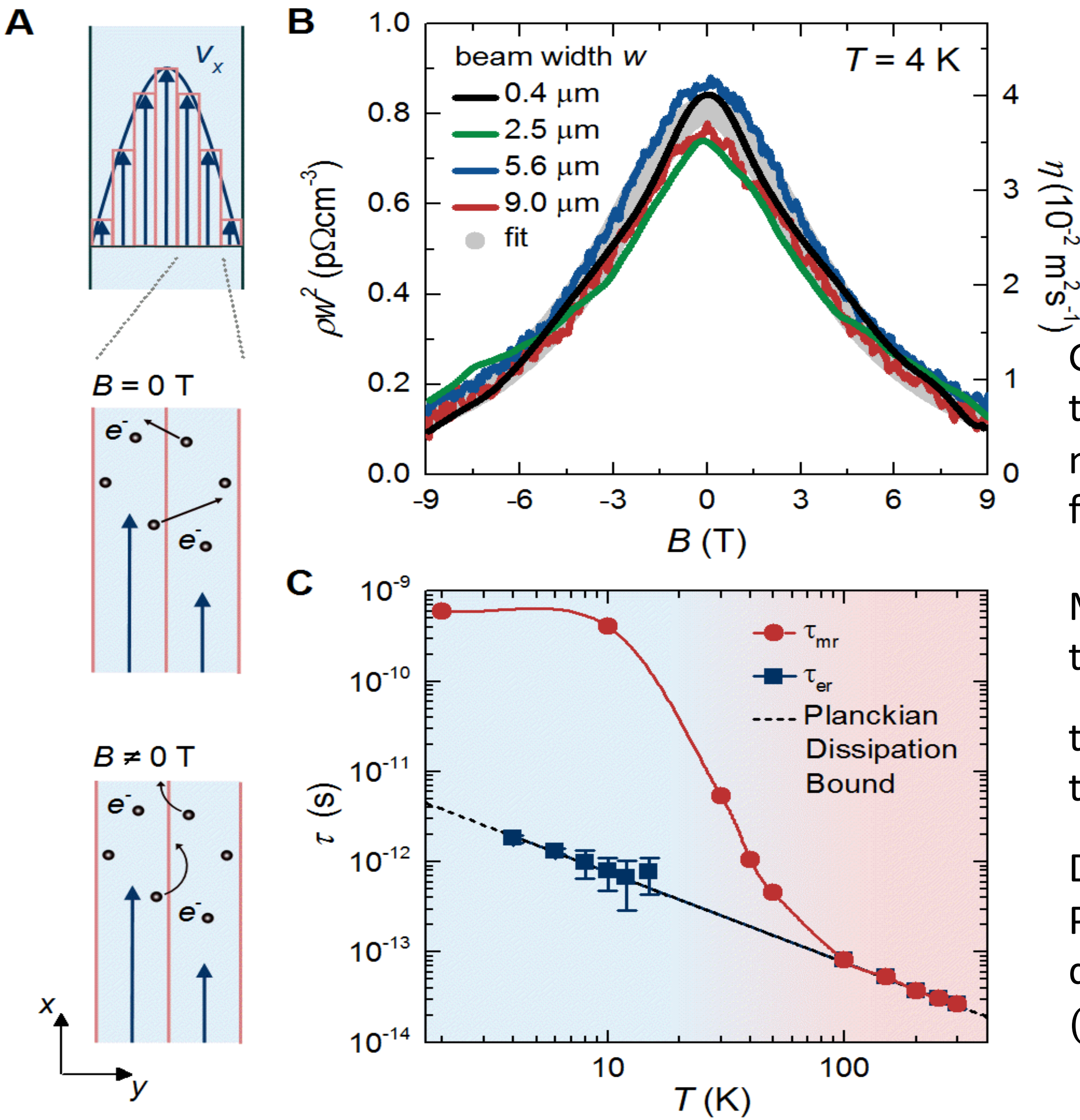

Grey dots:
the magnetohydrodynamic model in the Navier-Stokes flow limit

Momentum relaxation times t_{mr}

thermal energy relaxation times t_{er},

Dashed line marks the Planckian bound on the dissipation time $\tau_\hbar = \hbar/(k_B T)$.

J. Gooth et al. submitted, arXiv:1706.05925

Viscosity of the electron fluid in WP_2

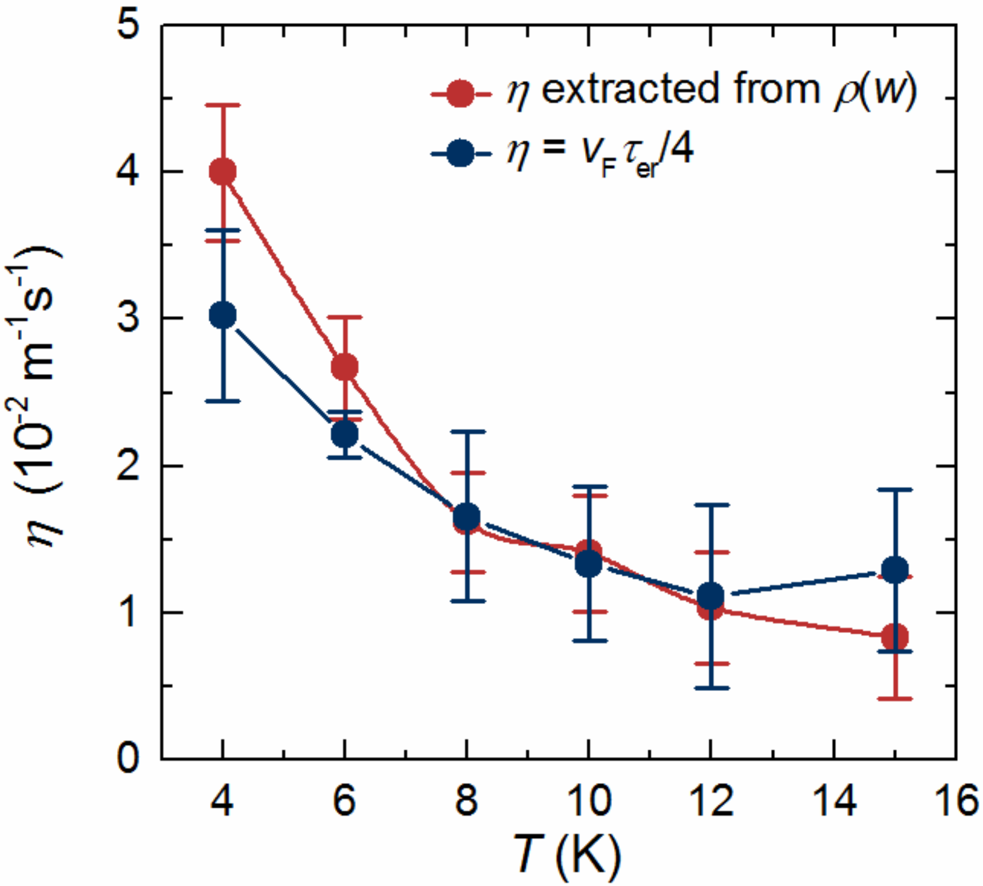

The dynamic viscosity is $\eta_D = 1\times10^{-4}$ kgm^{-1}s^{-1} at 4 K.

TaAs

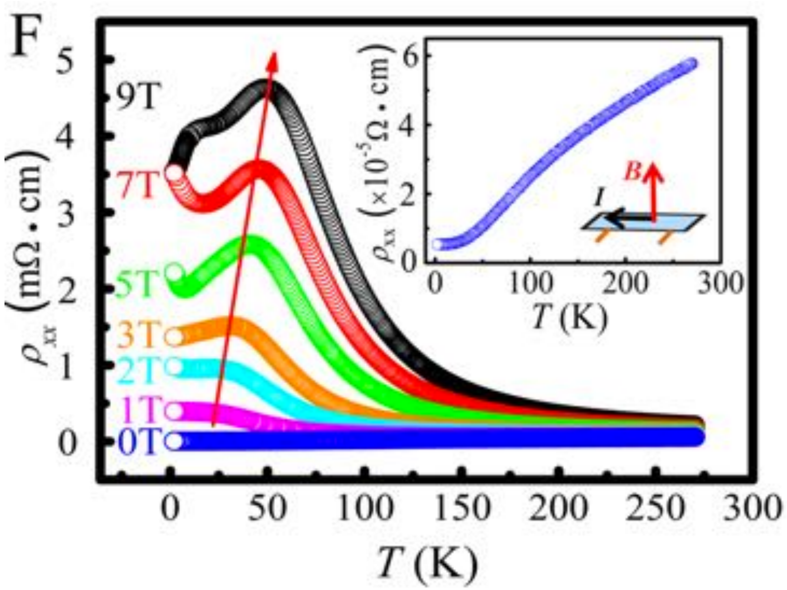

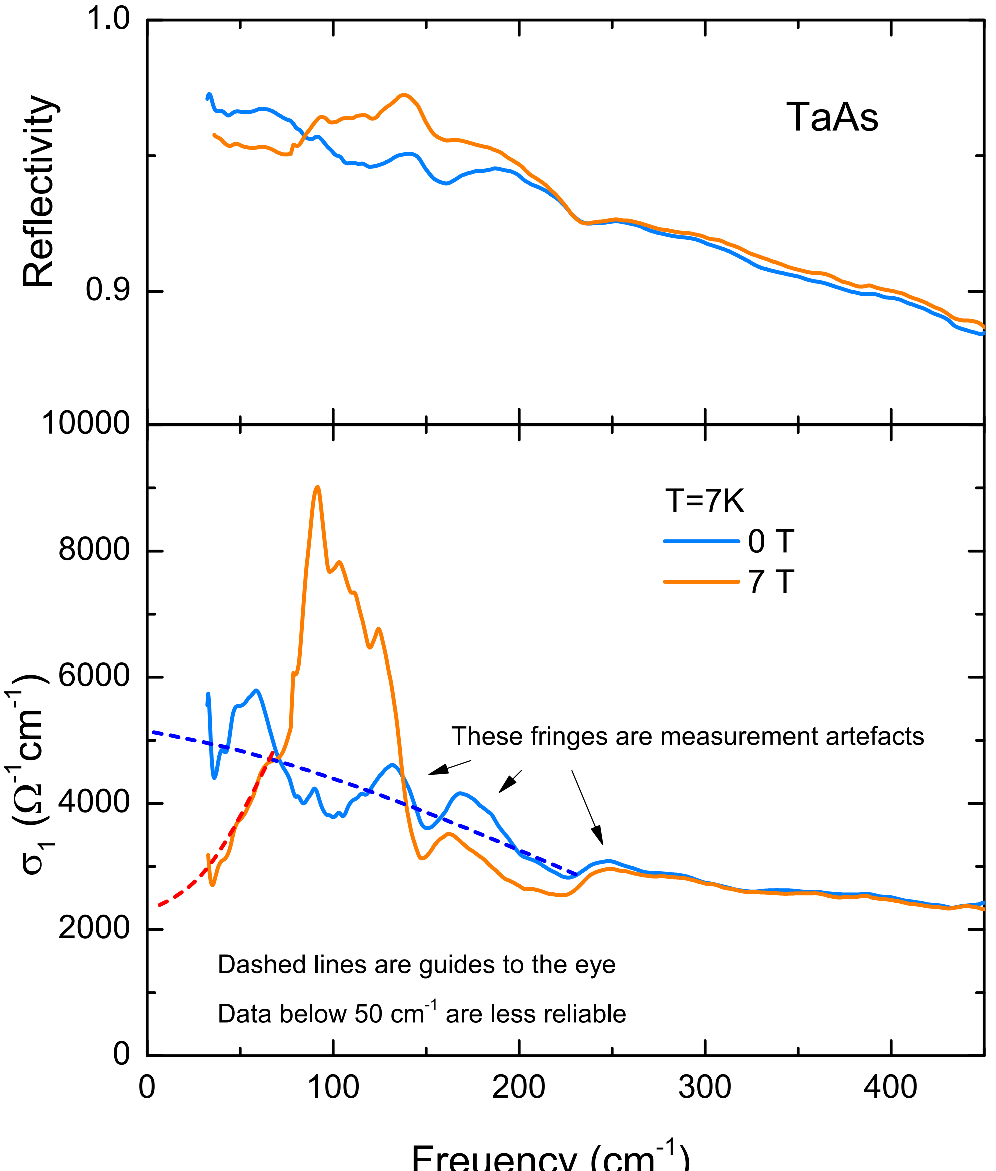

Huang et al. Phys. Rev. X 5, 031023 (2015)

A. Pronim unpublished

Design scheme: Dirac and Weyl

- Semimetal
- Band inversion – e.g. inert pair effect
- Crossing band due to enforced degeneration
- New quantum effects – electron liquid

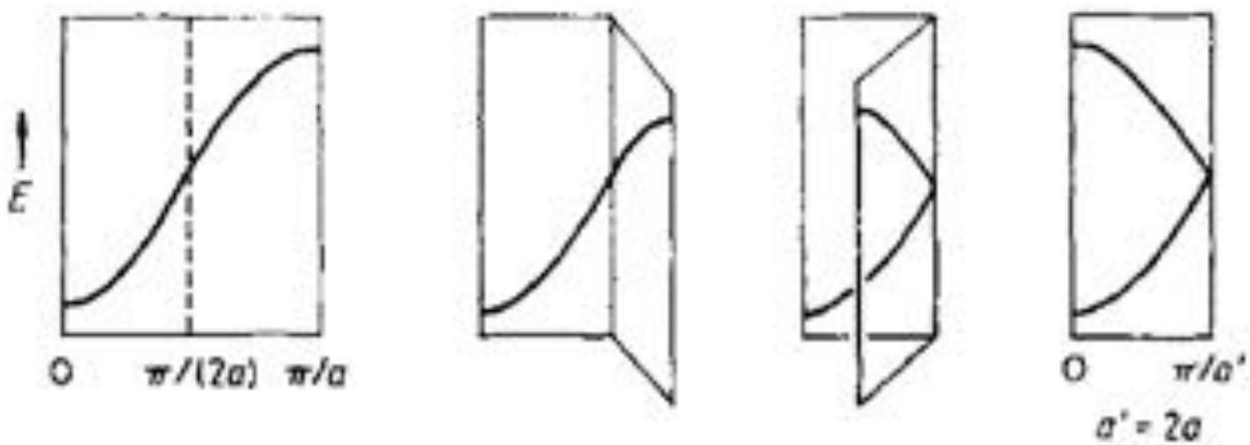

Hoffmann Angewandte. Chem. 26 (1987) 846

Weyl Semimetals

Magnetically induced

Predicting topological insulators

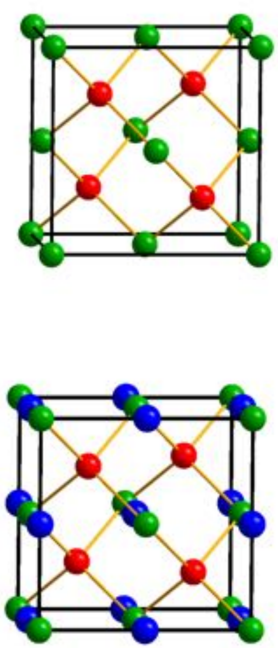

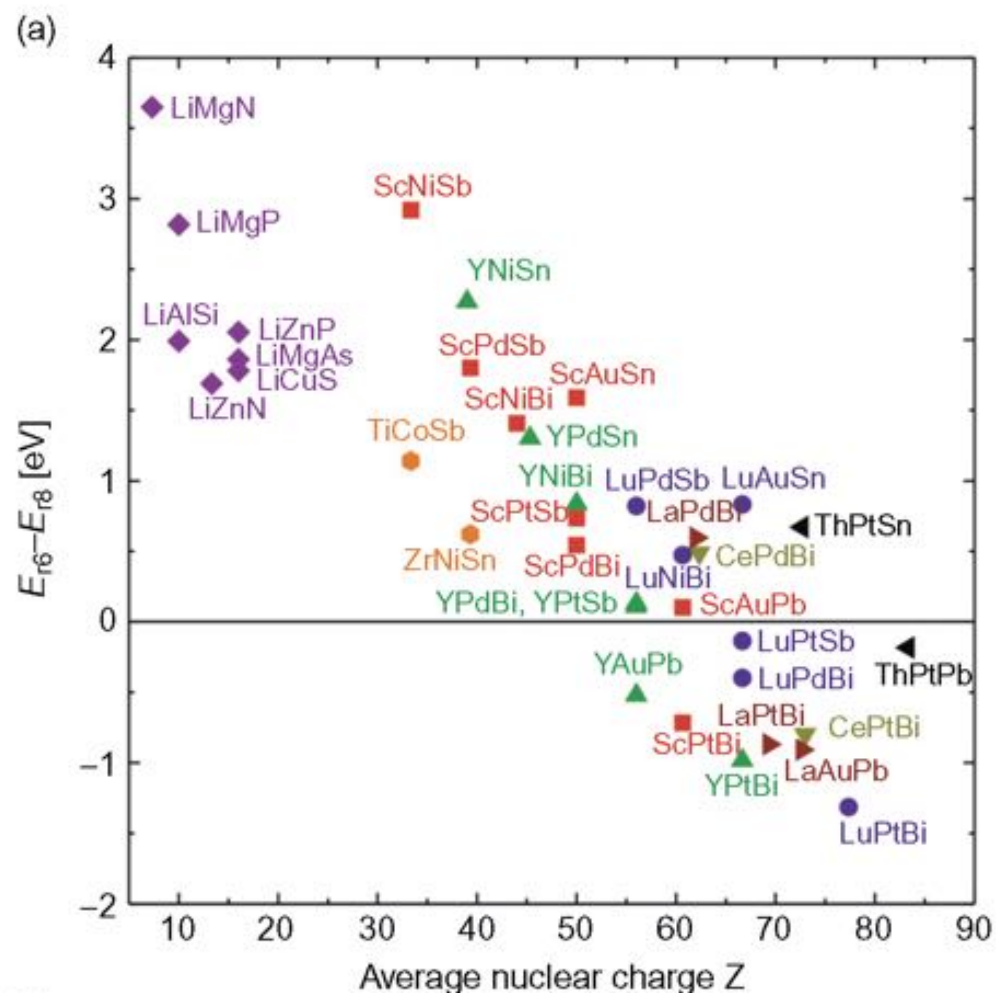

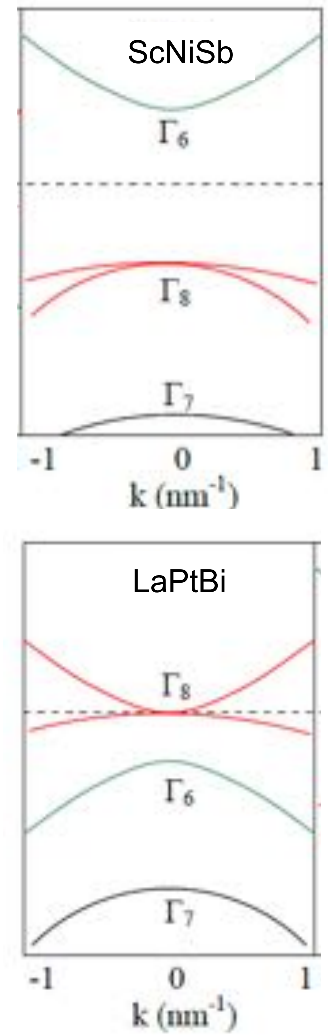

S. Chadov et al., Nat. Mater. **9** 541 (2010).
H. Lin et al., Nat. Mater. **9** 546 (2010).

REPtBi …multifunctional topologic insulators

Magnetism and heavy fermion-like behavior in the RBiPt series

P. C. Canfield, J. D. Thompson, W. P. Beyermann, A. Lacerda, M. F. Hundley, E. Peterson, and Z. Fisk
Los Alamos National Laboratory, Los Alamos, New Mexico 87545

H. R. Ott
ETH, Zurich, Switzerland

J. Appl. Phys. **70** (10), 15 November 1991

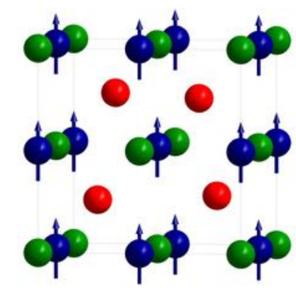

Multifunctional properties

- RE: Gd, Tb, Sm Magnetism and TI
  - Antiferromagnetism with GdPtBi
- RE: Ce
  - complex behaviour of the Fermi surface
- RE: Yb Kondo insulator and TI
  - YbPtBi is a super heavy fermion with the highest γ value

Pt — **RE** — **Bi**

$10 + 3\ (+f^n) + 5 = 18$

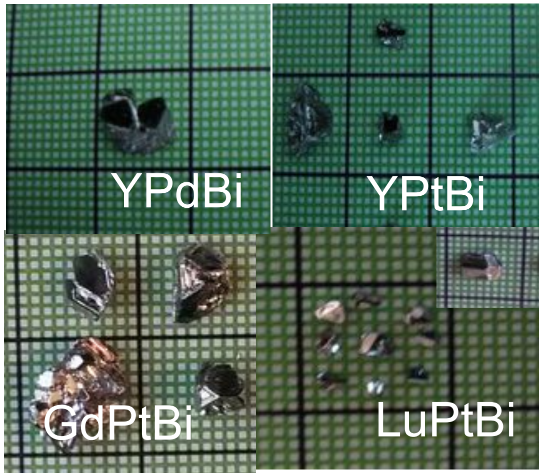

S. Chadov et al., Nat. Mater. 9, 541 (2010).
H. Lin et al., Nat. Mater. 9, 546 (2010).

Weyl semimetals

3D topological Weyl semimetals - breaking time reversal symmetry – in transport measurement we should see

1. Intrinsic anomalous Hall effect

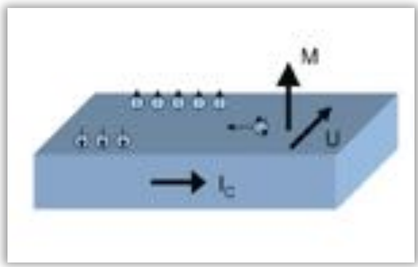

2. Chiral anomaly

$$\partial_\mu j^\mu_\chi = -\chi \frac{e^3}{4\pi^2\hbar^2}\boldsymbol{E}\cdot\boldsymbol{B}$$

$$\sigma_a = \frac{e^3 v_f^3}{4\pi^2\hbar\mu^2 c} B^2,$$

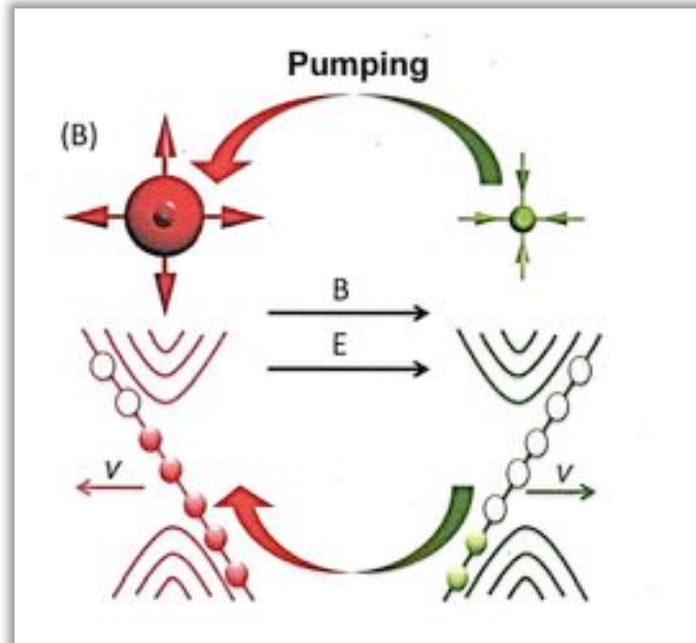

S. L. Adler, Phys. Rev. 177, 2426 (1969)
J. S. Bell and R. Jackiw, Nuovo Cim. A60, 47 (1969)
AA Zyuzin, AA Burkov - Physical Review B (2012)
AA Burkov, L Balents, PRL 107 12720 (2012)

Weyl GdPtBi in a magnetic field

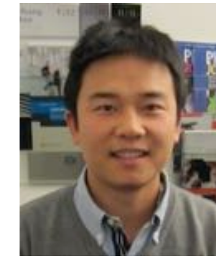

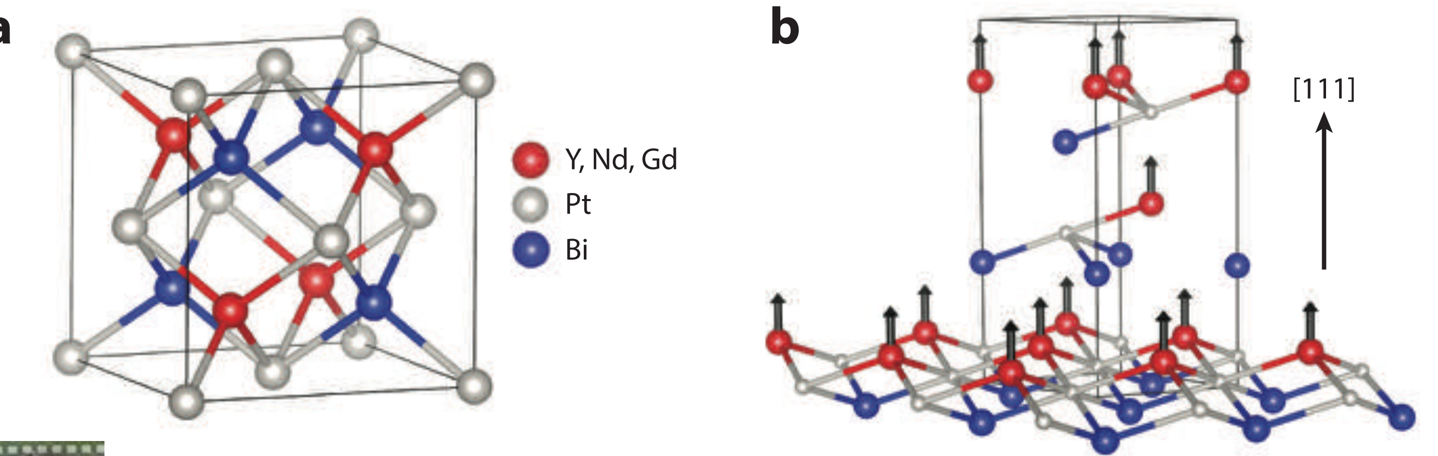

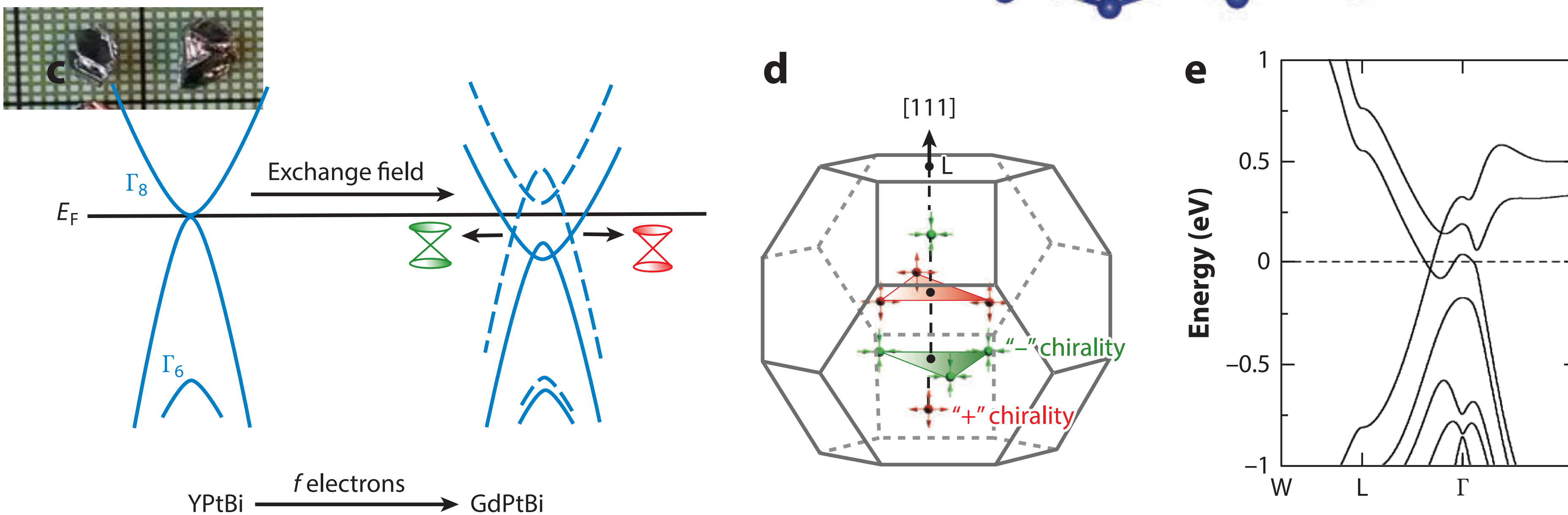

C. Shekhar et al., arXiv:1604.01641, (2016).

M. Hirschberger et al.,. Nature Mat. Online arXiv:1602.07219, (2016).

Chiral Anomaly – neg. quadratic MR

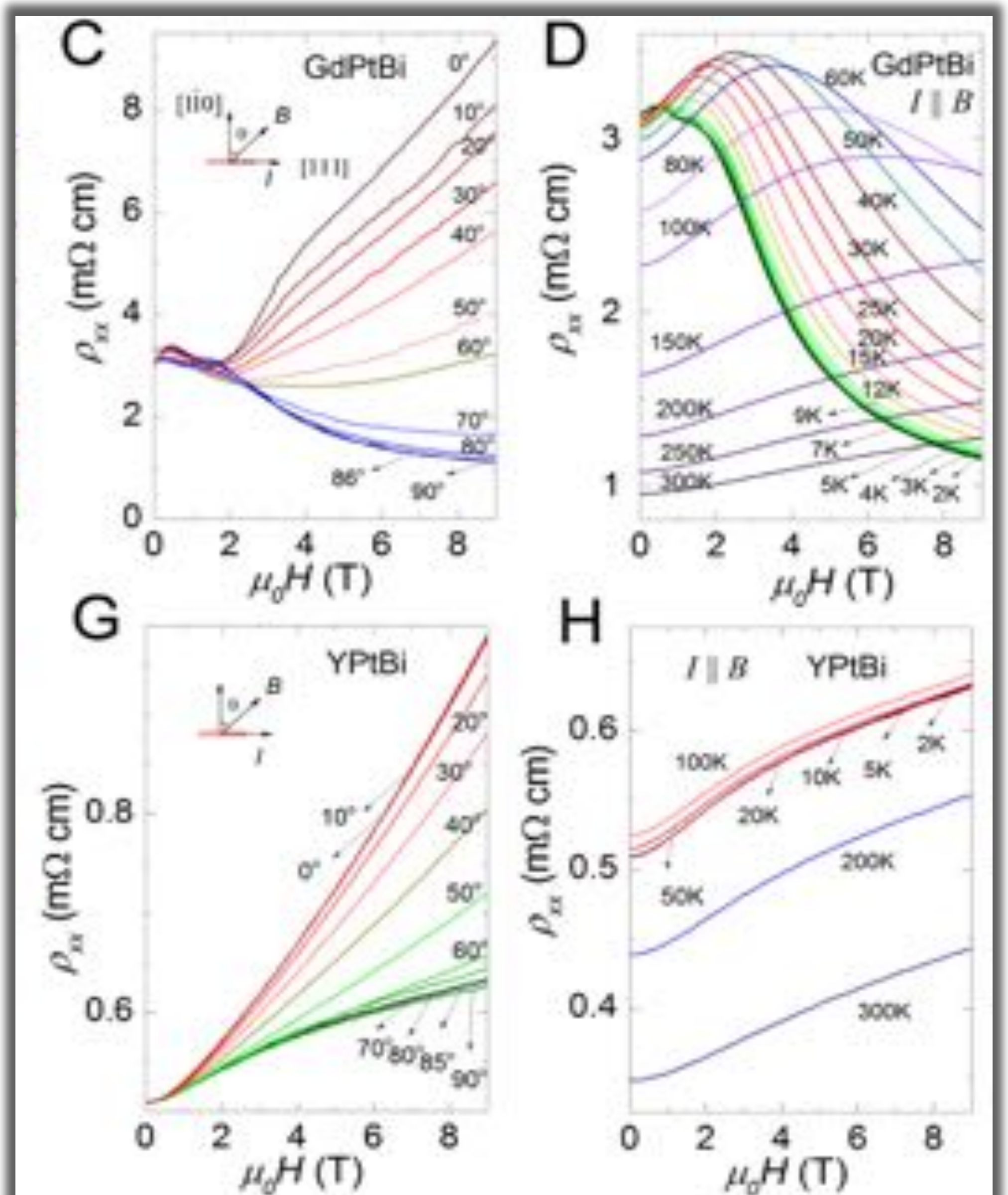

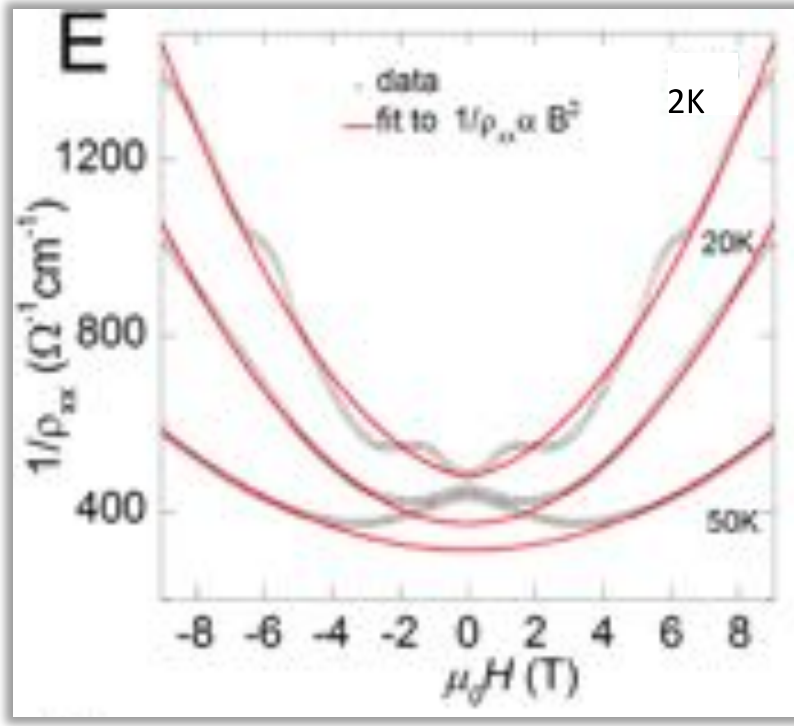

C. Shekhar et al., arXiv:1604.01641, (2016).

Claudia Felser and Binghai Yan, Nature Materials 15 (2016) 1149

M. Hirschberger et al. Nature Mat. online, arXiv:1602.07219, (2016).

GdPtBi – Anomalous Hall Effect

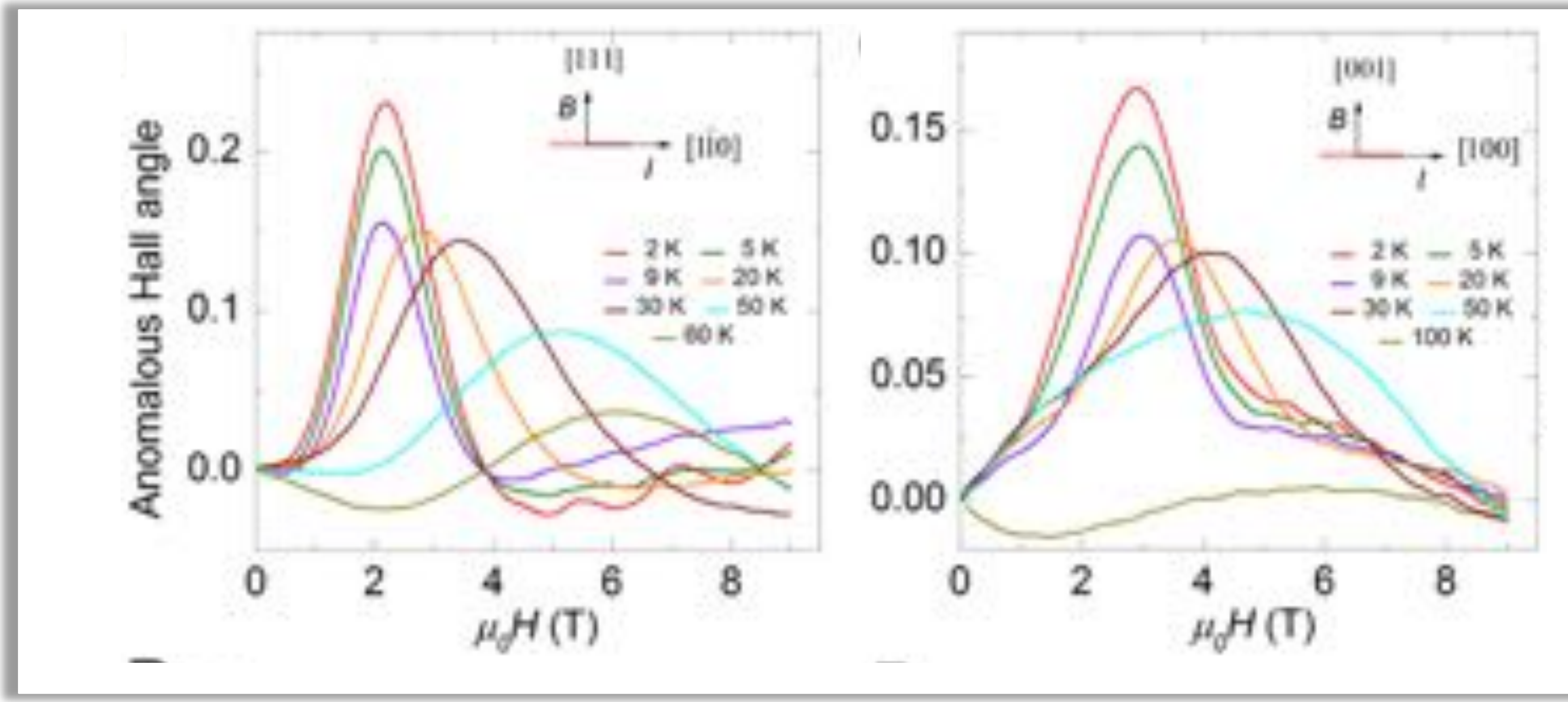

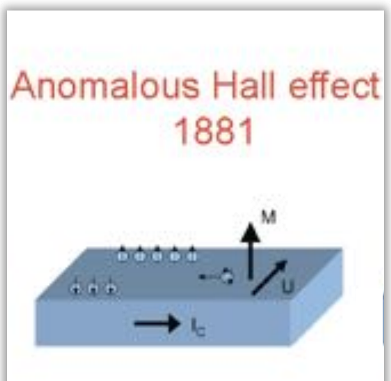

In Ferromagnets an AHE scales with the magnetic moment
Antiferromagnets show no AHE
A Hall angle of 0.2 is exceptional high

$$\rho_H = R_0 B + \boxed{4\pi R_s M}$$

Shekhar et al., arXiv:1604.01641, (2016).
T. Suzuki,… & J. G. Checkelsky, Nature Physics (2016) doi:10.1038/nphys3831

Chiral Anomaly – neg. quadratic MR

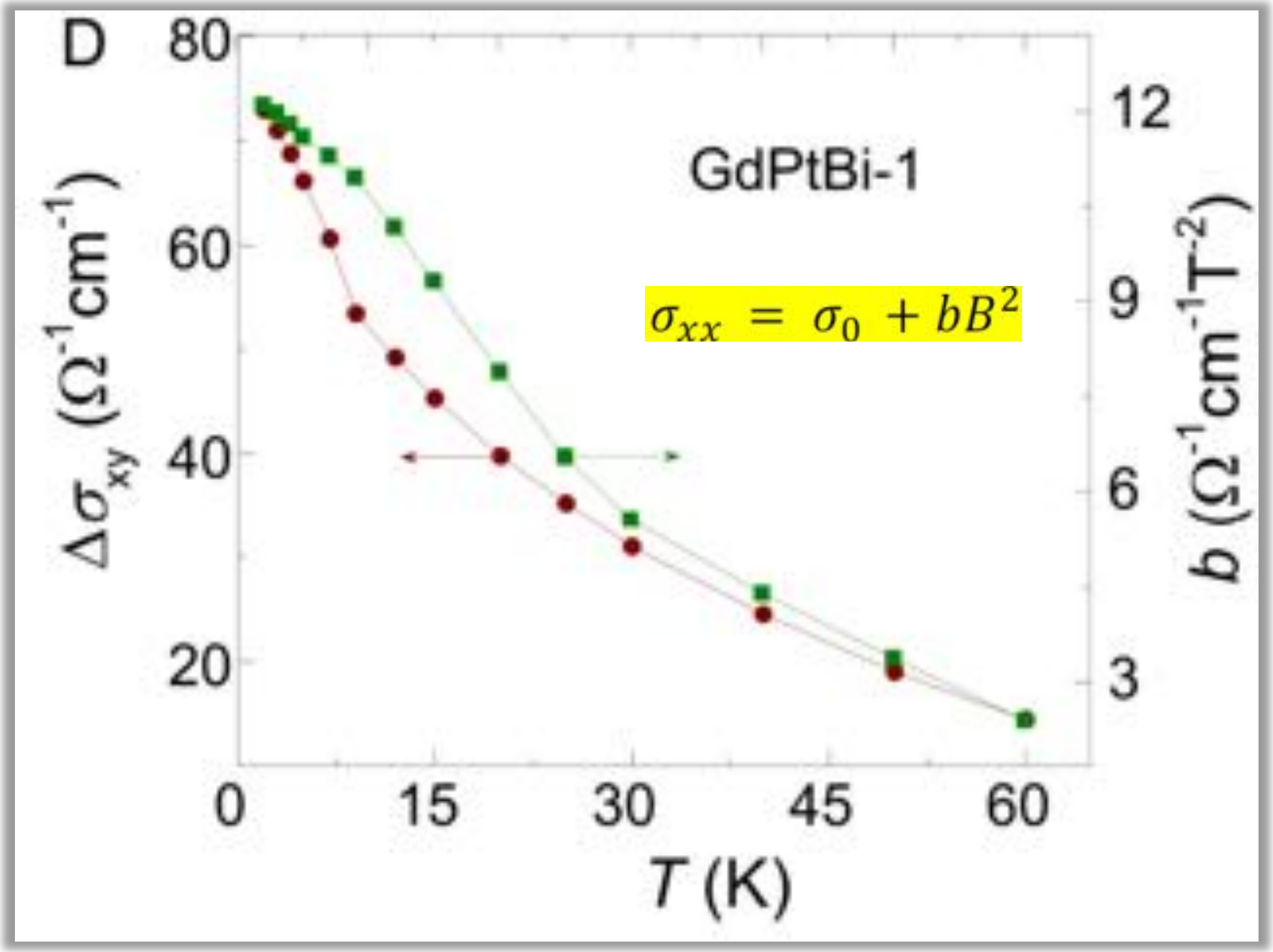

C. Shekhar et al., arXiv:1604.01641, (2016).
Claudia Felser and Binghai Yan, Nature Materials 15 (2016) 1149
M. Hirschberger et al. Nature Mat. online, arXiv:1602.07219, (2016).

GdPtBi – Anomalous Hall Effect

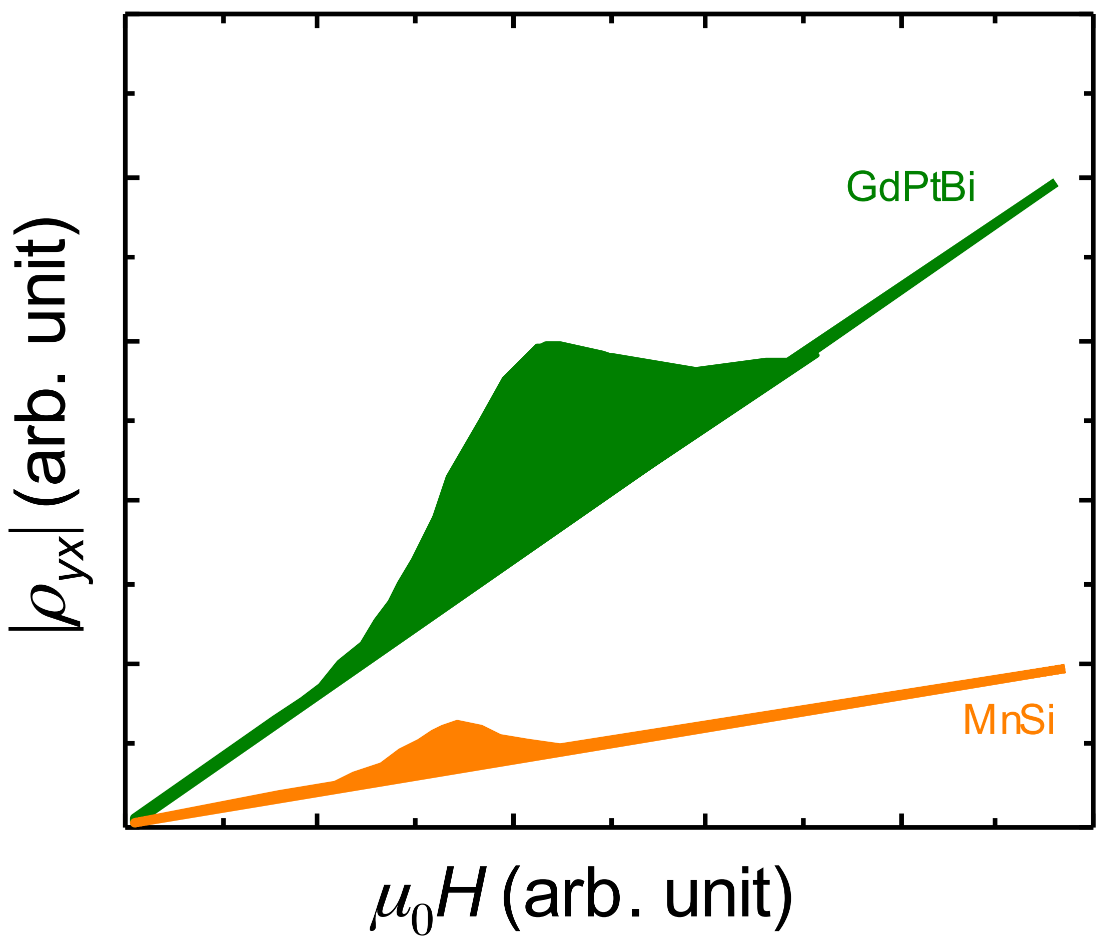

Do Antiferromagnets have AHE

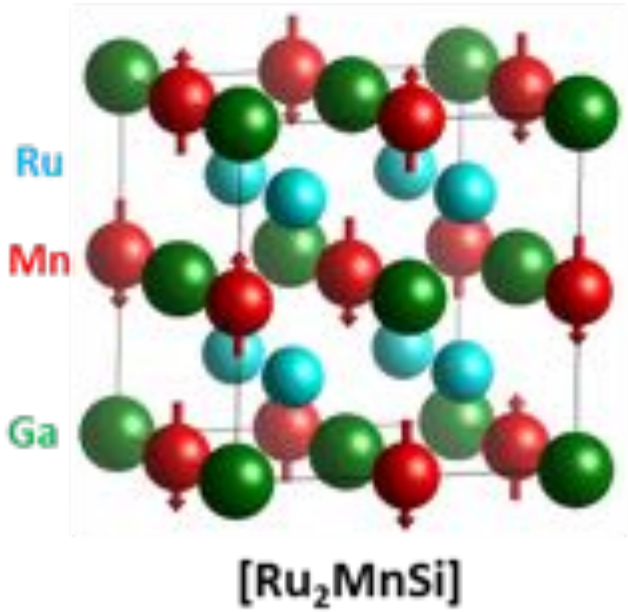

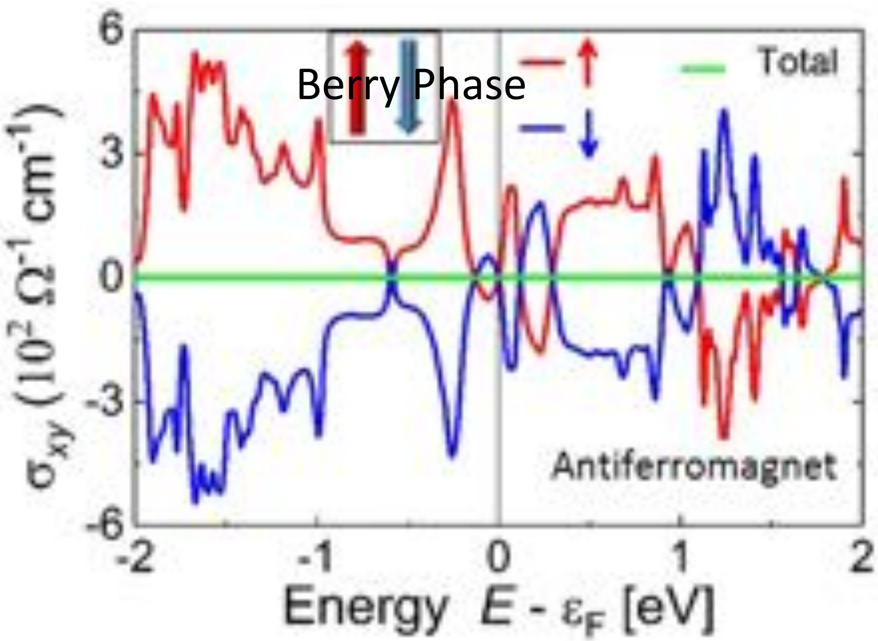

$$\rho_H = R_0 B + \boxed{4\pi R_s M}$$

No ! – No Berry phase

Heusler Weyl and Berry

Materials: … to half metallic ferromagnets

X_2YZ

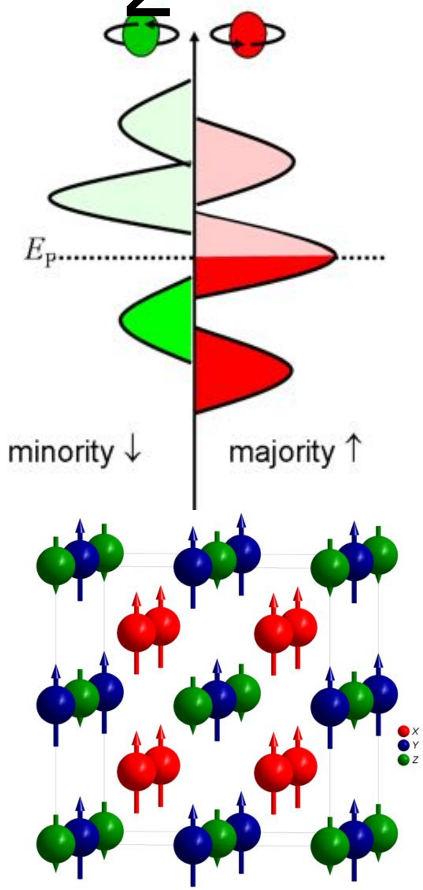

Kübler *et al.*, PRB **28**, 1745 (1983)
de Groot RA, et al. PRL **50** 2024 (1983)
Galanakis *et al.*, PRB **66**, 012406 (2002)

Example: Co_2MnSi

- magic valence electron number: 24
- valence electrons = 24 + magnetic moments

Co_2MnSi: $2\times9 + 7 + 4 = 29$ Ms = $5\mu_B$

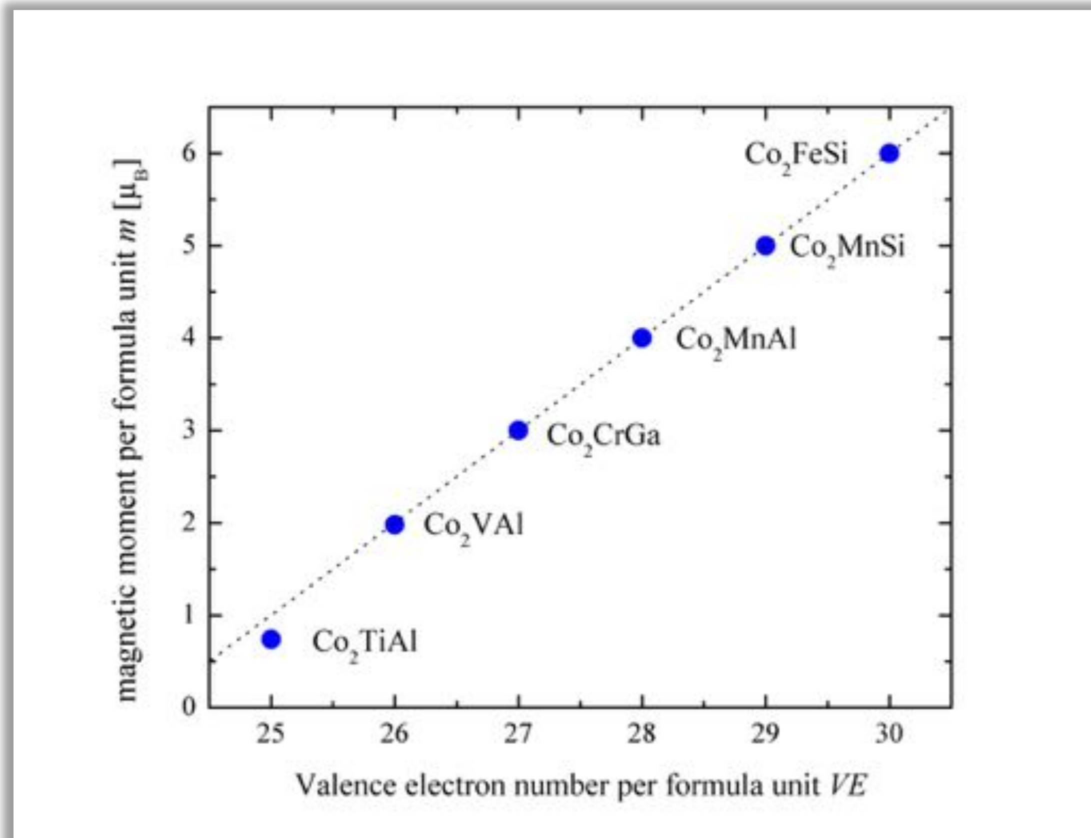

Weyl semimetals in Heusler compounds

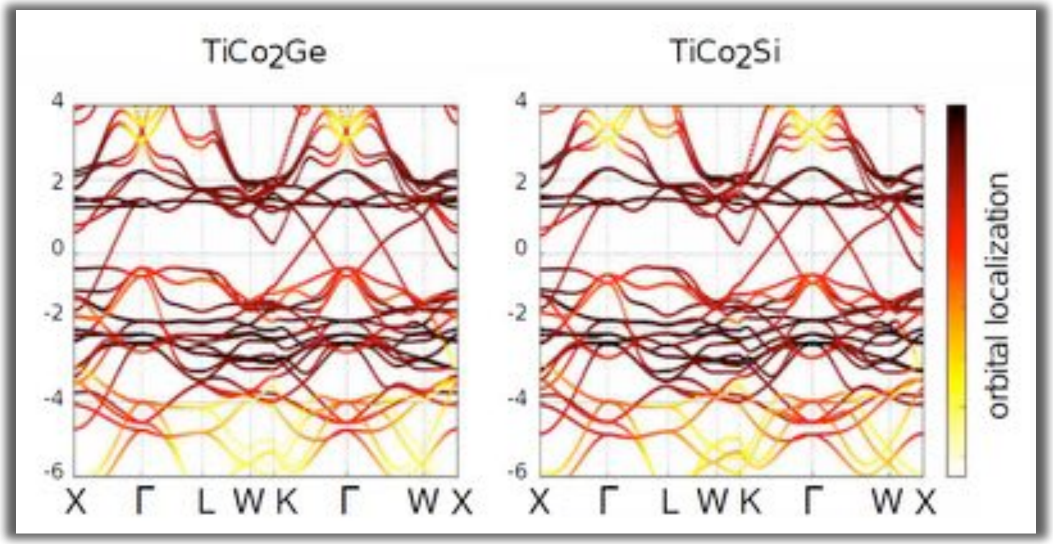

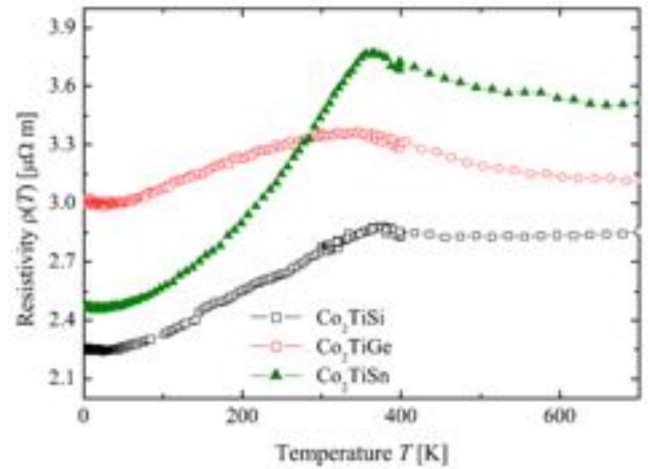

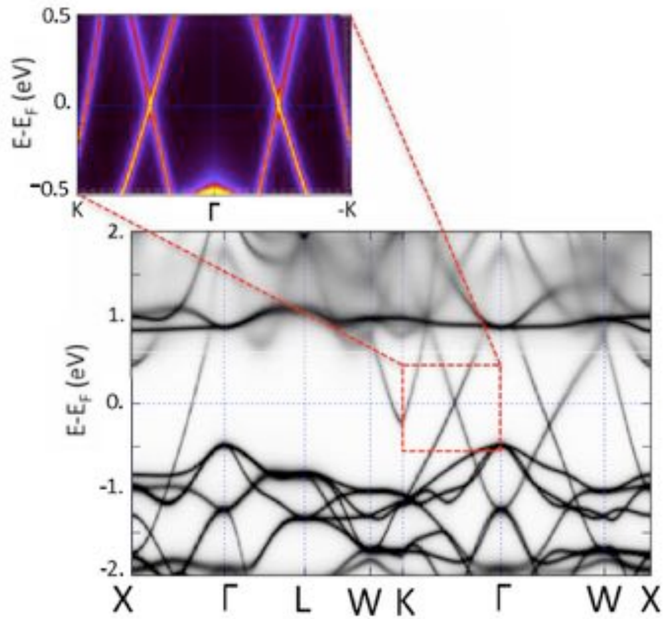

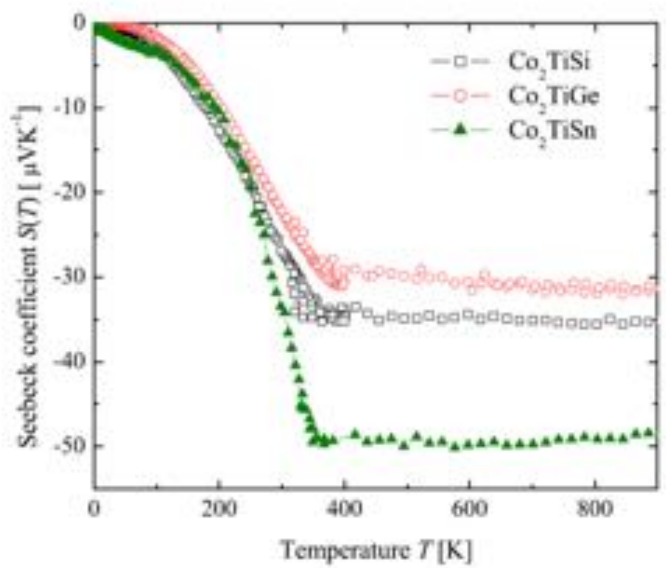

Zhijun Wang, et al., arXiv:1603.00479
Guoqing Chang et al., arXiv:1603.01255

Barth et al. PRB 81, 064404 2010

AHE in half metallic ferromagnets

PHYSICAL REVIEW B **85**, 012405 (2012)

Berry curvature and the anomalous Hall effect in Heusler compounds

Jürgen Kübler[1,*] and Claudia Felser[2]

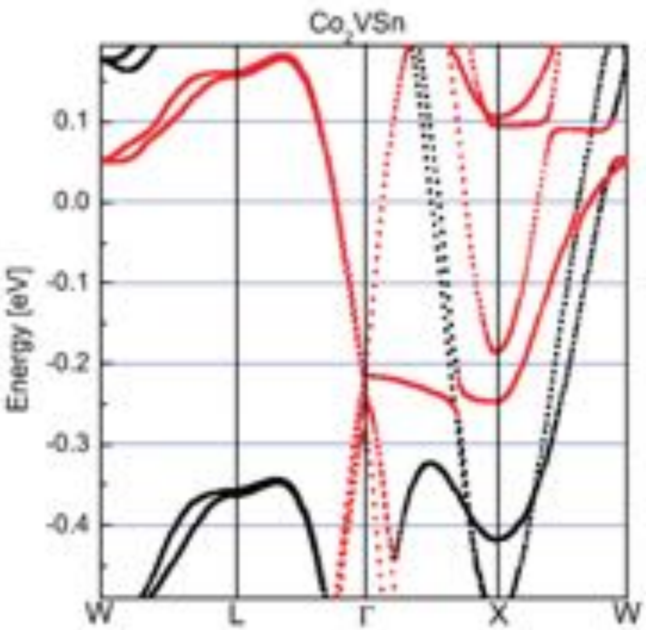

FIG. 4. (Color online) Band structure near the Fermi edge of Co$_2$VSn. Majority-spin electron states appear in red, minority-spin states in black. Note the Dirac cone at the Γ point at about −0.22 eV.

Compound[a]	N_V	a (nm)	M^{exp}	M^{calc}	σ_{xy}	P (%)
Co_2VGa	26	0.5779	1.92	1.953	66	65
Co_2CrAl	27	0.5727	1.7	2.998	438	100
Co_2VSn	27	0.5960	1.21	1.778	−1489	35
Co_2MnAl	28	0.5749	4.04	4.045	1800	75
Rh_2MnAl	28	0.6022		4.066	1500	94
Mn_2PtSn[b]	28	0.4509 (1.3477)		6.66	1108	91
Co_2MnSn	29	0.5984	5.08	5.00	118	82
Co_2MnSi	29	0.5645	4.90	4.98	228	100

The AHE depends only on the Berry curvature in Heusler compounds and not on the magnetisation

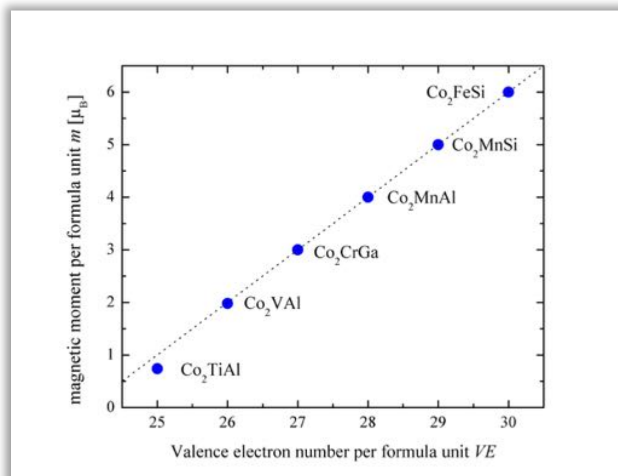

$$\rho_H = R_0 B + \boxed{4\pi R_s M}$$

Kübler, Felser, PRB 85 (2012) 012405
Vidal et al Appl.Phys.Lett. 99 (2011) 132509
Kübler, Felser, EPL 114 (2016) 47005.

AHE in half metallic ferromagnets with Weyl

Giant AHE in Co_2MnAl

$$\sigma_{xy} = 1800\,\mathrm{S/cm}\ \ \mathrm{calc.}$$
$$\sigma_{xy} \approx 2000\,\mathrm{S/cm}\ \ \mathrm{meas.}$$

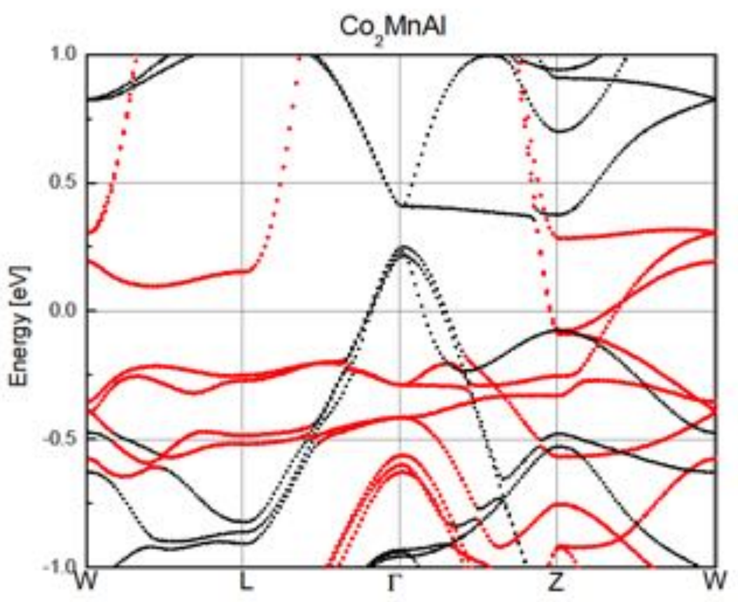

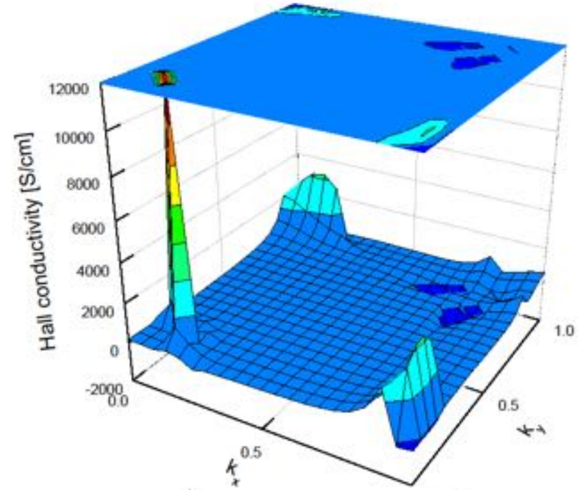

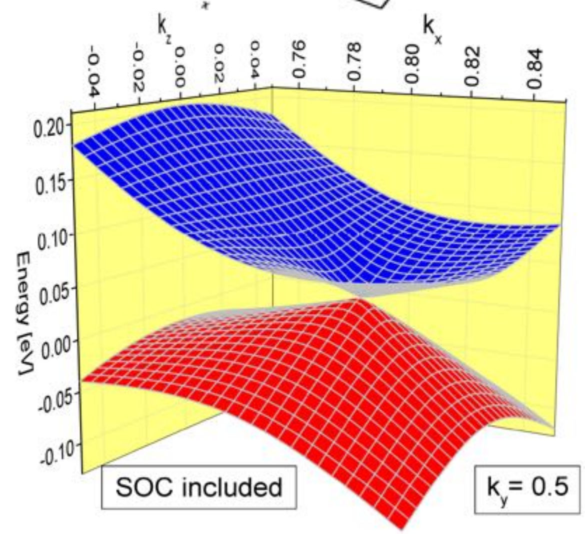

Weyl points are the origin for a large Berry phase and a Giant AHE

Kübler, Felser, PRB 85 (2012) 012405
Vidal et al Appl.Phys.Lett. 99 (2011) 132509
Kübler, Felser, EPL 114 (2016) 47005.

Heusler, Weyl and Berry

Can we design an AFM with a Berry curvature

Hexagonal Antiferromagnet

A Letters Journal Exploring the Frontiers of Physics

December 2014

EPL, 108 (2014) 67001

www.epljournal.org

doi: 10.1209/0295-5075/108/67001

Non-collinear antiferromagnets and the anomalous Hall effect

J. Kübler[1] and C. Felser[2]

PRL 112, 017205 (2014) PHYSICAL REVIEW LETTERS week ending 10 JANUARY 2014

Anomalous Hall Effect Arising from Noncollinear Antiferromagnetism

Hua Chen, Qian Niu, and A. H. MacDonald

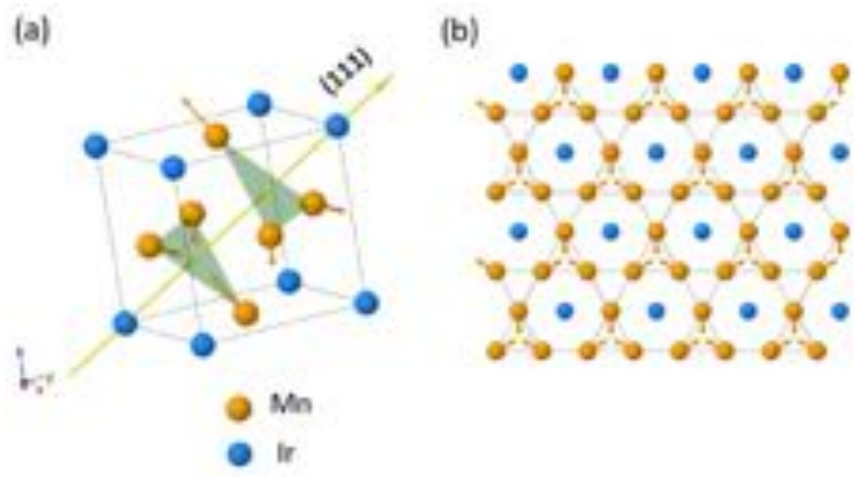

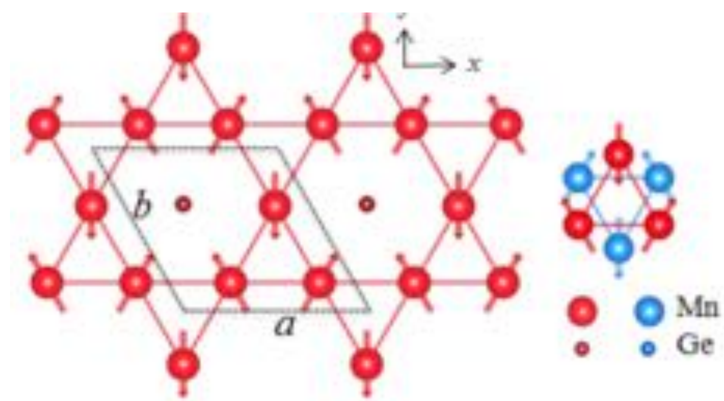

Chen, Niu, and MacDonald, Phys. Rev. Lett., 112 (2014) 017205

Kübler and Felser EPL 108 (2014) 67001

Non-collinear AFM in metallic Mn_3Ge

The anomalous Hall conductivities are normally assumed to be proportional to magnetization

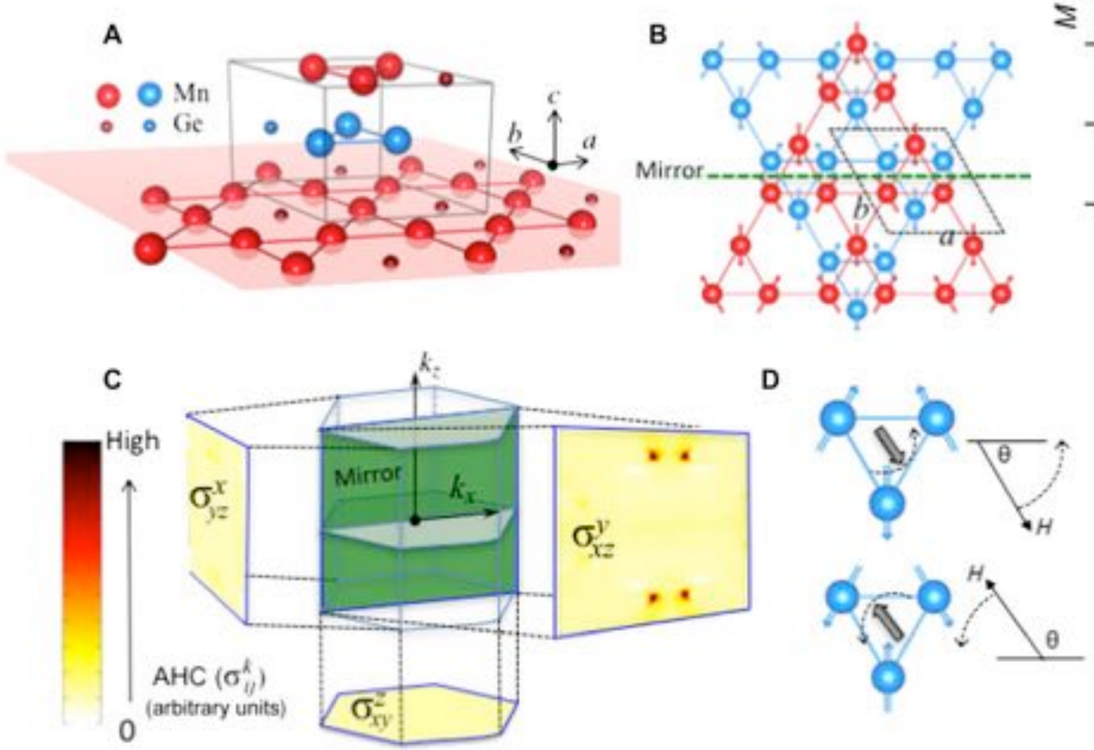

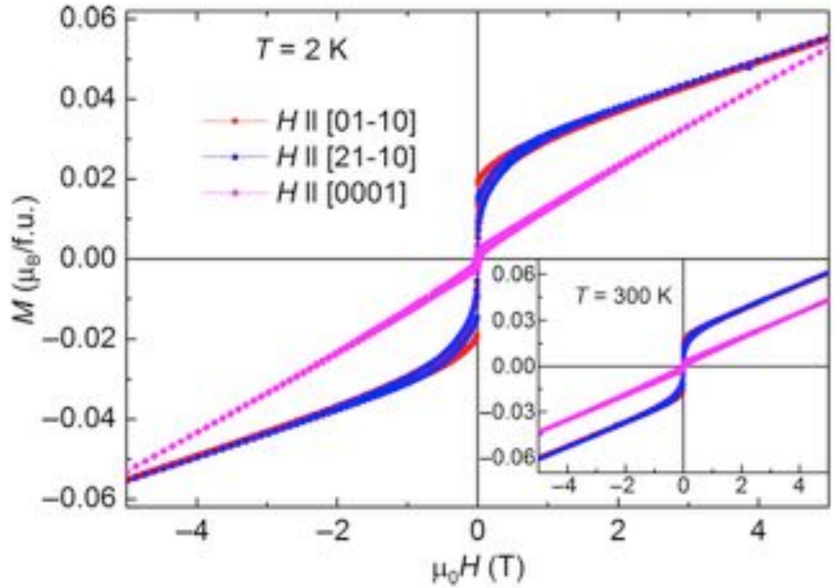

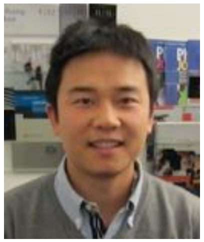

Kübler and Felser EPL 108 (2014) 67001
Nayak et al. preprint: arXiv:1511.03128, Science Advances 2 (2016) e1501870

Non-collinear AFM Mn_3Ge/Mn_3Sn

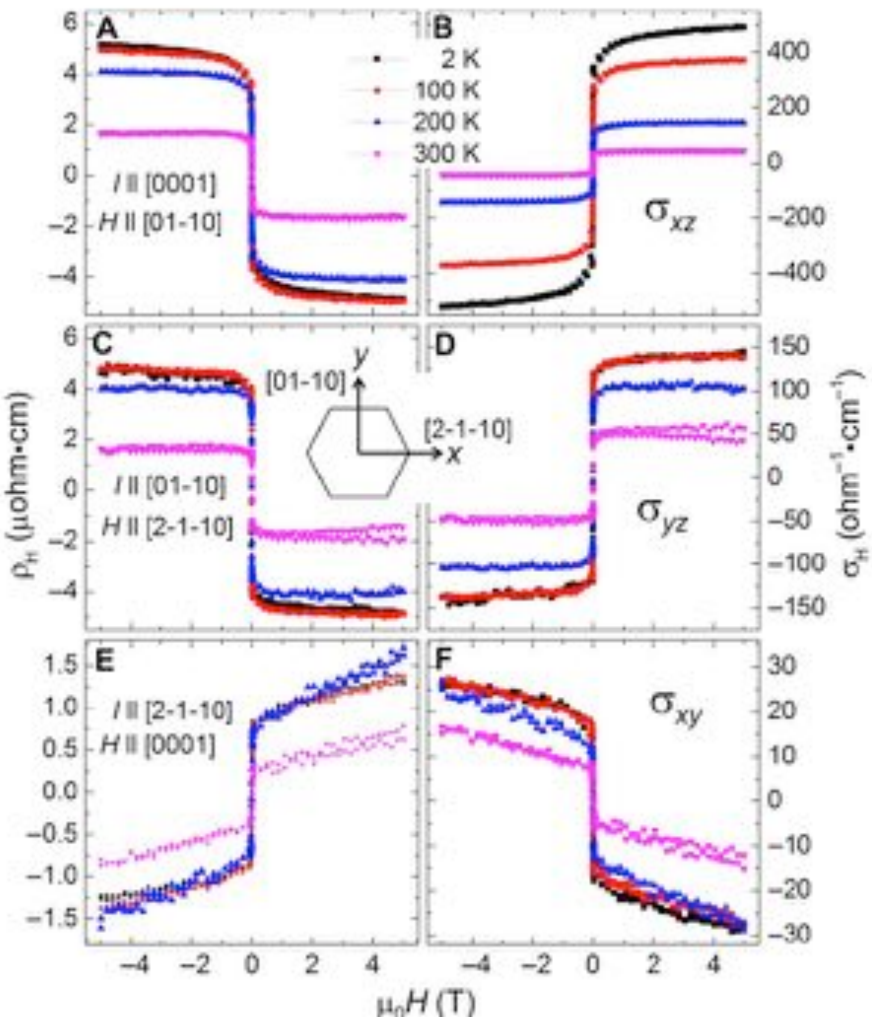

LETTER

doi:10.1038/nature15723

Large anomalous Hall effect in a non-collinear antiferromagnet at room temperature

Satoru Nakatsuji[1,2], Naoki Kiyohara[1] & Tomoya Higo[1]

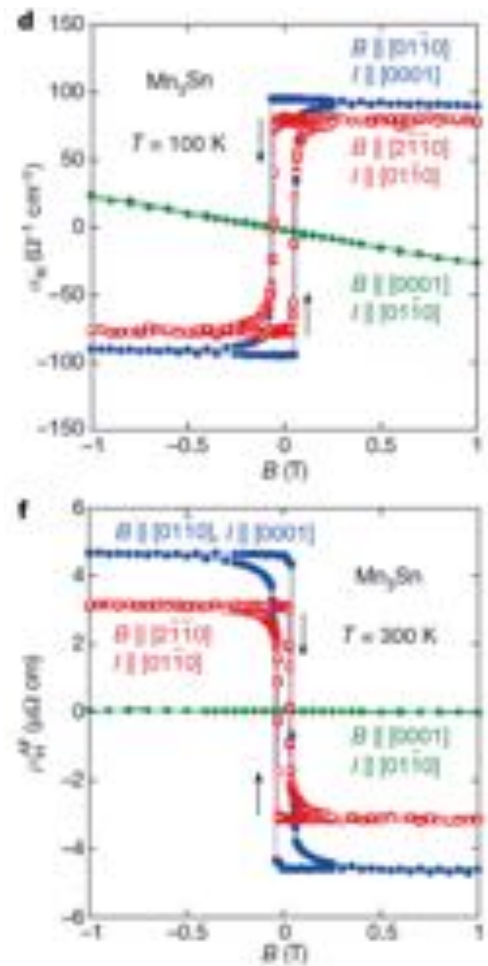

Nayak et al. preprint: arXiv:1511.03128, Science Advances 2 (2016) e1501870

Kiyohara, Nakatsuji, preprint: arXiv:1511.04619,

Nakatsuji, Kiyohara, & Higo, Nature, doi:10.1038/nature15723

Neel Temperature

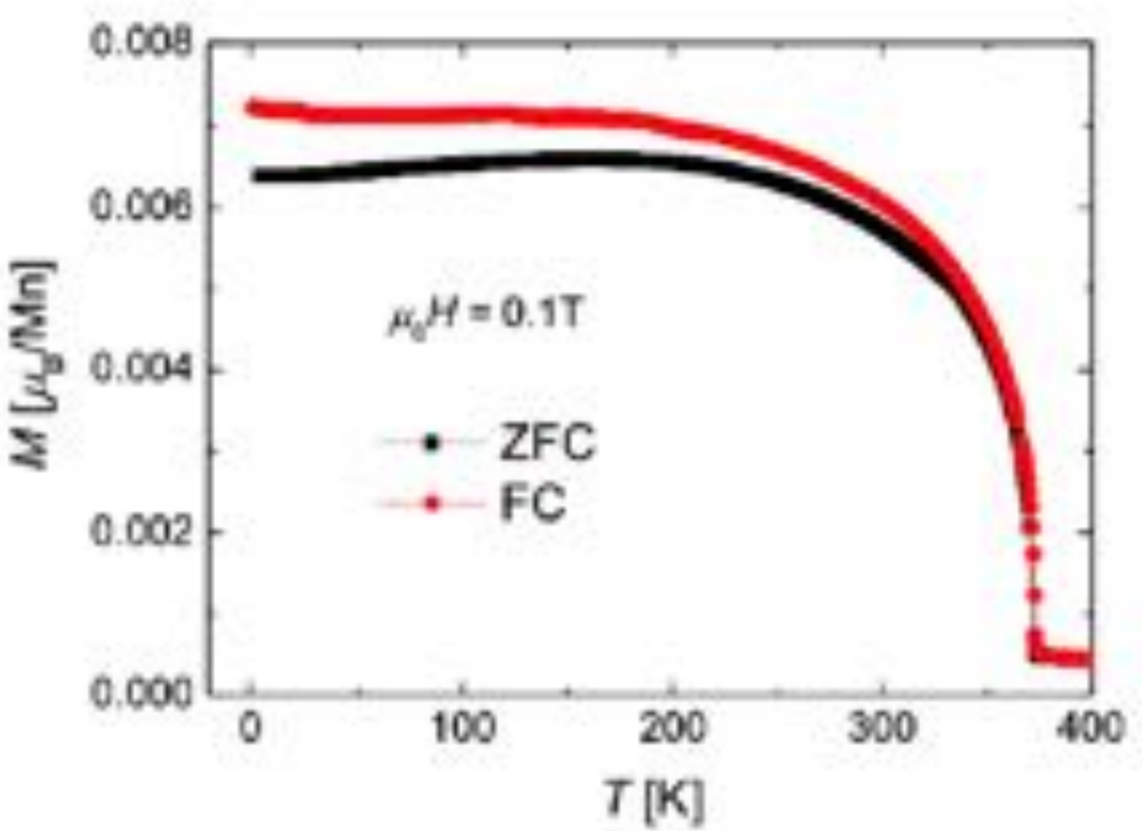

And more … Giant Nernst, has already shown switching …

Nayak et al. preprint: arXiv:1511.03128, Science Advances 2 (2016) e1501870
Kiyohara, Nakatsuji, preprint: arXiv:1511.04619,

Fermiarcs in the Weyl AFM

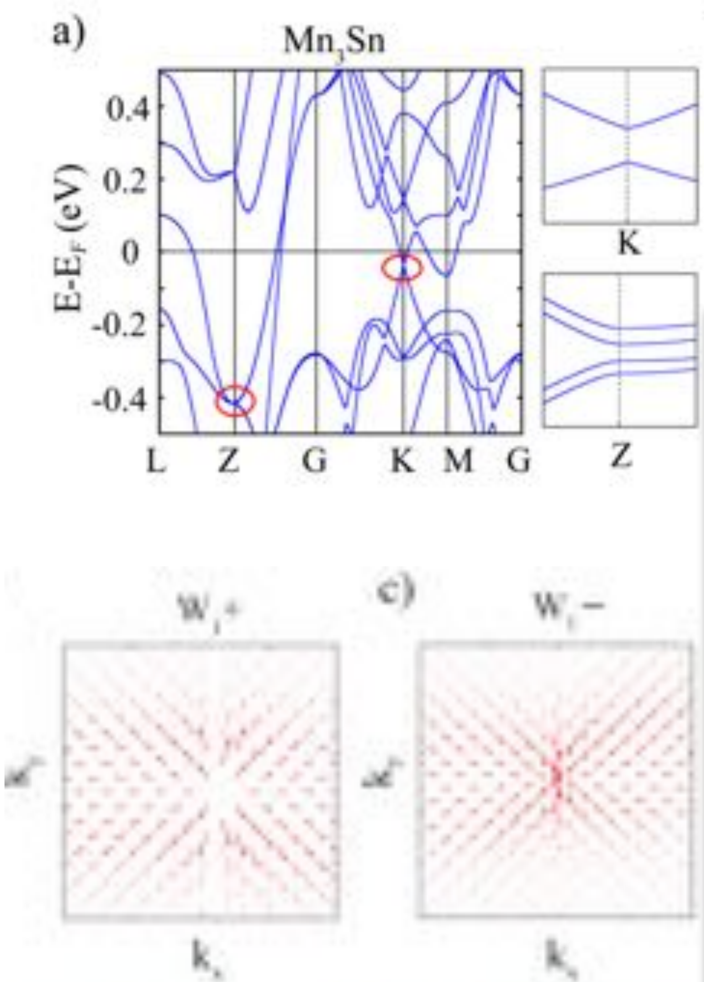

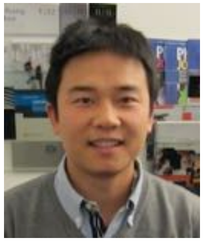

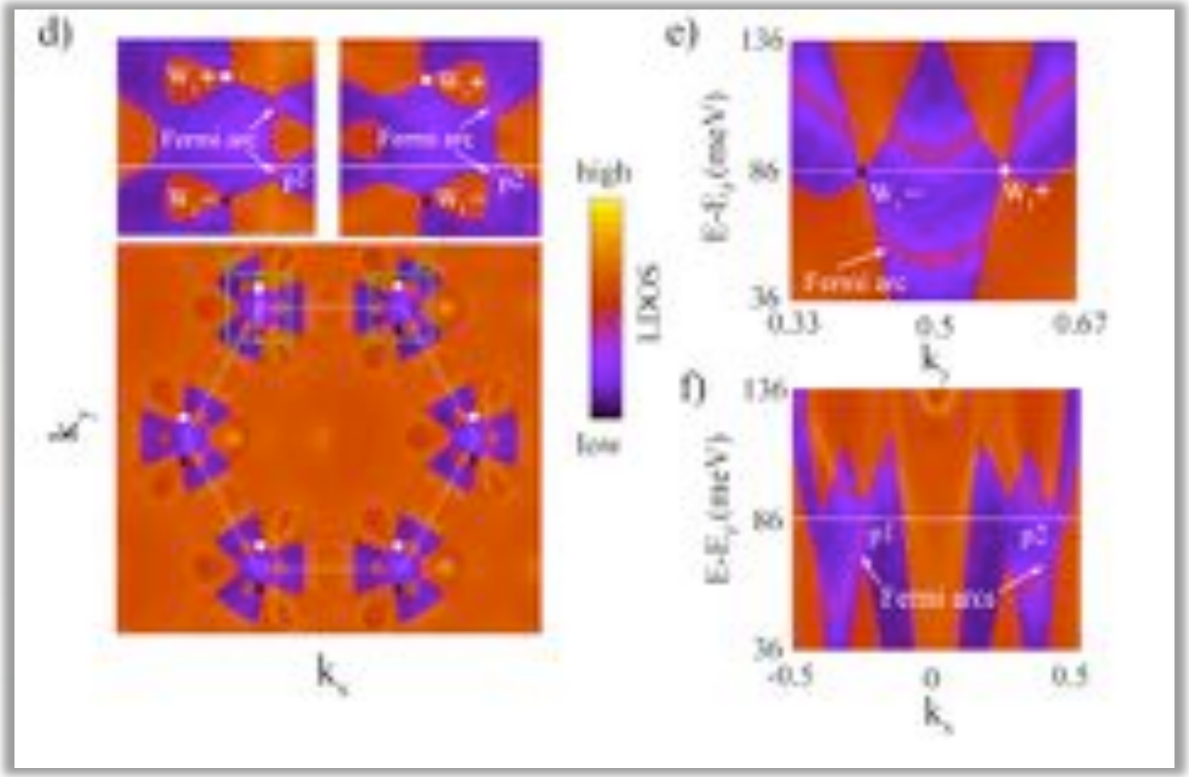

Hao Yang, et al. , preprint: arXiv:1608.03404

Application Spin Hall Effect

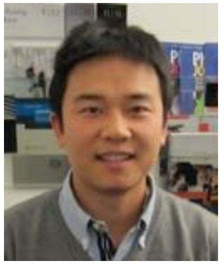

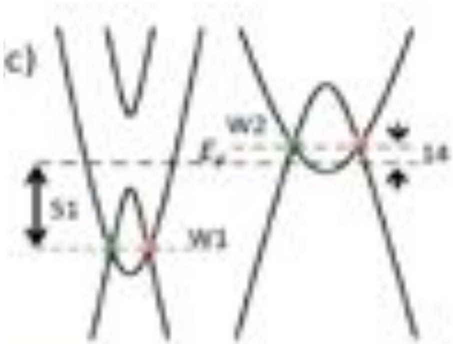

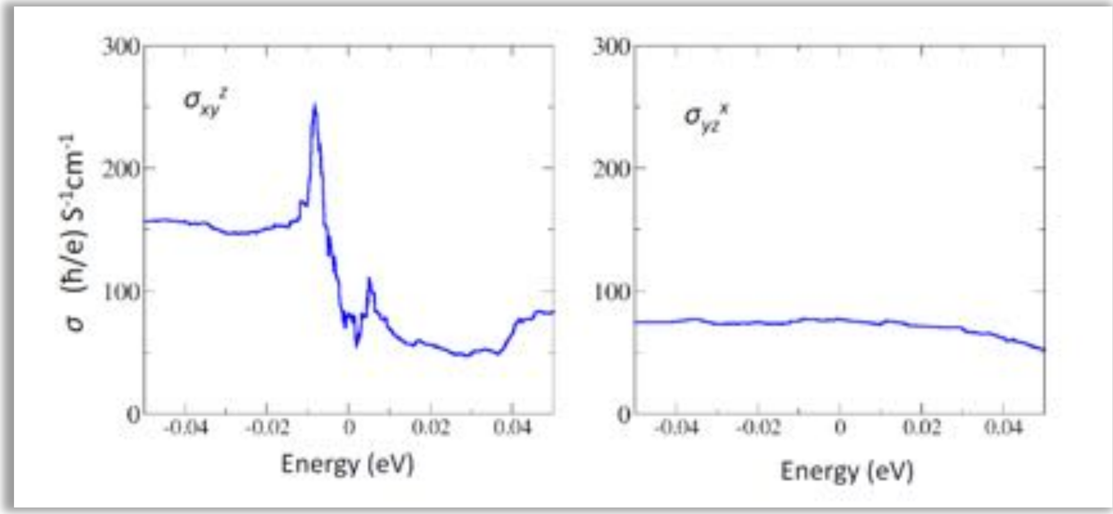

Yan Sun et al., Physical Review Letter 117 (2016) 146401

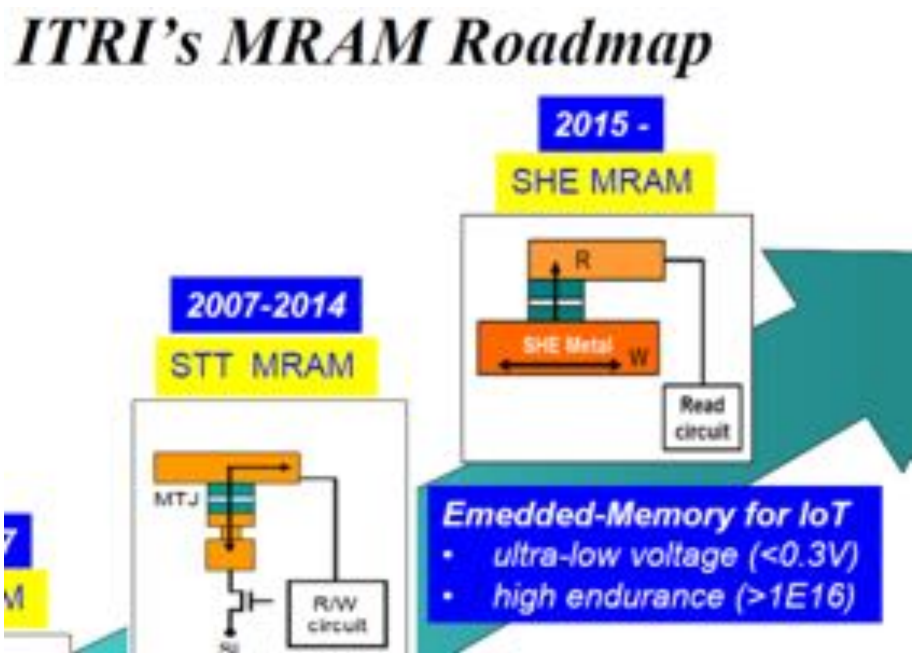

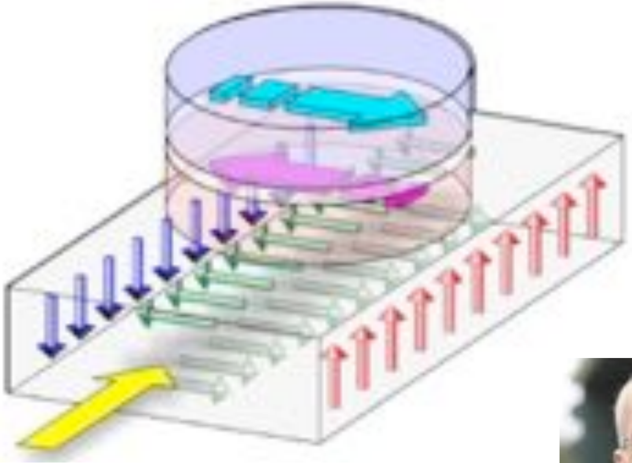

Giant AHE in AFM

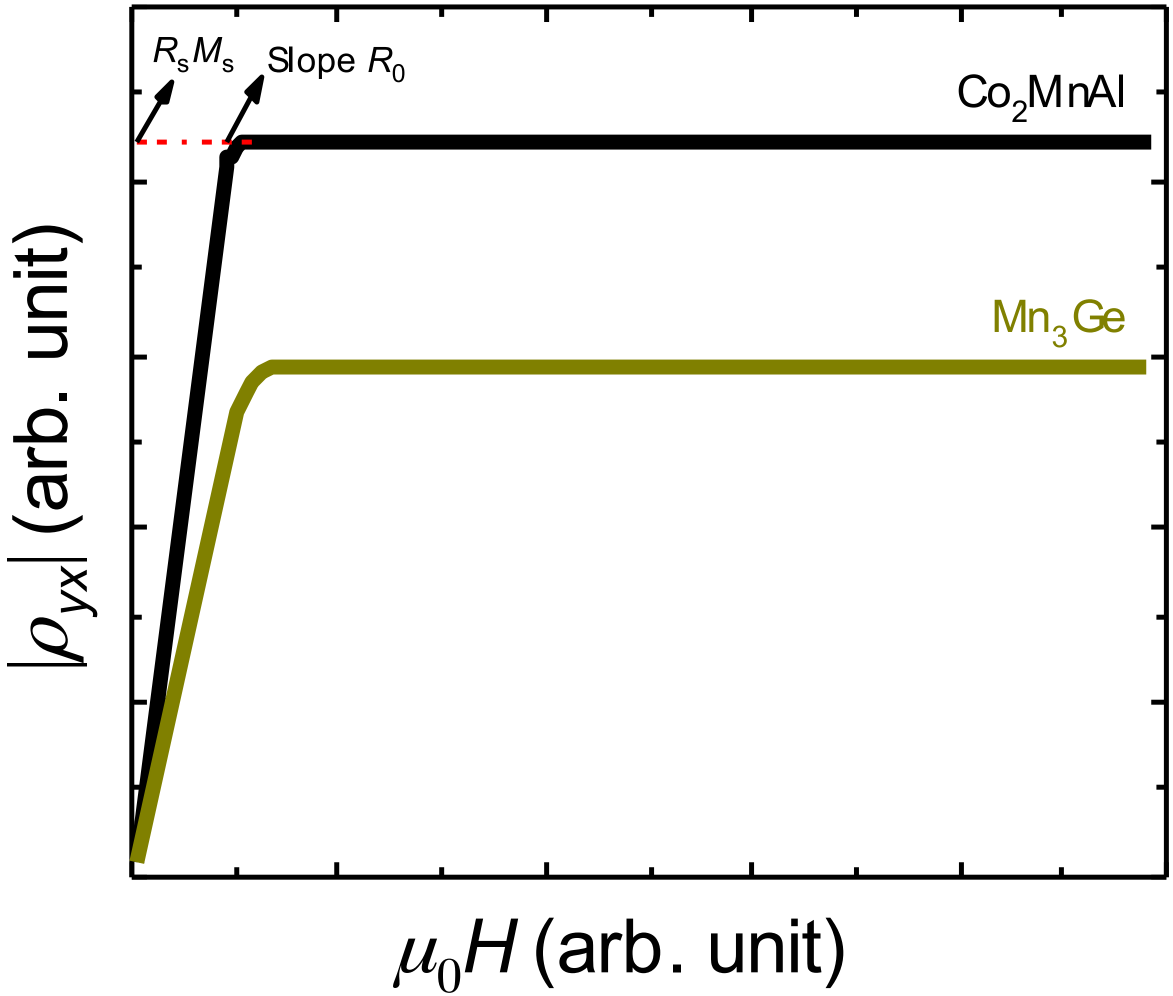

Heusler, Weyl and Berry

Can we design an a Ferro/Ferrimagnet with a zero Berry curvature

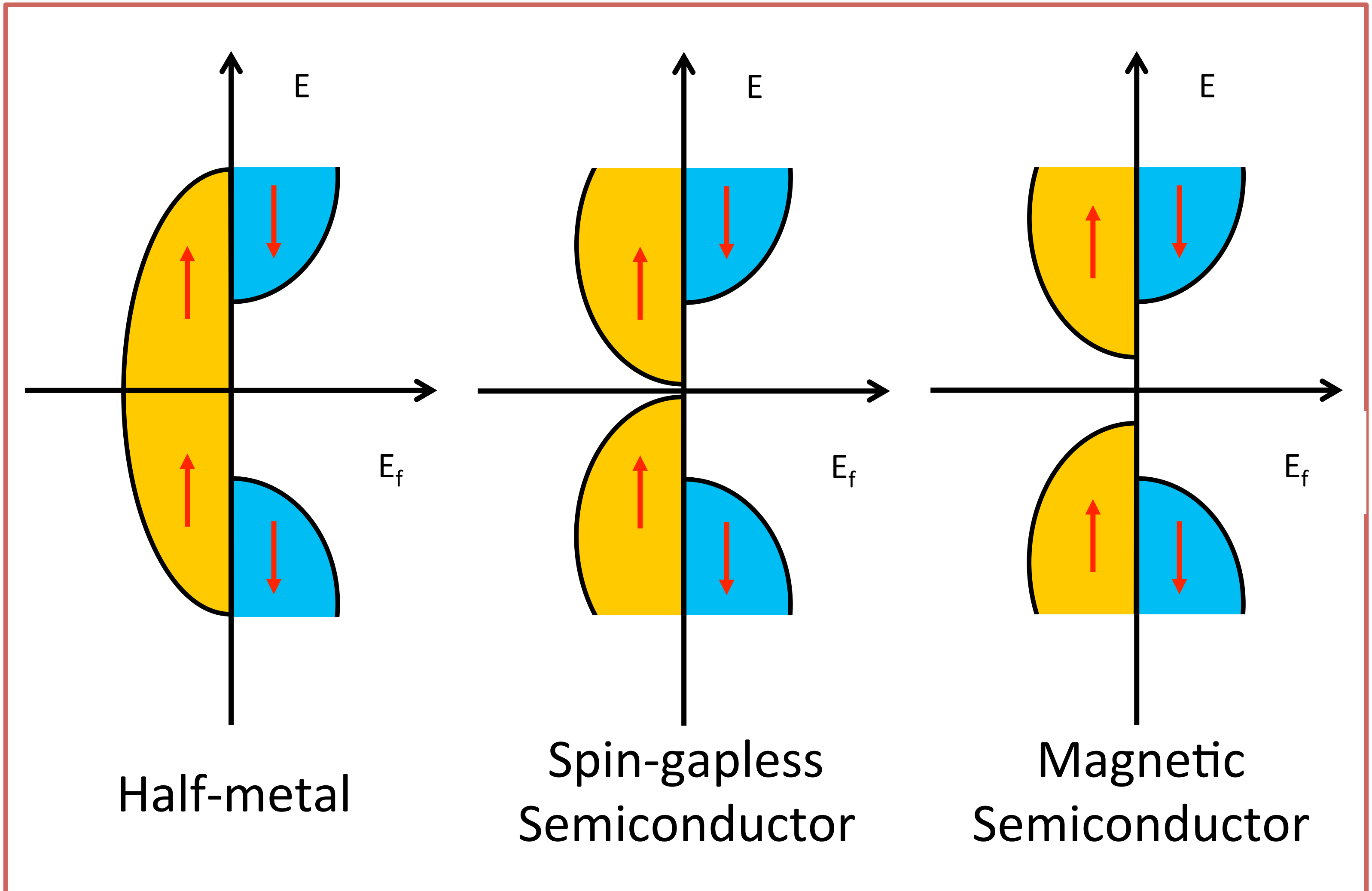
E
E
E
E_f
E_f
E_f
Half-metal
Spin-gapless
Semiconductor
Magnetic
Semiconductor

Weyl or Spingapless

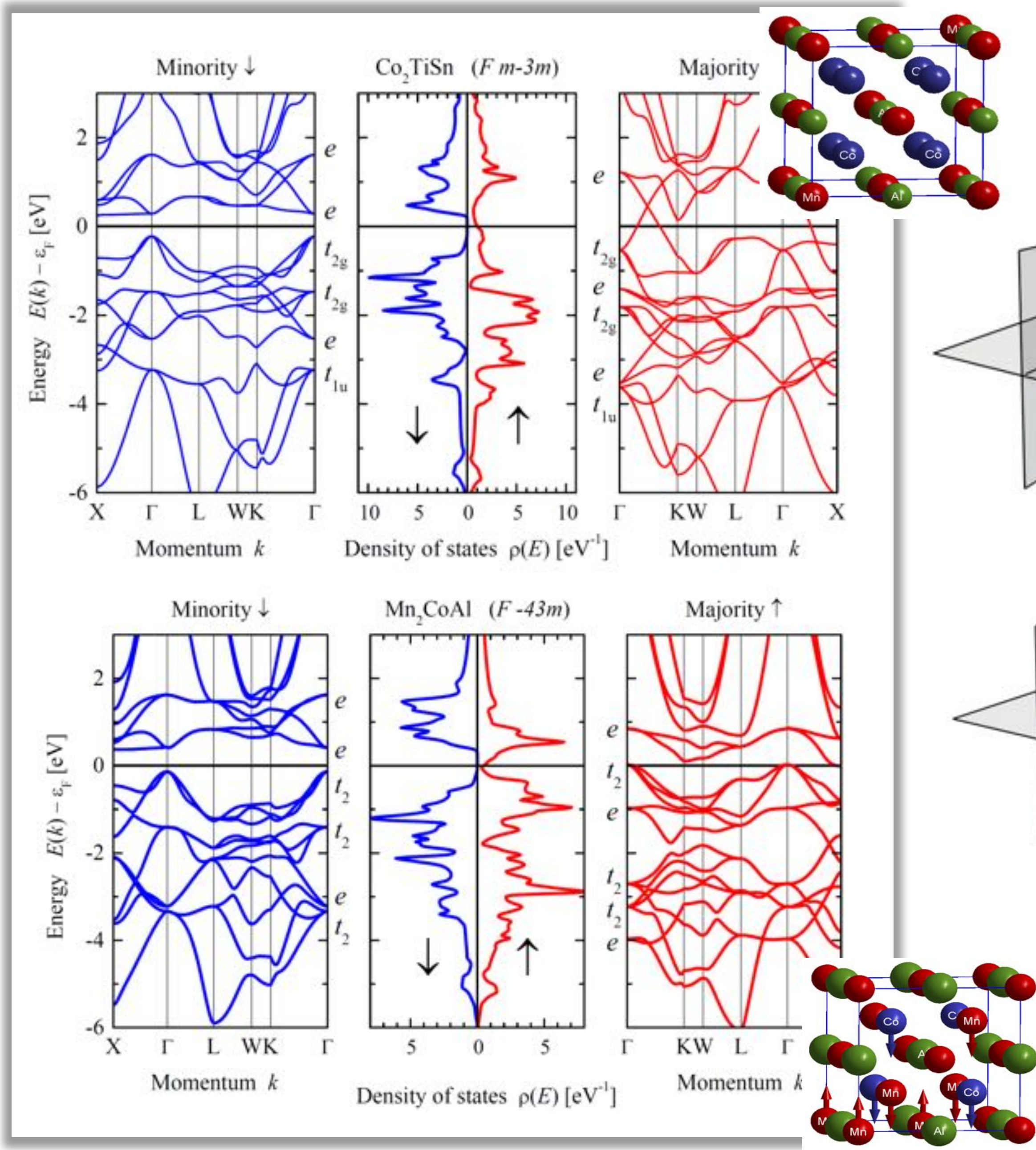

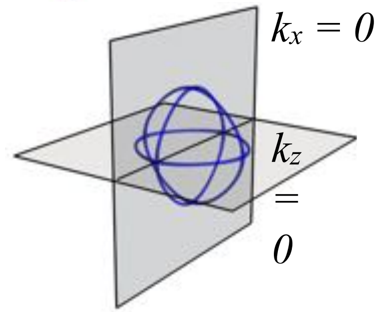

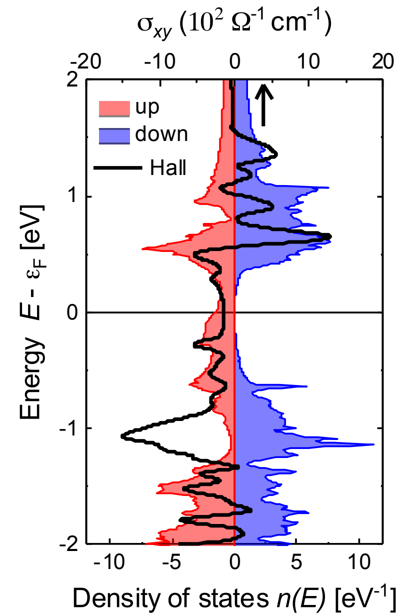

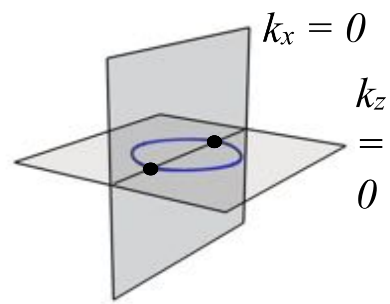

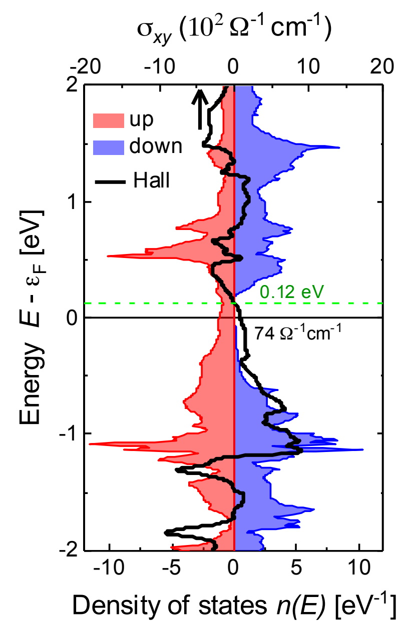

Weyl or Spingapless

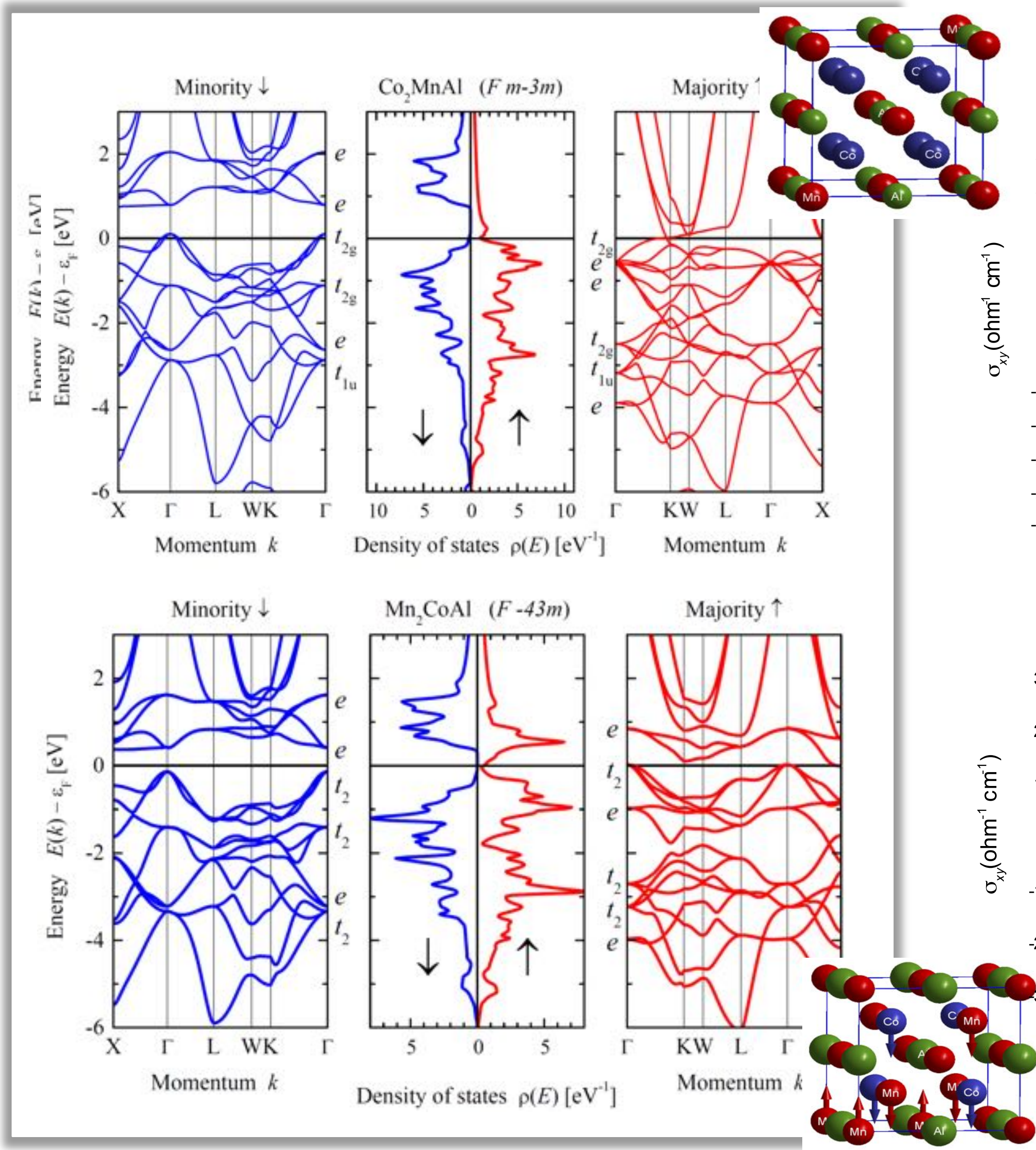

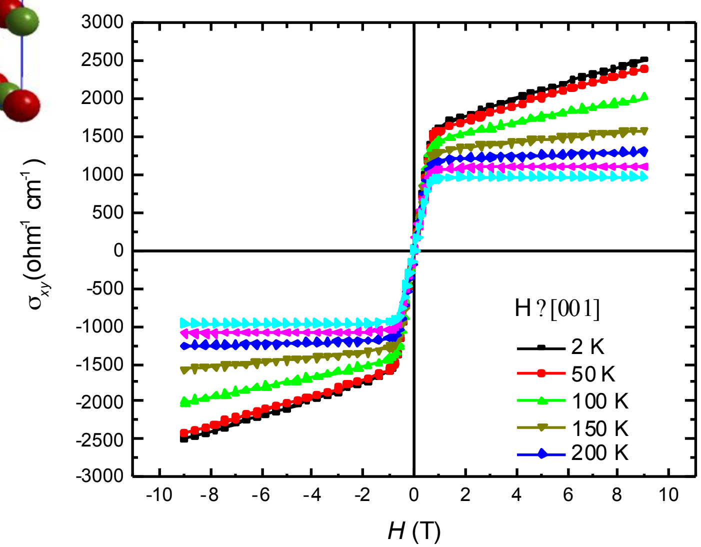

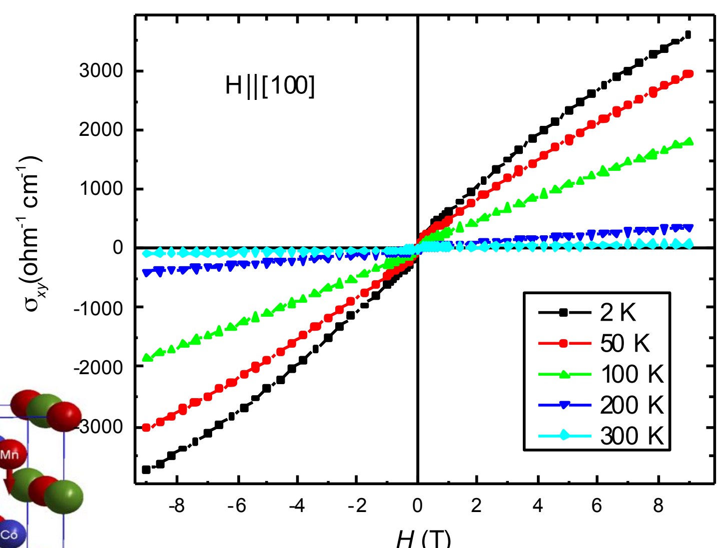

Weyl or Spingapless

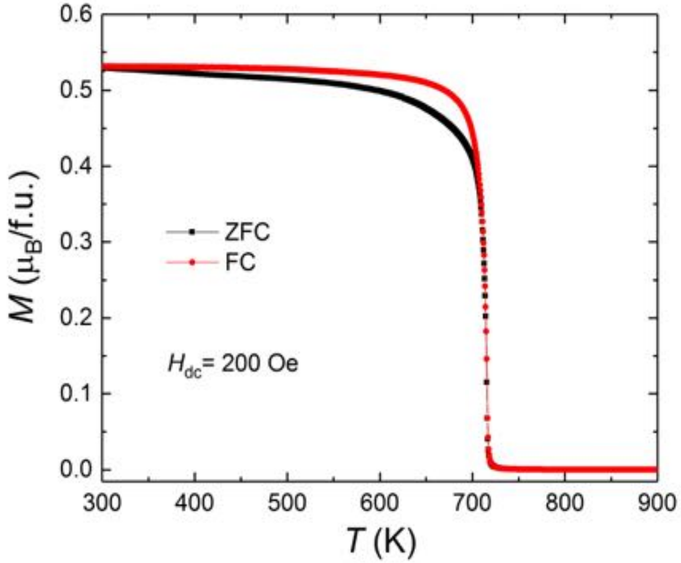

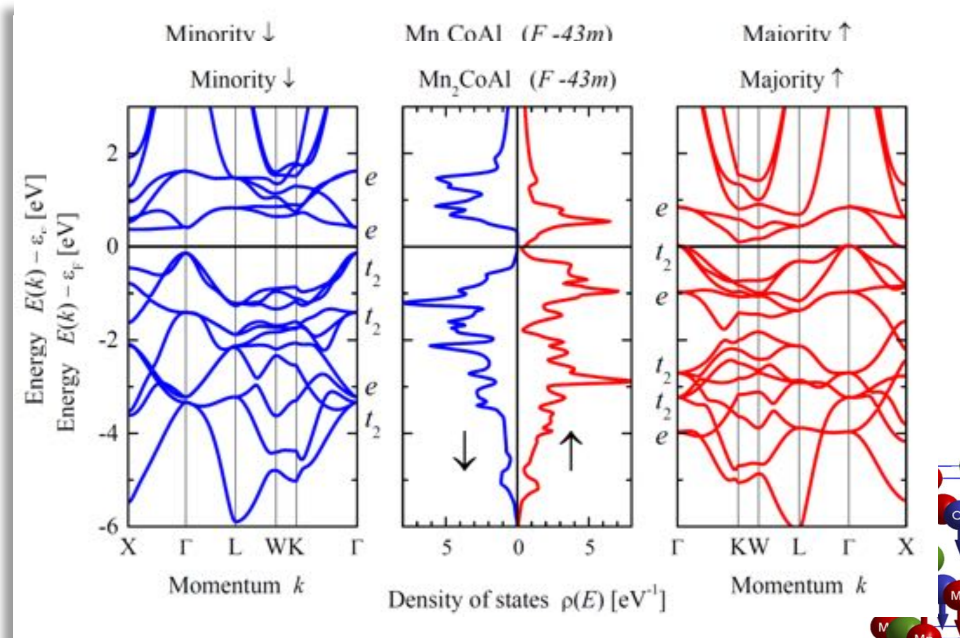

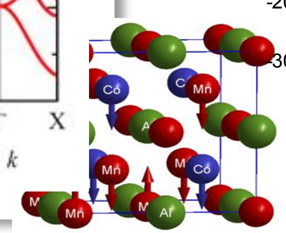

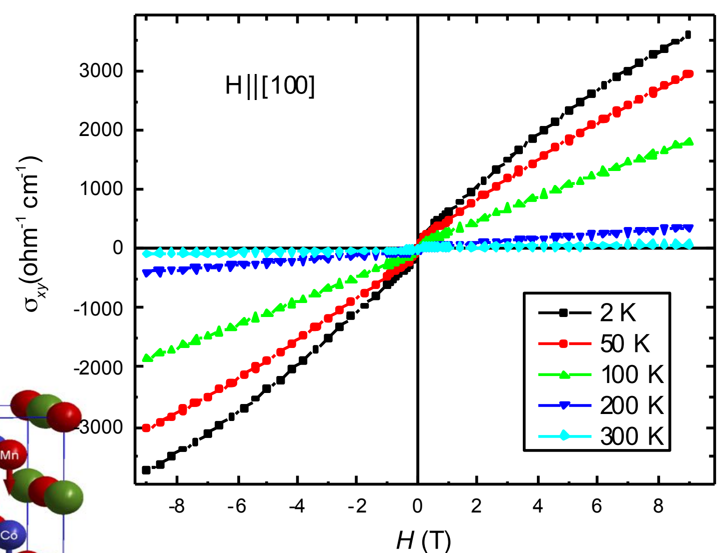

More semiconductors

26

Mn2CoAl

CoMn2Al

CoFeCrAl

CoMnCrSi

CoFeVSi

FeMnCrSb

18

V_3Al

21

FeVTiSi

CoVScSi

FeCrScSi

FeVTiSi

FeMnScAl

28

CoFeMnSi

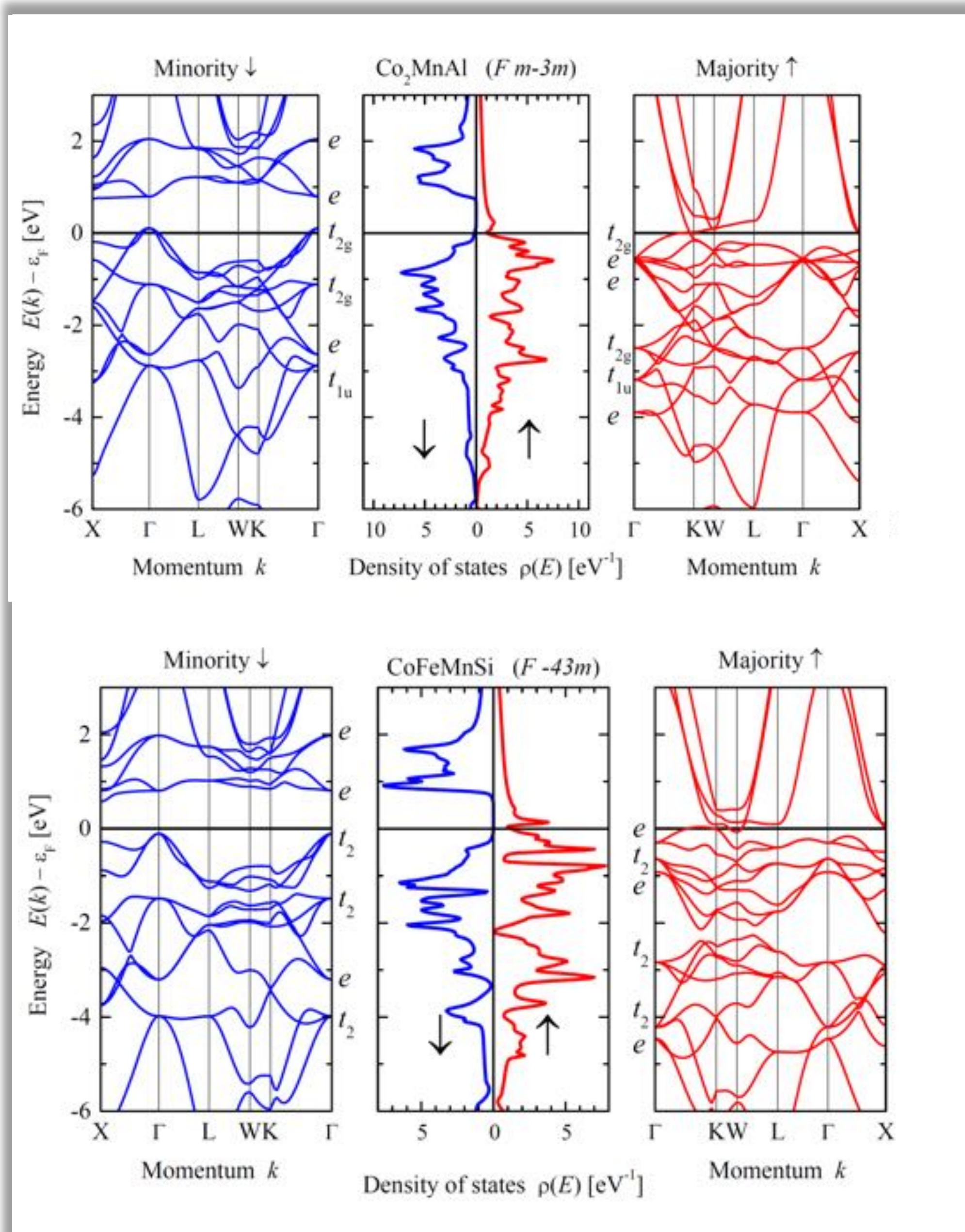

Anomalous Hall effect

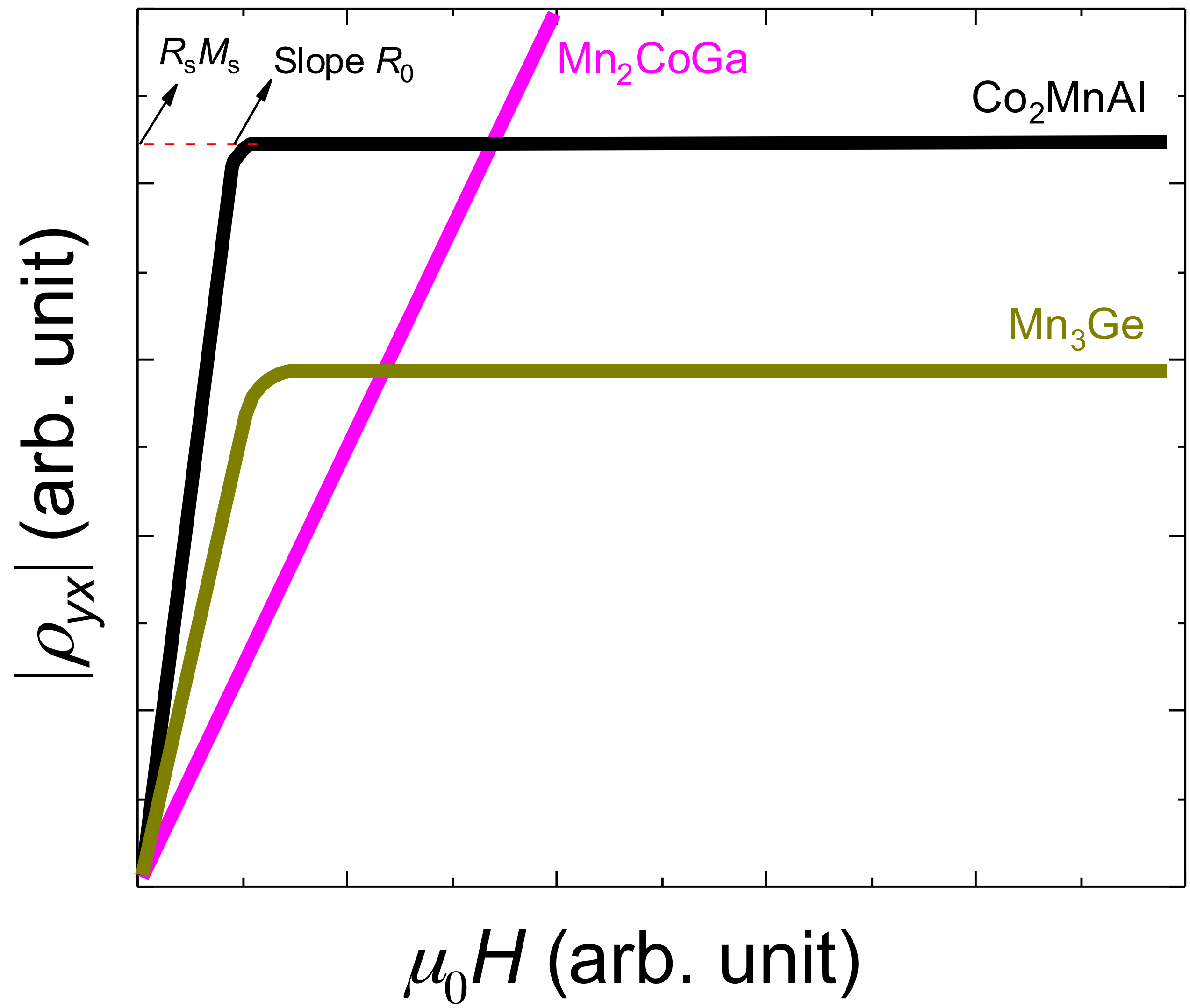

Anomalous Hall effect

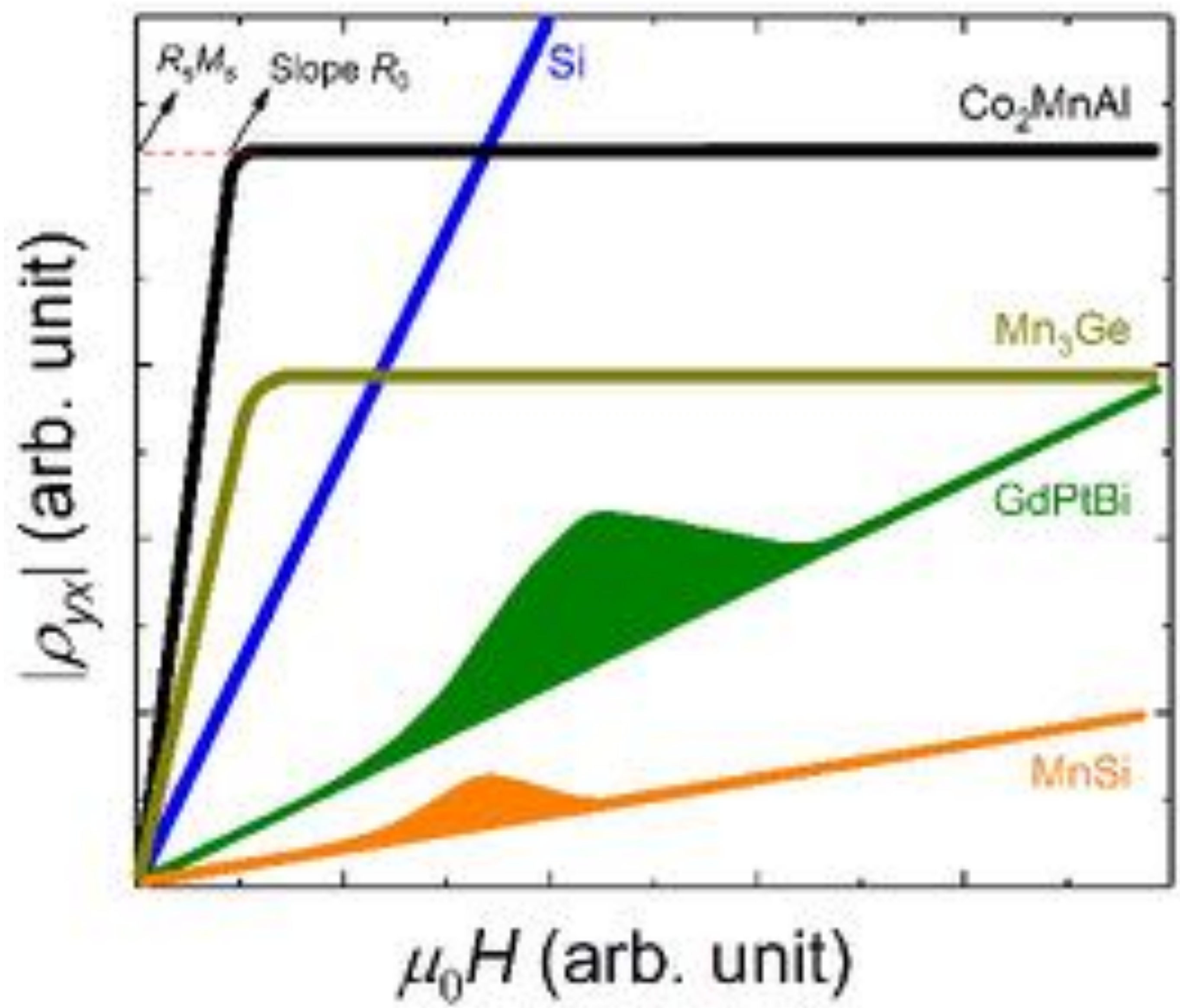

Single Crystals available

BaCr2As2
BaCrFeAs2

CaPd3O4
SrPd3O4
BaBiO3

Bi2Te2Se
Bi2Te3
Bi2Se3
BiSbTe2S
BiTeI
BiTeBr
BiTeCl

LaBi, LaSb
GdBi, GdSb

HfSiS

Bi4I4

BaSn2

AlPt
GdAs
CoSi

MoP
WP

TaP
NbP
NbAs
TaAs
NbP-Mo
NbP-Cr
TaP-Mo
TaAsP

CrNb3S6
V3S4
Cd3As2

MnP
MnAs

MoSe2-xTex
MoTe2-xSex
MoTe2 (T´/2H)

PtTe2
PtSe2
PdTe2
PdSe2
OsTe2
RhTe2
TaTe2
NbTe2
WSe2
HfTe5
MoTe2
TaS2
PdSb2
CuxWTe2
FexWTe2
WTe2
Co0,4TaS2
Fe0,4TaS2

Ag2Se
IrO2
OsO2
ReO2
WP2
MoP2

VAl3
Mn3Ge
Mn3Ir
Mn3Rh
Mn3Pt
[illegible]

YPtBi
NdPtBi
GdPtBi
YbPtBi
ScPdBi
YPdBi
ErPdBi
GdAuPb
TmAuPb
AuSmPb
AuPrPb
AuNdPb
[illegible]
AuLuSn
AuYSn
ErAuSn
EuAuBi

CaAgAs

KMgSb
KMgBi
KHgSb
KHgBi
LiZnAs
LiZnSb

YbMnBi2
Ni2Mn1.4In0.6
YFe4Ge2

Mn1.4PtSn

CuMnSb
CuMnAs

Co2Ti0.5V0.5Sn
Co2VAl0.5Si0.5
Co2Ti0.5V0.5Si
Mn2CoGa
Co2MnGa
Co2Al9
Co2MnAl
Co2VGa0.5Si0.5
Co2TiSn
Co2VGa
Co2V0.8Mn0.2Ga
CoFeMnSi

Thank you!

Real space topology - Skyrmions

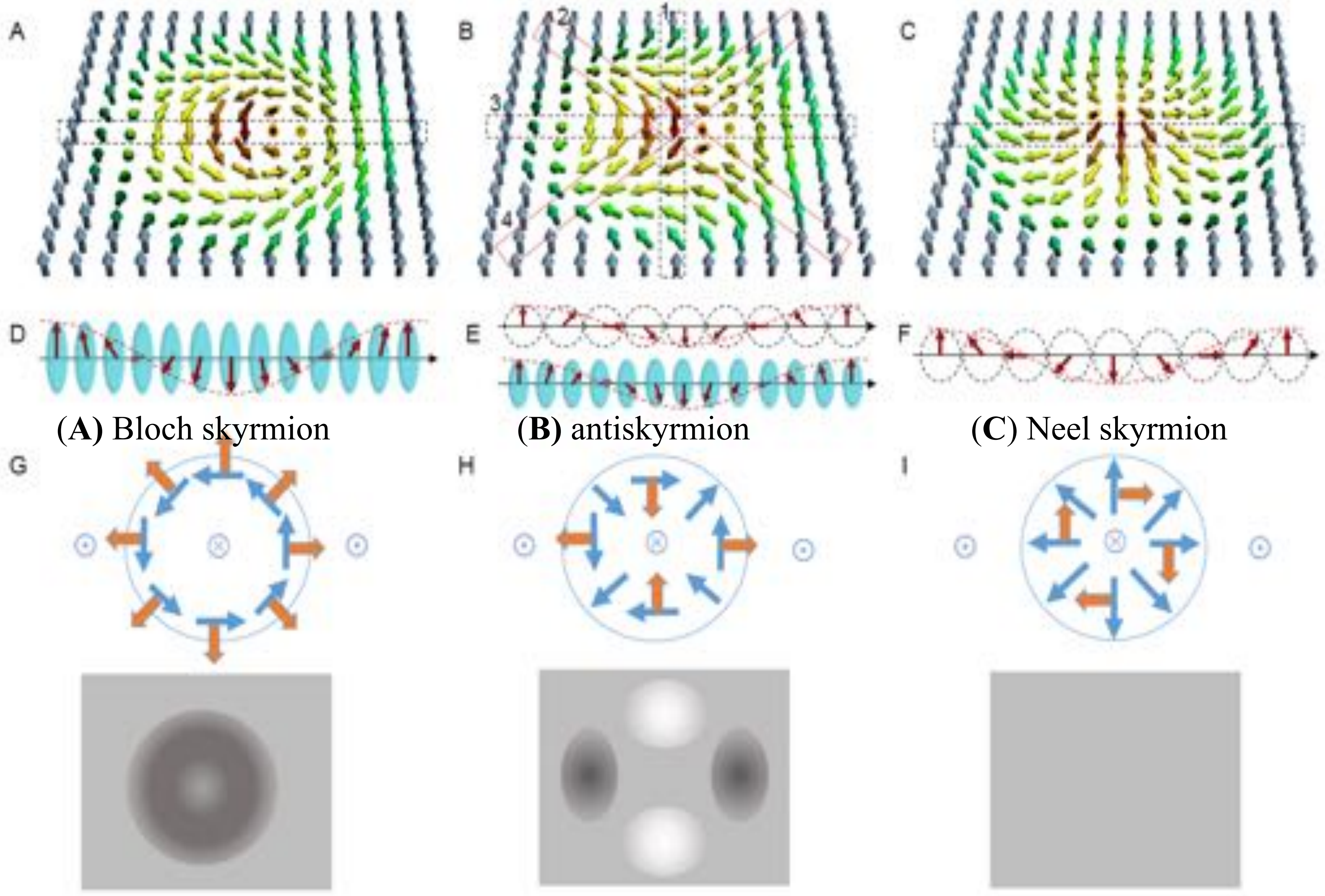

$Mn_{1.4}Pt_{0.9}Pt_{0.1}Sn$: Anti-Skyrmions

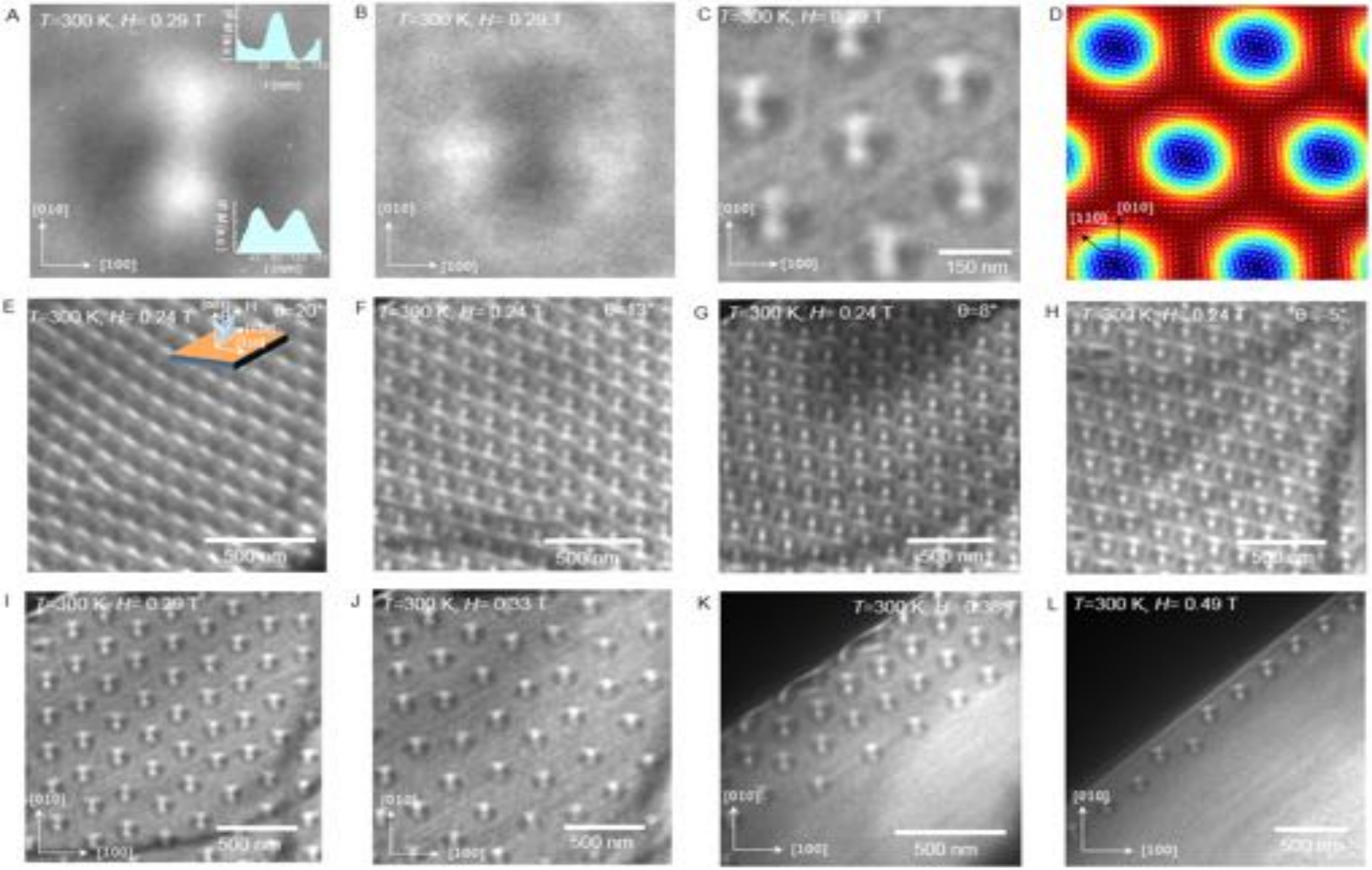

Nayak, et al. preprint arXiv:1703.01017

Bogdanov et al PRB **66**, 214410 (2002)

Single Crystals available

BaCr2As2
BaCrFeAs2

CaPd3O4
SrPd3O4
BaBiO3

Bi2Te2Se
Bi2Te3
Bi2Se3
BiSbTe2S
BiTeI
BiTeBr
BiTeCl

LaBi, LaSb
GdBi, GdSb

HfSiS

Bi4I4

BaSn2

AlPt
GdAs
CoSi

MoP
WP

TaP
NbP
NbAs
TaAs
NbP-Mo
NbP-Cr
TaP-Mo
TaAsP

CrNb3S6
V3S4
Cd3As2

MnP
MnAs

MoSe2-xTex
MoTe2-xSex
MoTe2 (T´/2H)

PtTe2
PtSe2
PdTe2
PdSe2
OsTe2
RhTe2
TaTe2
NbTe2
WSe2
HfTe5
MoTe2
TaS2
PdSb2
CuxWTe2
FexWTe2
WTe2
Co0,4TaS2
Fe0,4TaS2

Ag2Se
IrO2
OsO2
ReO2
WP2
MoP2

VAl3
Mn3Ge
Mn3Ir
Mn3Rh
Mn3Pt
[illegible]

YPtBi
NdPtBi
GdPtBi
YbPtBi
ScPdBi
YPdBi
ErPdBi
GdAuPb
TmAuPb
AuSmPb
AuPrPb
AuNdPb
[illegible]
[illegible]
AuYSn
ErAuSn
EuAuBi

CaAgAs

KMgSb
KMgBi
KHgSb
KHgBi
LiZnAs
LiZnSb

YbMnBi2
Ni2Mn1.4In0.6
YFe4Ge2

Mn1.4PtSn

CuMnSb
CuMnAs

Co2Ti0.5V0.5Sn
Co2VAl0.5Si0.5
Co2Ti0.5V0.5Si
Mn2CoGa
Co2MnGa
Co2Al9
Co2MnAl
Co2VGa0.5Si0.5
Co2TiSn
Co2VGa
Co2V0.8Mn0.2Ga
CoFeMnSi

Thank you!